Universidad de Oviedo

Universidá d'Uviéu

University of Oviedo

Programa de Doctorado en Materiales

DESIGN OF SELECTIVE ADSORPTION MATERIALS FOR THE REMOVAL OF HAZARDOUS ORGANIC COMPOUNDS

DISEÑO DE ADSOBENTES SELECTIVOS PARA LA ELIMINACIÓN DE COMPUESTOS ORGÁNICOS PELIGROSOS

TESIS DOCTORAL

Tetiana Hubetska

Julio 2021

Universidad de Oviedo

Universidá d'Uviéu

University of Oviedo

Programa de Doctorado en Materiales

DESIGN OF SELECTIVE ADSORPTION MATERIALS FOR THE REMOVAL OF HAZARDOUS ORGANIC COMPOUNDS

DISEÑO DE ADSOBENTES SELECTIVOS PARA LA ELIMINACIÓN DE COMPUESTOS ORGÁNICOS PELIGROSOS

TESIS DOCTORAL

Directores de tesis

Dr. D. José Rubén García Menéndez

Dra. Dña. Natalia Kobylinska

Universidad de Oviedo
Universidá d'Uviéu
University of Oviedo

RESUMEN DEL CONTENIDO DE TESIS DOCTORAL

1.- Título de la Tesis	
Español: Diseño de adsorbentes selectivos para la eliminación de compuestos orgánicos peligrosos.	Inglés: Design of selective adsorption materials for the removal of hazardous organic compounds.

2.- Autora	
Nombre: Tetiana Hubetska	NIE:
Programa de Doctorado: Materiales	
Órgano responsable: Comisión Académica Programa de Doctorado en Materiales	

RESUMEN (en español)

Se desarrollaron métodos de preparación de materiales para la recuperación y pre-concentración de contaminantes orgánicos, tanto en aire como en medio acuoso. En la primera parte de esta Tesis Doctoral, se sintetizaron carbones activados (ACs) con porosidad y morfología diversas. En el caso de materiales mesoporosos, se utilizaron sílice SBA-15 y MCM-48 como plantilla. Los ACs se obtuvieron mediante pirolisis con vapor y activación química. El poliestireno mejoró la resistencia mecánica de los ACs mesoporosos de morfología esférica. ACs de morfología esférica se utilizaron como adsorbentes en la extracción de componentes peligrosos en humo de cigarrillos. Se utilizaron subproductos de pipas de girasol, procedentes de una central eléctrica industrial, para la síntesis en tres etapas (pretratamiento ácido-base/disolventes, carbonización y activación química) de ACs, con capacidad de adsorción hacia azul de metileno superior a la de ACs comerciales. La segunda parte de este trabajo se focalizó hacia la síntesis de nanopartículas de magnetita tipo *core-shell* y la aplicación de estos materiales como adsorbentes o agentes de limpieza para la determinación de contaminantes orgánicos en matrices diversas. Se han obtuvieron nanopartículas de magnetita decoradas con capas de sílice y modificadas con el tensioactivo no iónico Triton X-100 (Fe_3O_4@Triton). Fe_3O_4@Triton pre-concentó eficazmente pesticidas organoclorados (OCPs) en medio acuoso. Los nanocompuestos magnéticos se separaron fácilmente de la disolución mediante un campo magnético externo, sin centrifugación ni filtración. Asimismo, se desarrolló el procedimiento QuEChERS con el Fe_3O_4@Triton como agente limpiador de componentes no polares. El procedimiento QuEChERS modificado se utilizó para monitorizar el seguimiento de 20 OCPs en muestras de frutas, hortalizas y suelos. Los adsorbentes desarrollados son susceptibles de aplicación práctica, tanto desde una perspectiva económica como ecológica.

RESUMEN (en Inglés)

In the present PhD Thesis is to develop methods preparation of effective materials for the removal and pre-concentration of organic contaminants in air/water medium. In the first part, the synthesis activated carbon (AC) materials with various porosity and morphology were described. The synthesis of the mesoporous samples was based on the using of SBA-15 and MCM-48 silica as templates. The steam-pyrolysis and chemical activation has been used for obtained AC. Then, polystyrene was used to increase the mechanical resistance of the mesoporous AC with spherical morphology. The adsorption performance of spherical AC was studied by extraction of cigarette smoke. The possibility of using on sunflower husk by-products obtained at industrial power plant as precursor for the synthesis of AC also investigated. The AC has been synthesized in three steps: acid-alkali/solvents pretreatment, carbonization and chemical activation. The adsorption capacity toward methylene blue was higher than commercial AC. The second part of work focuses on the synthesis core-shell type magnetite nanoparticles and application of these materials as adsorbents or clean-up agent for determination organic pollutants in various matrixes. Magnetite nanoparticles decorated with silica layers and modified with non-ionic surfactant Triton X-100 (Fe_3O_4@Triton) have been obtained. The Fe_3O_4@Triton is effectively pre-concentrate the organochlorine pesticides (OCPs) in the water medium. The magnetic nanocomposites can be easily separated from the solution by an external magnetic field without centrifugation or filtration. Also, the QuEChERS procedure with the Fe_3O_4@Triton as clean-up agent of non-polar components was developed. The modified QuEChERS procedure has been applied for the monitoring of 20 OCPs in fruit, vegetable and soil samples. This study opens up possibilities for the developed adsorbents with focus on the economic and eco-friendly effects.

SR. PRESIDENTE DE LA COMISIÓN ACADÉMICA DEL PROGRAMA DE DOCTORADO EN MATERIALES

Universidad de Oviedo

Universidá d'Uviéu

University of Oviedo

Programa de Doctorado en Materiales

DESIGN OF SELECTIVE ADSORPTION MATERIALS FOR THE REMOVAL OF HAZARDOUS ORGANIC COMPOUNDS

DISEÑO DE ADSOBENTES SELECTIVOS PARA LA ELIMINACIÓN DE COMPUESTOS ORGÁNICOS PELIGROSOS

TESIS DOCTORAL

Tetiana Hubetska

Julio 2021

Universidad de Oviedo

Universidá d'Uviéu

University of Oviedo

Programa de Doctorado en Materiales

DESIGN OF SELECTIVE ADSORPTION MATERIALS FOR THE REMOVAL OF HAZARDOUS ORGANIC COMPOUNDS

DISEÑO DE ADSOBENTES SELECTIVOS PARA LA ELIMINACIÓN DE COMPUESTOS ORGÁNICOS PELIGROSOS

TESIS DOCTORAL

Directores de tesis

Dr. D. José Rubén García Menéndez

Dra. Dña. Natalia Kobylinska

Contents

Acknowledgements

On the first place I would like to thank the professors who supervised this work Prof. José Rubén García Menéndez and Dr. Natalia Kobylinska for all the faith they put in me, for directing, advising, supporting and simply for being excessively kind and understanding in many occasions.

I express my gratitude to all the friends and colleagues from University of Oviedo I have had pleasure to work with in the recent years, to Sergei, Olena, Igor, Arancha, Mohammed, Rafa, Marina, Camino, Beatriz, and of course to Prof. Santiago García Granda, who made everything started. I would like to acknowledge all the technical and scientific assistance I received from the SCTs staff Alfonso, David, Jorge, Victor.

I am enormously grateful to the group of Prof. Ana Paula Carvalho, to Ana Sofia for accommodating me in Lisboa and giving me the possibility to not only do a fruitful research, but also spend a great time.

Finally, I thank my friends (too many to list here but you know who you are!) for providing support and friendship that I needed. I also give my gratitude to all of my family I have seen so little in the ultimate years, but who supported me in spite of the distance.

Abstract

The technological progress of human society has resulted in contamination of water and air manifesting in the presence of toxic pollutants. Effects of toxic inorganic (metal ions and anions) and organic pollutants on human health are continuously being analyzed by international organizations such as World Health Organization (WHO), Environmental Protection Agency (EPA), and European Union (EU). High concentrations of these toxic elements cause several adverse effects on human health. Environmentally pollutants include phenolic compounds, pesticides, herbicides, fertilizers, organic acids, dyes, pharmaceutical substances such as antibiotics, cosmetics, and personal care products, detergents, and heavy metals. The main sources of environmental water contamination include wastewater discharge from industries, agriculture, and other global activities. Environmental contamination is an existence of a symbiotic relationship between human health and environmental protection. Hence, water decontamination is a very important processes for further human civilization.

Adsorption has several advantages over the other methods of removal pollutants because of its simple design and can involve low investment in terms of both initial cost and land required. In this way, in recent years, the search for low-cost adsorbents that have pollutant-binding capacities is intensified. In this context, the present *PhD Thesis* was develop methods preparation effective materials for removal and pre-concentration organic contaminants in air/water medium.

Optimization of the synthesis conditions was used out taking into account various factors on the final properties of the obtained adsorbents. In the first part of this research, activated carbon-based materials with various porosity and morphology have been synthesized, and their adsorption activities toward toxic components in water medium and air have been tested.

The synthesis of the mesoporous activated carbon was based on the applying of periodically ordered mesoporous silica dioxide as a template for carbon preparation. For this approach, carbo-thermal reduction of the organic precursor by means of the filling of mesoporous silica pores with organic polysaccharide (sucrose). In the next stage, powder carbon replicas are obtained by annealing samples in an inert atmosphere. Also, using periodic mesoporous silica dioxide such as SBA-15 and MCM-48 was synthesized mesoporous carbon replicas with large specific surface areas and a high degree of ordering. In addition, polystyrene was used to increase the mechanical resistance of the spherical mesoporous carbon after removal silica dioxide template. The steam-pyrolysis at 900 °C, and chemical activation with HNO_3, H_2O_2 and their mixture at thermal

treatment has been used for obtained activated carbon-based adsorbents. The effect morphological and physico-chemical characteristics of samples to adsorption properties were determined. The adsorption properties of the obtained materials were studied using tetracycline (TC) antibiotics as the model analytes. Adsorption kinetics, isotherms characteristics, and pH effect to the affinity of the antibiotics on different adsorbents were studied. Moreover, the hypothetical mechanism of antibiotics adsorption on the obtained samples was proposed. The mesoporous activated carbon exhibited high adsorptive activity even after five cycles adsorption/desorption, which was potentially able for high efficiency and low-cost water purification.

Also, mesoporous carbon materials with spherical morphology and micron size were synthesized especially for the removal of gaseous pollutants. It has been established that the adsorbents have a high specific surface area with protolytically active oxygen-containing groups. The adsorption properties of the carbon adsorbent were investigated by extraction and concentration of main components of cigarette smoke. Adsorption of smoke components was performed as dynamic and static conditions; therefore, developed materials can be applied as fillers in stationary smoking rooms and in spaces equipped with a fume hood. The spherical mesoporous adsorbents show superior properties compared to the commercial materials used for air remediation in smoking rooms. The chemical regeneration of the mesoporous adsorbents has been reached through extraction by organic solvents without additional thermal treatment.

It was also investigated the possibility of using biowaste as a low-cost precursor for the synthesis of activated carbon. Biomass wastes based on sunflower seed husk residues obtained at industrial energy pyrolysis plant were tested as to raw material for AC. The AC has been synthesized by three steps: (1) pretreatment of raw materials by acid-alkali/organic solvents, (2) simple carbonization at 600 C, and (3) chemical activation by HNO3 or NaOH. The adsorption capacity toward Methylene blue dye as a model molecule by the AC sample was higher (379.0 $mg \cdot g^{-1}$) than the value of commercial activated carbon (Norit).

The second part of this work focuses on the synthesis of new modified core-shell magnetite nanoparticles and the application of these magnetic solids as adsorbents and clean-up agents before the determination of organic pollutants in various matrixes.

Novel hydrophobically functionalized magnetic nanocomposites have been prepared as new adsorbents for the effective removal of organic compounds. Magnetite (Fe_3O_4) nanoparticles decorated with layers of silica and modified with a non-ionic surfactant Triton X-100 (Fe_3O_4@Triton) have been prepared through a step-by-step core-shell technique. Hydrophobic

groups grafted to the surface of magnetic nanoparticles can be effectively pre-concentrate the organochlorine pesticides (OCPs) present in the water medium. Effective adsorption and selective uptake of OCPs are observed on the prepared composite due to the high concentration of hydrophobic functional groups on the nanocomposites of the surface. Then the magnetic nanocomposites can easily be separated from the extract by an external magnetic field avoiding additional steps of centrifugation or filtration.

In addition, the target analyte sample preparation *Quick-Easy-Cheap-Effective-Rugged-Safety* (QuEChERS) procedure with the novel magnetic nanocomposite (Fe_3O_4@Triton) as a clean-up agent of non-polar components (fat, pigment, etc.) was developed. The modified QuEChERS procedure has been applied for the monitoring of 20 OCPs present in fruit, vegetable, and soil samples. Modified MNPs were found to more effective clean-up agents for purification extract than typical commercial adsorbents (octadecyl silica and granular carbon black) or bare Fe_3O_4. The magnetic nanocomposites have provided the lower level of co-extracted interferences (including pigments) in the extraction process. The type and amount of clean-up adsorbents, the volume and polarity of the solvent and the extraction time were optimized. Under the found optimal conditions the developed QuEChERS procedure was validated through linearity, recovery, precision and accuracy studies. Thus, the results have shown good linearity and satisfactory average recoveries of various OCPs. The QuEChERS procedure using modified Fe_3O_4 MNPs improves the rapidity sample pretreatment and exhibits an enhanced performance in removing pesticide impurities employing budget-conscious laboratory equipment.

The materials proposed in this work can be implemented in routine practice for monitoring, determination, and removal of organic compounds in different types of contaminated samples.

Resumen

El progreso tecnológico de la humanidad ha provocado un alarmante aumento en la contaminación ambiental, que se manifiesta en la cuasi-omnipresencia de componentes tóxicos en multitud de lugares (agua, aire, suelo, alimentos, etc.). A pesar de que los efectos de los contaminantes (orgánicos e inorgánicos) sobre la salud humana son analizados continuamente por instituciones internacionales como la Organización Mundial de la Salud (OMS), la Agencia de Protección Ambiental (EPA) o la Unión Europea (EU), sus elevadas concentraciones provocan cada vez un mayor número de efectos sanitarios adversos.

Los contaminantes ambientales incluyen compuestos fenólicos, pesticidas, herbicidas, fertilizantes, ácidos orgánicos, tintes, sustancias farmacéuticas (con especial mención a los antibióticos), cosméticos y productos de cuidado personal, detergentes y metales pesados, entre otros muchos. Las principales fuentes de contaminación ambiental del agua deben buscarse en la descarga de aguas residuales de industrias, agricultura y otras actividades globales. Dado que la contaminación ambiental incide negativamente en la salud humana, la protección del medio ambiente, incluyendo la descontaminación eficaz de las aguas, es una cuestión decisiva para nuestro futuro.

La adsorción presenta varias ventajas sobre otros métodos de eliminación de contaminantes, incluyendo un diseño simple, acompañado de una baja inversión, tanto en términos de costes iniciales como de espacios requeridos para su ejecución. Como consecuencia, en los últimos años se ha intensificado la búsqueda de adsorbentes de precio asumible con buena capacidad de captar contaminantes. En este contexto, en la presente Tesis Doctoral se desarrollaron nuevos métodos de preparación de materiales para la remoción y preconcentración de contaminantes orgánicos en aire/agua.

En la primera parte de esta investigación, se sintetizaron materiales basados en carbones activados, con porosidad y morfologías diversas, y se determinaron sus propiedades de adsorción hacia componentes tóxicos en medios acuosos y en aire.

La preparación de carbones activados se efectuó usando como plantilla dióxido de silicio mesoporoso ordenado periódicamente, con reducción carbo-térmica posterior del precursor orgánico (sacarosa) empleado como relleno de los mesoporos de la sílice. Utilizando materiales periódicos, SBA-15 y MCM-48, se sintetizaron réplicas carbonosas con elevadas superficies específicas y alto grado de ordenación. Además, se empleó poliestireno para aumentar la resistencia mecánica de los

carbones mesoporosos esféricos, después de la eliminación de la plantilla de sílice. Se estudió la pirolisis con vapor a 900 °C, y la activación química con HNO_3, H_2O_2 y sus mezclas. Se determinó el efecto de las características morfológicas y físico-químicas de los materiales sobre sus propiedades de adsorción, utilizando tetraciclinas como sistemas modelo. Se estudió la cinética de adsorción, las características de las isotermas y el efecto del pH en la afinidad de estos antibióticos hacia diferentes adsorbentes. Además, se propuso un mecanismo de adsorción de tetraciclinas en las muestras obtenidas. Los carbones activados mesoporosos preparados exhibieron elevada actividad de adsorción, incluso después de cinco ciclos de adsorción/desorción, siendo potencialmente utilizables para la purificación de aguas a bajo costo.

Se sintetizaron materiales carbonosos mesoporosos, de morfología esférica y tamaño micrométrico, útiles en la eliminación de contaminantes gaseosos, con elevada área superficial específica y grupos oxigenados protolíticamente activos. Se testaron sus propiedades de adsorción en la extracción y concentración de componentes tóxicos del humo de cigarrillos, en condiciones dinámicas y estáticas, proponiéndose su uso como adsorbentes en salas de fumadores (tanto en espacios equipados con recirculadores de aire como en ambientes estacionarios) debido a sus propiedades superiores a los materiales comerciales más comunes (además, la regeneración de estos adsorbentes se consiguió por extracción con disolventes, sin tratamiento térmico adicional).

La segunda parte de este trabajo se centró en la síntesis de nuevas nanopartículas de magnetita núcleo-capa modificadas, y la aplicación de estos materiales magnéticos como adsorbentes y agentes de limpieza, previos a la determinación de contaminantes orgánicos en matrices diversas.

Se prepararon nuevos nanocompuestos magnéticos, funcionalizados hidrofóbicamente. Se sintetizaron nanopartículas de magnetita decoradas con capas de sílice y modificadas con un tensioactivo no iónico (Fe_3O_4@Triton). Los grupos hidrófobos injertados en la superficie de las nanopartículas magnéticas lograron preconcentrar eficazmente plaguicidas organoclorados (OCPs) presentes en medio acuoso, al tiempo que los nanocompuestos se separaron magnéticamente del extracto, evitando procesos más lentos y costosos (centrifugación o filtración).

Se desarrolló un procedimiento de preparación de muestras *Quick-Easy-Cheap-Effective-Rugged-Safety* (QuEChERS), utilizando Fe_3O_4@Triton como agente de limpieza de componentes no polares, y se aplicó al seguimiento de una veintena de OCPs presentes en frutas, hortalizas y suelos. El procedimiento desarrollado demostró mayor eficiencia que cuando se usan adsorbentes comerciales, con menores interferencias en procesos de coextracción. Se optimizó el tipo y la cantidad de adsorbente de limpieza, el volumen y la polaridad del disolvente y el tiempo de extracción. El

procedimiento QuEChERS desarrollado se validó mediante estudios de linealidad, recuperación, precisión y exactitud. Por tanto, los materiales objeto de esta investigación podrán ser implementados, a bajo coste, para el seguimiento, determinación y remoción de compuestos orgánicos en diferentes tipos de muestras contaminadas.

Índices de calidad

De acuerdo con el Reglamento de los Estudios de Doctorado aprobado por el Consejo de Gobierno de la Universidad de Oviedo el 17 de Junio de 2013 (Boletín Oficial del Principado de Asturias Nº 146, de 25-06-2013), para presentar la Tesis Doctoral como Compendio de Publicaciones es necesario incluir en la presente Memoria un informe con el factor de impacto de las publicaciones presentadas, junto con un detalle informativo sobre la calidad de las mismas, basado en el índice de impacto y en la posición que ocupa la revista científica dentro de una determinada categoría. El informe correspondiente a los índices de impacto de las revistas en las que se han publicado los artículos que forman parte de la presente Memoria de Tesis Doctoral se resume en la siguiente Tabla.

Relación de publicaciones derivadas de la presente Tesis Doctoral
(datos obtenidos de Journal Citations Reports®).

Nombre de la publicación	Año	Factor de Impacto	Categoría de JCR®	Clasificación, en la categoría	Cuartil, en la categoría
IEEE Magnetics Letters	2018	1.540 (2019) 1.539 (5 años)	PHYSICS, APPLIED	103/155	Q3
Protection of Metals and Physical Chemistry of Surfaces	2019	0.985 (2019) 0.879 (5 años)	METALLURGY & METALLURGICAL ENGINEERING	56/79	Q3
Adsorption	2020	1.949 (2019) 2.639 (5 años)	ENGINEERING, CHEMICAL	77/143	Q3
Journal of Agricultural and Food Chemistry	2020	4.192 (2019) 4.290 (5 años)	CHEMISTRY, APPLIED	15/71	Q1
Journal of Analytical and Applied Pyrolysis	2021	3.905 (2021) 4.296 (5 años)	ENGINEERING, CHEMICAL	34/143	Q1

Comunicaciones a congresos

1. T.S. Hubetska, N.G. Kobylinska, J.R. García, Approaches for the solid-phase extraction of pollutants from water and food products, NALS - Nanomaterials Applied to Life Sciences, Gijón (Spain), 2017. *Poster.*

2. T.S. Hubetska, A.S. Mestre, N.G. Kobylinska, A.P. Carvalho, J.R. García, Sisal derived activated carbons: New synthesis approach, characterization and application for removal of pharmaceutical compounds, 16th Polish- Ukrainian Symposium, Lublin (Poland), 2018. *Poster.*

3. T.S. Hubetska, N.G. Kobylinska, J.R. García, Efficient adsorption of pharmaceutical drugs in aqueous solution using a mesoporous activated carbon, 41 RIA-IBA3, Gijón (Spain), 2018. *Poster.*

4. T.S. Hubetska, A.S. Mestre, N. Kobylinska, J.R. García, A.P. Carvalho, Superactivated carbons synthetized by steam activation of acid-chars for pharmaceuticals removal, CESEP 19- International Conference on Carbon for Energy Storage and Environmental Protection, Alicante (Spain), 2019. *Oral.*

5. A.P. Carvalho, T.A.G. Duarte, T.S. Hubetska, C. Nunes, J.R. García, L.M.D.R.S. Martins, A.S. Mestre, Acid-chars as platform materials for adsorption and catalysis, Carbon 2019, Lexington (USA), 2019. *Oral.*

6. T.S. Hubetska, N.G. Kobylinska, J.R. García, Optimization of QuEChERS procedure by hydrophobic magnetic nanocomposites for residual OCPs determination coupled with GC-MS, Euroanalysis XX, Istanbul (Turkey), 2019. *Poster.*

7. Tetiana S. Hubetska, Natalia G. Kobylinska, José R. García, Development of carbon adsorbents from industrial pyrolyzed biowaste by-products under varying conditions of $ZnCl_2$ and H_2O_2/HNO_3 activation, AdvPhotoCat EE2021, Bucharest (Romania)/Crete (Greece) 2021. *Poster*

Nomenclature

AC – Activated carbon;

BET – Brunauer-Emmett-Teller;

BJH – Barrett-Joyner-Halenda;

DTA – Differential thermal analysis;

FTIR – Fourier transform infrared spectroscopy;

GC-MS – Gas chromatography with mass-spectrometry;

GC-FID – Gas chromatography with flame ionization detection;

HPLC – High performance liquid chromatography;

MNPs – Magnetic nanoparticles;

SPE – Solid phase extraction;

MSPE – Magnetic solid phase extraction;

SPIONs – Superparamagnetic iron oxide nanoparticles;

OMC – Ordered mesoporous carbon;

XRD – X-ray diffraction;

SEM – Scanning electron microscopy;

TEM – Transmission electron microscopy;

TGA – Thermogravimetry analysis;

MS – Mass spectrometry;

TGA-MS - Thermogravimetry analysis coupled to mass spectrometry;

XPS – X-ray photoelectron spectroscopy;

QuEChERS – Quick, easy, cheap, effective, rugged, safety;

OCPs – Organochloride pesticides;

MB – Methylene blue;

TC – Tetracycline;

CTC – Chlortetracycline;

OTC – Oxytetracycline;

DC – Doxycycline;

MC – Mesoporous carbon;

NLDFT – Non-local density functional theory;

α-BHC – α-Hexachlorocyclohexane;

4,4-DDD – Dichlorodiphenyldichloroethane;

4,4-DDE – Dichlorodiphenyldichloroethylene;

4,4-DDT – Dichlorodiphenyltrichloroethane;

OFN – Octafluoronaphthalene;

SS – Standart solution;

IS – Internal standards;

ME – Matrix effect;

LOD – Limits of detection;

LOQ – Limits of quantification;

GCB – Granulated carbon black.

List of Figures

1. Introduction

The essential aim of this work is to fill the gap that exists between the fields of materials and its adsorption properties, an area that, to our knowledge, has not been completely encompassed. Adsorption technology is a recognized method for the removal of most contaminants from liquid and gas phases by various types of materials. The phenomenon of adsorption from both a fundamental and an applied perspective was summarized. There is a vacuum of knowledge between adsorption properties and material parameters that, if filled, could give birth to new concepts and ideas in this part of the *Ph.D. thesis*.

1.1 Adsorption air/water treatment and purification of organic contaminants

Nowadays, people are exposed to a wide range of synthetic environmental chemicals, and some studies have suggested the potential for harmful effects to human health for many of these compounds [1]. There are over 100,000 chemicals are currently in use or present in consumer products with over 30,000 considered to be in wide commercial use (in consumer products at > 907 $kg \cdot year^{-1}$) [2].

A rigorous evaluation of environmental contamination requires constant innovation in technologies, chromatographic materials, and analytical approaches to gain early identification and accurate quantification of every substance able to compromise flora, fauna, and public health integrity. Due to the public interest in environmental issues, the research in such a field is extremely active and many papers have continuously been published every year. In the same way, the literature is rich in reviews that have been aimed at covering the several facets of environmental investigations: Development of novel extraction strategies, fast chromatographic methods, use of mass spectrometry (MS) for target and non-target analysis, strategies for identification of transformation products [3].

Efficient techniques for the removal of highly toxic organic compounds from water and air have drawn significant interest A number of chemical technologies are applied with varying degrees of results to control water pollution. Some of them are coagulation [4], filtration with coagulation, precipitation, ozonation, solvent extraction [5], adsorption, ion-exchange [6], reverse osmosis, and advanced oxidation processes have been used for the removal of organic pollutants from polluted water and wastewater. These methods have been found to be limited since they often involve high

capital and operational costs. On the other hand, ion-exchange and reverse osmosis are more attractive processes because the pollutant values can be recovered along with their removal from the effluents. Reverse osmosis, ion-exchange, and advanced oxidation processes do not seem to be economically feasible because of their relatively high investment and operational cost.

Among the possible techniques for water and treatments, the adsorption process by solid adsorbents shows potential as one of the most efficient methods for the treatment and removal of organic contaminants in wastewater treatment. Adsorption has advantages over the other methods because of its simple design and can involve low investment in terms of both initial cost and land required. The adsorption process is widely used for the treatment of industrial wastewater from organic and inorganic pollutants and meets great attention from researchers. In recent years, the search for low-cost adsorbents that have pollutant–binding capacities has intensified. Adsorption can also remove soluble and insoluble organic pollutants. The removal capacity by this method may be up to 99.9% [7].

The adsorption of pollutants from aqueous solutions plays an important role in wastewater treatment since it eliminates the need for huge sludge-handling processes. Adsorption is a surface phenomenon with a common mechanism for organic and inorganic pollutants removal. When an environment containing absorbable comes into contact with a solid with a highly porous surface structure, liquid-solid or air-solid intermolecular forces of attraction cause some of the molecules from the solution or air to be concentrated or deposited at the solid surface. The substance retained (on the solid surface) in adsorption processes is called adsorbate, whereas, the solid on which it is retained is called an adsorbent. This surface accumulation of adsorbate on adsorbent is called adsorption. This creation of an adsorbed phase having a composition different from that of the bulk fluid or air phase forms the basis of separation by adsorption technology. In a bulk material, all the bonding requirements (be they ionic, covalent, or metallic) of the constituent atoms of the material are filled by other atoms in the material. However, atoms on the surface of the adsorbent are not wholly surrounded by other adsorbent atoms and therefore can attract adsorbates. The exact nature of the bonding depends on the details of the species involved, but the adsorption process is generally classified as physisorption (characteristic of weak van der Waals forces) or chemisorption (characteristic of covalent bonding). It may also occur due to electrostatic attraction. Physical adsorption has been found to be more significant in the case of separation processes. Physical adsorption is again classified into Thermal Swing Adsorption and Pressure Swing Adsorption, based on the operation of the process. Both the processes have their advantages and disadvantages.

Physical adsorption occurs when organic molecules are held on the surface and in the pores of the adsorbent by the weak van der Waals force of attraction and are generally characterized by low heat of adsorption, and by the fact that the adsorption equilibrium is reversible and rapidly established.

It is assumed that the weak van der Waal forces bind the adsorbent and adsorbate together. There is no transfer or sharing of electrons though new equilibrium adjustment takes place without losing the original association of electrons with their respective interacting species. The presence of these weak bonds is characterized by low heat of adsorption usually less than 42 kJ $\cdot mol^{-1}$. This adsorption is appreciable only at a temperature below the boiling point of adsorbate, it is reversible in nature and non-specific with respect to the adsorbent (the physical adsorption may be leading to the formation of multilayer, with more dependence on the nature of the adsorbate than that of solid adsorbent).

In many cases, the adsorption of a substance at a surface involves the formation of chemical bonds between the adsorbate and adsorbent due to the transfer or sharing of electrons. It is generally characterized by a high degree of heat of adsorption (i.e. 20-150 $kcal \cdot mol^{-1}$) and can occur at high temperatures. It is usually irreversible in nature and nonspecific with both adsorbate and adsorbent. Due to high initial heat which leads to a large amount of adsorption is indicative of chemical adsorption to form something like a monolayer, followed by the formation of a multilayer that is bound by physical forces.

The most common techniques with using inorganic and polymeric adsorbents for the preparation of aqueous samples for an analysis trace amount of organic or clean-up matrix before analysis are solid-phase extraction (SPE) or its micro-extraction variants. The sorbent-based microextraction techniques have been proposed in recent years as an alternative to conventional sample preparation techniques for the control of pollutants in the environment. This technique involves advantages such as minimal solvent and sample consumption, fewer treatment steps, and reduction of waste generation, and also presents some drawbacks: Batch to batch variation, the fragility of fibers, restricted choice of commercially available stationary phases, and fiber coatings, and insufficient selectivity of these materials [8]. SPE is an exhaustive sample preparation technique that possesses advantages over other traditional sample preparation techniques, including low organic solvent consumption, simplicity, rapidity, and improved sample clean-up. These advantages of SPE have made it a very attractive technique in different bio/analytical research areas such as environmental, clinical, biological, and food studies [9].

Although natural adsorbents are abundant and inexpensive, these attributes may not offset the effects of impurities and inconsistency of properties relative to the more uniform synthetic adsorbents. Recently, a novel SPE procedure using magnetic or magnetizable materials has been introduced and the new method is called magnetic solid-phase extraction (MSPE) [10]. MSPE requires the addition of magnetic sorbent particles to the target ions-containing solution. The target ions are adsorbed onto the surface of magnetic material and the magnetic particles containing the analytes are collected by applying an external magnetic field. The adsorbed analyte is then eluted with a suitable solvent, analysed, and the purified solution sent to other downstream processes or refining. MSPE offers several advantages compared to conventional solid-phase extraction methods:

(1) simplified sample pre-treatment in contrast with the time-consuming column packing;

(2) fast and easy analyte separation since sample pre-treatment (i.e., centrifugation, filtration, etc.) is not required;

(3) magnetic sorbent particles render high selectivity towards environmental and biological compounds treated even with the presence of suspended solids;

(4) typical sample impurities that hinder the adsorption process during the magnetic separation are repelled due to its diamagnetic properties;

(5) opportunity for automation procedures (off- and online) with flow injection analysis and other related methods providing fast, selective, sensitive, and repeatable methods for conventional analysis [11].

1.2. Adsorption isotherms in liquid phase: Equilibrium, kinetics, modeling and interpretations

Well-designed adsorption processes have high efficiency resulting in a high-quality effluent after treatment. The adsorption process is presumed to involve the following stages (Fig. 1): Mass transfer of the adsorbate molecules across the external boundary layer towards the adsorbent solid (1), adsorbate molecules transport from the adsorbent surface into the active sites by diffusion within the pore-filled liquid and migrate along the solid surface of the pores (2), solute molecules adsorption on the active sites on the interior surfaces of the pores (3), and once the molecules adsorbed, it may migrate on the pore surface trough surface diffusion (4). It is therefore understandable that the study of adsorption equilibrium, kinetics in wastewater treatment is significant as it provides valuable insights into the reaction pathways and into the mechanism of sorption reactions.

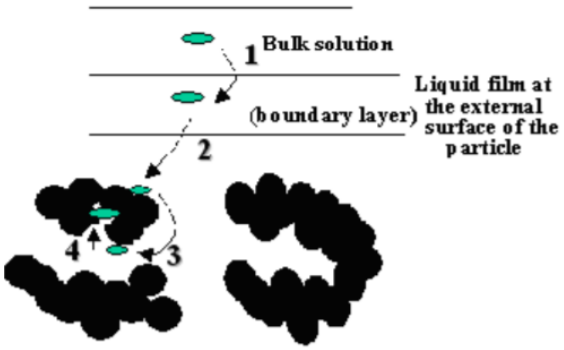

Fig. 1. Schematic representation of an adsorption process in liquid phase [12].

Between the adsorbate and adsorbent dynamic equilibrium is established, which results from the equalization of the number of adsorbed molecules with that of molecules undergoing desorption:

$$A \leftrightarrow A_{ads}$$

where A are the adsorbate molecules in the gas/liquid phase, A_{ads} are in the adsorbed state. This follows as in the same time unit the same number of adsorbate molecules is undergoing adsorption and desorption. As adsorption measure the amount of the adsorbed substance it is assumed that is expressed in grams, moles, or cm^3 per the adsorbent mass unit. In adsorption equilibrium, these quantities depend on the gas and temperature pressure.

To develop adsorption equilibrium and kinetics, knowledge of the rate law describing the adsorption system is required. The rate law is determined by experimentation and it cannot be inferred by more examination of the overall chemical reaction equation. The rate law has three primary requirements:

- Knowledge of all the molecular details of the reaction including the energetics and stereochemistry.
- Interatomic distances and angles throughout the course of the reaction.
- Individual molecular steps involved in the mechanism.

Adsorption kinetics. The kinetics of adsorption is important because this is what controls the efficiency of the process and the equilibrium time of adsorption reaction. It also describes the rate of the adsorbate uptake on adsorbents. To identify the potential rate -controlling steps involved in the process of adsorption, three kinetic models were studied and used to fit the experimental data from the adsorption of organic molecules onto various adsorbents. These models are the pseudo-first-

order [13], pseudo-second-order [14], intra particle diffusion [15], Boyd [16] and Elovich [17] kinetic models.

The Lagergren pseudo-first order model is most commonly used to describe the adsorption of solute from a liquid solution [13]. The pseudo-first-order kinetic model can be represented by the following Lagergren rate equation:

$$ln\frac{(qe-q)}{qe} = -k1t \qquad (1)$$

where q and q_e are the amounts of adsorbate adsorbed ($mg \cdot g^{-1}$) at any time (min) and at equilibrium, respectively; and k_1 is the rate constant of first-order sorption (min^{-1}). The value of k_1 is determined by plotting $ln(q_e - q_t)$ vs. t [18]. The pseudo-first-order equation was used infrequently to describe the sorption kinetics.

The non-popular pseudo-first-order Lagergren equation can be applied to correlate kinetic adsorption data only in the adsorption systems that are not far from equilibrium. Also, the Lagergren equation is then the limiting form of the kinetic equations developed by assuming both diffusional and surface reaction kinetic models [19].

Another model for the analysis of sorption kinetics is pseudo-second-order (PSO) [14]. PSO model assumes that the rate of adsorption of solute is proportional to the available sites on the adsorbent, and the reaction rate is dependent on the amount of solute on the surface of the adsorbent. The driving force ($q_e - q_t$), proportional to the number of active sites available on the adsorbent, can be rearranged to obtain a linear form:

$$\frac{t}{q} = \frac{1}{k_2 q_e^2} + \frac{1}{q_e}t \qquad (2)$$

The plot of t/q versus t gives a straight line with slope of $1/k_2 q_e^2$ and intercept of $1/q_e$. So the gram of solute sorbed per gram of sorbent at equilibrium (q_e) and sorption rate constant (k_2) could be evaluated from the slope and intercept, respectively [20].

Even though the PSO model may be affected by pH, dose amount, particle size, and temperature, the model assesses the impact of observable rate parameters. PSO can be used to determine the initial solute uptake and adsorption capacity of an adsorbent. Studies have shown that adsorption behavior that fits the PSO model well often can be explained by diffusion-based mechanisms. Hypothetical data generated using the assumption of pseudo-first-order rate behavior has been shown to fit the PSO model very well. In light of published evidence, adsorption kinetics of

materials is expected to mainly depend on diffusion-limited processes, as affected by heterogeneous distributions of pore sizes and continual partitioning of solute species between a dissolved state and a fixed state of adsorption [21].

These theoretical approach mental results indicate that when the initial concentration of solute is low, then the pseudo-second-order model is suitable for analysis of sorption kinetics, and when the initial concentration is high, the pseudo-first-order model becomes suitable. Of course, one may face the situation that, even at longer adsorption times, the popular Lagergren equation does not apply. This would mean that either the experimental conditions are not proper for the lumped pseudo-first-order expression to be used or that the underlying physical model is not applicable. This conclusion is in complete agreement with a lot of experimental results of the adsorption of organic compounds in solution. Most of the researchers selected the pseudo-second-order kinetic model [**Ошибка! Закладка не определена.**] the experiment better and it has been concluded that the adsorption mechanism is chemisorption in nature, involving the transfer of electrons between the adsorbate and adsorbent [22].

Thus, the pseudo-second-order adsorption mechanism is predominant and that the overall rate of the dye and huge organic molecules adsorption process appears to be controlled by the chemisorption process [**Ошибка! Закладка не определена.**]. Similar phenomena have also been observed in the adsorption of dye (Remazol Black B, etc.) on biomass [23]. In general, the rate constant decreases with an increase of initial dye concentration for the pseudo second-order model.

Adsorption capacity and isotherm models. As the adsorption progress, an equilibrium of adsorption of the solute between the solution and adsorbent is attained (where the adsorption of solute is from the bulk onto the adsorbent is minimum). Adsorption equilibrium is established when an adsorbate phase is in contact with the adsorbent for a long time.

The isotherm is depicted graphically expressing the adsorbent concentration against its residual concentration. It provides a perception of the mechanism of adsorption, degree of harmony of the adsorbents, and surface. The adsorption amount (q_e, $mmol \cdot g^{-1}$) of the molecules at the equilibrium step determined according to the following equation:

$$q_e = \frac{V(C_0 - C_e)}{M} \qquad (3)$$

where V is the solution volume (L); M is the mass of monolithic adsorbents (g); and C_o and C_e are the initial and equilibrium adsorbate concentrations, respectively.

The amount adsorbed from the solution on a solid depends upon a number of factors such as the nature of the adsorbent and adsorbate, the interfacial tension between solution and adsorbent, the temperature of the system, concentration. The pH of the solution, the porosity of the adsorbent, presence of the foreign material, time duration allowed, and the procedure adopted for the systems. Typically, adsorption capacity data are gathered at a fixed temperature and various adsorbate concentrations (or partial pressures for vapor or gas), and the data are plotted as an isotherm (loading versus concentration at constant temperature).

Equilibrium data, commonly known as adsorption isotherms, describe how the adsorbate interacts with adsorbents, and give a comprehensive understanding of the nature of the interaction. It is basically important to optimize the design of an adsorption system. Many theoretical and empirical models have been developed to represent the various types of adsorption isotherms. At present, there is no single equation that satisfactorily describes all mechanisms and shapes. The parameters obtained from the different models provide important information on the surface properties of the adsorbent and its affinity to the adsorbate. Several isotherm equations have been developed and employed for such analysis and the three important isotherms, the Langmuir, Freundlich and, Temkin isotherms are applied in this study.

Langmuir model. The Langmuir isotherm model is widely used in the literature because since incorporates an easily interpretable constant that corresponds to the highest possible adsorbate uptake (i.e. the complete saturation isotherm-curve plateau). Langmuir isotherm model is an empirical model assuming that adsorption can only occur at a finite number of definite localized sites, and the adsorbed layer is one molecule in thickness or monolayer adsorption [24].

The Langmuir non-linear equation is expressed as:

$$q_e = q_m K_L \frac{C_e}{1 + K_L C_e} \qquad (4)$$

where C_e is the concentration of analyte solution at equilibrium ($mg \cdot L^{-1}$); q_e is the corresponding adsorption capacity ($mg \cdot g^{-1}$); q_m ($mg \cdot g^{-1}$) and K_L ($L \cdot mg^{-1}$) are constants which are related to adsorption capacity and energy or net enthalpy of adsorption, respectively. The linear forms of the Langmuir isotherm

$$\text{I} \quad \frac{C_e}{q_e} = \frac{1}{q_m K_L} + \frac{C_e}{q_m} \qquad (5)$$

$$\text{II} \quad \frac{1}{q_e} = \left[\frac{1}{q_m K_L}\right] \frac{1}{C_e} + \frac{1}{q_m} \qquad (6)$$

$$\text{III} \quad q_e = q_m - \left[\frac{1}{K_L}\right]\frac{q_e}{C_e} \qquad (7)$$

$$\text{IV} \quad \frac{q_e}{C_e} = K_L q_m - K_L q_e \qquad (8)$$

Among the four linear forms which will result in different parameter estimates, type I is one of the most popular the fitted equation used in literature. Hence by plotting C_e/q_e against C_e it is possible to obtain the value of the Langmuir constant K_L (K_L is related to the adsorbent-adsorbate affinity) and q_m.

The Langmuir theory is a basic assumption, that adsorption occurs on the surface containing the adsorbing sites is a perfectly flat plane with no folds and each site can hold at most one molecule of Adsorbent (mono-layer coverage only). Also, assumptions including there are no interactions between adsorbate molecules on adjacent sites; dynamic equilibrium there is between the adsorbed molecules and free molecules, and all sites are equivalent [25]. In brief, the Langmuir adsorption model ignores adsorbate-adsorbate interactions and fails to account for the surface roughness of the adsorbent. Despite this, many adsorption processes can be described using the Langmuir model, such as the interaction of methylene blue or lead with chemical activated carbons [26], or the adsorption of nitrobenzene on several zeolite types [27].

Freundlich model. The Freundlich isotherm describes heterogeneous surface adsorption. The energy distribution for adsorptive sites in Freundlich isotherm follows an exponential type function that is close to the real situation. The rate of adsorption/desorption varies with the strength of the energy at the adsorptive sites. The Freundlich non-linear equation is expressed as:

$$q_e = K_F C_e^{1/n} \qquad (9)$$

where K_F and n are the constants, which measure the adsorption capacity and intensity, respectively.

The linear form of the Freundlich isotherm is:

$$lnq_e = lnK_F + \frac{1}{n} lnC_e \qquad (10)$$

Plotting $\ln q_e$ against $\ln C_e$, the Freundlich constant (K_F) and n can be determined. A higher n value suggests the non-linearity of the data while an n value above 10 indicates that the adsorption process was irreversible [28]. The K_F constant relates to the effectiveness of adsorbents to adsorb

compounds. High values of K_F indicate larger capacities of adsorption. The constant *n* is a function of the strength of the adsorbent and indicates the favorability of adsorption determined (an *n* value above 10 is related to a non-reversible adsorption process [29]). It is generally stated that the values n in the range of 2–10 represent good, 1–2 moderately difficult and 1 poor adsorption characteristics [30].

Many adsorption processes can be described using the Freundlich model, such as the extraction of diclofenac from aqueous solutions using graphene oxide aerogel [31], the efficiency of natural zeolites for remove ammonium from water [32], or the adsorption of methylene blue by using magnetic metal-organic frameworks [33].

In all cases, Freundlich isotherms described adsorbent-adsorbate interactions on mesoporous or macroporous solids with weak attractive forces. This weakness causes a small uptake in the beginning, but once a molecule has been adsorbed, the adsorbate-adsorbate forces will promote the adsorption of further molecules.

Temkin model. Temkin isotherm, useful for chemisorption processes, takes into account the effects of indirect adsorbate-adsorbate interactions on adsorption, and suggests that the heat of adsorption of all the molecules in the layer would decrease linearly with coverage due to these interactions by ignoring the extremely low and large value of concentrations [34, 35]. Mathematically, it is described by the equations:

$$q_e = \frac{RT}{b} ln(AC_e) \qquad (11)$$

$$q_e = \frac{RT}{b} lnA + \frac{RT}{b} lnC_e \qquad (12)$$

where q_e is the amount of adsorbed substance per unit weight of adsorbent ($mg \cdot g^{-1}$), C_e is the amount of unabsorbed substance concentration in solution at equilibrium ($mg \cdot L^{-1}$), R is the gas constant, T is the temperature (K), and *A* and *b* are the Temkin constants which characterize the adsorption capability and energy of adsorption, respectively [36].

Many solid-liquid processes can be described using the Temkin isotherm, as the multicomponent adsorption isotherms of BTEX (benzene, toluene, ethylbenzene, and xylenes) onto zeolites [37], the sorption of Eu(III) on activated carbon [38], or the adsorption of TCP (2,4,6-trichlorophenol) with activated carbon in aqueous solutions [39]. In all cases, Temkin isotherm corresponds to adsorbents with a high surface area and highly developed porosity.

1.3. Adsorbents: Optimization and design of adsorption systems

One of the advantages of the adsorption process is the possibility to use different solid adsorbents. Many times, the adsorption materials are thermally stable and easy to prepare while, usually, the adsorption process is simple to design and operate. In addition, the process does not produce redundant side-products and the solid materials can be regenerated by desorption, being, therefore, a reversible technique, so it is considered a technology that is not aggressive with the environment [40]. Typical requirements for commercial adsorbents are following [41]:

- High porosity and accessible internal surface.
- High adsorption efficiency in a wide range for adsorbate concentrations.
- Good balance between macro-pores (for fast internal transport) and micro-pores (for large internal surfaces).
- Hydrophobic chemical structure (for treatment of moist gases) unless the adsorbent is to be used as a desiccant.
- Thermal stability is unaffected by cyclic regeneration.
- Mechanical integrity during handling.
- Low-pressure drop over the adsorber bed.
- Low cost for acquisition (and, eventually, disposal) of adsorbents.

During the last few years, several reviews have appeared on water and wastewater treatment where adsorption technology has been adopted [42]. In one such study, Wang [42] reviewed the use of natural zeolites and their modified forms for various water pollutants and concluded that natural zeolites were very good adsorbent. However, these zeolites showed varying ion selectivity and competitive adsorption for a multicomponent system. Besides this, cationic surfactant could change the surface charge of natural zeolite, making them more suitable for the adsorption of anions and organics.

Different types of solid materials using in the separation process are classified into natural and synthetic adsorbents. Natural adsorbents include charcoal, clays [43], clay minerals, zeolites [32, 37] and ores. These natural materials, in many instances, are relatively cheap, abundant in supply and have significant potential for modification, and ultimately enhancement of their adsorption capabilities. Many synthetic adsorbents are prepared from waste, sewage sludge, silica, magnetic, metal oxide nanomaterials and polymeric adsorbents. Both natural and synthetic adsorbents are used in the removal of heavy metals, dyes, and organic compounds from water. Carbon-based adsorbents have been widely used to remove organic contaminants (see Fig. 2) from water and wastewater in

industrial-scale applications [44] while, till the present time, an only a small amount of reports focusing on pharmaceuticals and dyes removal from wastewater using alternative approach [45].

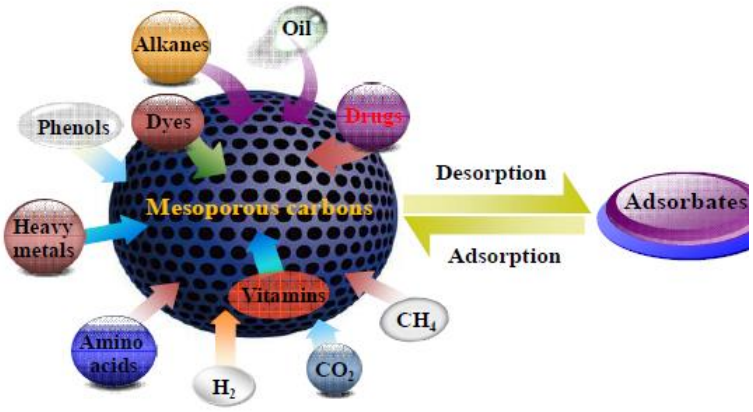

Fig. 2. Schematic diagram show the use of mesoporous carbons as sorbents [41].

The behavior of each adsorbent depends mainly on both their chemical composition and their accessible surface, affected by the presence of pores, edges, corners, cracks, and structural defects. Depending on the long-distance structural order, the adsorbents can be classified as amorphous or crystalline. Generally, the amorphous materials are characterized by high specific surface area (200-1000 $m^2 \cdot g^{-1}$) and very wide pore size ranges, while in the crystalline adsorbents the dimensions of the micropores are determined by the crystal framework and, therefore, the pore size distribution is narrow, while its specific surface area is usually not very high. Less important is the chemical nature of surfaces: polar (hydrophilic) or non-polar (hydrophobic). Water is a polar molecule very strongly adsorbed due to electrostatic forces onto hydrophilic adsorbents. In counterpart, is weakly adsorbed on any non-polar surfaces. Therefore, to remove contaminants from the aqueous environment it is better to carry them by adsorbents with hydrophobic functional groups. Activated carbon and many polymers are hydrophobic, while inorganic adsorbents are usually hydrophilic.

1.4. Carbon-based adsorbents

Carbonaceous material primarily consists of carbon element. Carbon has an atomic number of 6 and its ground-state electron configuration is $[He]2s^2 2p^2$. Like some other p-block elements (e.g., P, S, Sn), solid elemental carbon exhibits the phenomenon of allotropy (i.e., occurrence of the element in different forms that vary in structure and equation of state). Although other approaches have been used to justify the occurrence of different structures for this element in solid form, the hybridization

concept provides a very intuitive explanation and is very useful for classifying carbon-based solids. In this approach, one of the s electrons can be promoted and hybridized with different numbers of p orbitals to give rise to three types of hybrid orbitals: sp^3, sp^2, and sp. These are at the origin of the three basic carbon structures, respectively, diamond, graphite, and carbynes.

Graphite carbon is categorized into non-graphitic (without any measurable crystallographic order) and graphitic carbons (with measurable crystallographic order). Graphitizable carbon is soft, non-porous and has a high density. The microstructures of graphitizable carbons are arranged in preferential direction. Meanwhile, non-graphitizable carbon is hard, porous and has a low density. It also has very disordered microstructures.

Presence of heteroatoms (atoms except carbon such as hydrogen, oxygen, nitrogen, phosphorus and sulphur) on the surface of carbon materials usually used to determine its chemical properties. The presence of these atoms will influence its type and quantity. This occurred during the introduction of activating agent or by nature of the starting raw material. The heteroatoms and delocalized electron of the carbon on the surface of the carbon materials will form certain functional groups that will defined the chemical properties of it surface whether acidic or basic.

Carbon is an amazing element, not just because it is the element required for all life processes, but also due to the fact that it can exist in numerous allotropic forms. Additionally, by means of synthetic processes, carbon can be tailored into a myriad of structures, particularly those in the nanometre range [46]. Generally, different carbonaceous materials have various structures (specific surface area, pore size) and surface chemical properties (function groups, hydrophilicity, hydrophobicity) [47].

The groups that present on the surface (edge or outer surface of the activated carbon) which contains oxygen atoms usually related to the acidic surface properties. Concentration of the oxygen atoms on the surface plays an important role as these atoms really influenced the adsorption capability of the carbon itself. Carbonyl, carboxylic, chromene, ether, lactone, phenol, pyrone and quinone groups are the examples of the functional groups that contain oxygen which can be detected on the surface of the carbon. In addition, the basic characteristic of the carbon surface basically related with the presence of nitrogen atom that has ability to bind with protons and π-electrons resonance of carbon aromatic rings that attract protons.

Some outstanding properties make carbon materials advantageous over other proposed materials, such as zeolites or MOFs: low heat of adsorption (easy of regeneration), hydrophobic character (low

sensitivity to moisture conditions) or the possibility of been obtained through low-cost processes from different types of biomass and lignocellulosic waste [48].

There are varieties of approaches for the preparation of carbon materials, such as directly carbonizing from organic precursors, physically or chemically carbonizing from carbon, template methods using zeolites and mesoporous silica, solvothermal and hydrothermal methods with elevated temperature, the electrical arc methods, and chemical vapor decomposition (CVD) methods.

The carbon-silica composites (CSCs) are usually prepared by filling the carbon containing precursor chemicals into the mesopore silica followed by carbonization. The obtained CSCs are good candidates for VOC adsorption because of their large surface area, controllable pore size distribution, as well as high ignition temperature. The embeddedness of carbon into mesopore silica can reduce the large pores into micropore and shorten the diffusional path, both of which are contributed to VOC adsorption.

1.4.1. Ordered mesoporous carbons

Ordered mesoporous carbon (OMC) is synthesized for the first time by Ryoo et al. [49], who impregnated the carbon precursor into ordered mesoporous silica followed by carbonization and template removal. Some severe disadvantages of this method, such as need hard template, incompatibility between the template removal method and objective materials, and low synthesis efficiency, provoke the development of more effective self-assembly methods, which use low-molecular-weight resol as carbon source, silica as a triblock copolymer, and surfactant as a structure-directing agent.

The first hard templated ordered mesoporous that were synthesized used MCM-48 mesoporous silica molecular sieves as a template. The resulting replicated mesoporous carbon CMK-1 exhibited porous structures consisting of two disconnected interwoven three-dimensional pore systems. In a similar manner, a well-defined hexagonally ordered mesoporous carbon denoted CMK-3, was synthesized by using SBA-15 mesoporous silica as a template. Next to the sucrose solution, as in the original paper, also furfuryl alcohol or other carbon precursors such as glucose, xylose, acenaphthene, indene, *etc.* were impregnated in the silica template via the incipient wetness technique. Therefore, an amount of precursor solution equal to the total pore volume of the template is added. It is believed that the whole solution infiltrated the pores through capillary action. The carbon precursor was typically polymerized by means of a sulfuric acid catalyst and subsequently

carbonized under inert conditions. The silica template can be removed either under basic conditions or using of HF. Unfortunately, in all of the above-mentioned methods; the incipient wetness technique was unsuccessful to fill the pores uniformly due to the difficulty to homogenize a powder. Also, pore-blocking occurs upon subsequent impregnations of a precursor solution via the wet impregnation method. To obtain a high surface area, no carbon precursor must be deposited outside the template because this would lead to external carbon upon calcination. [50].

The synthesis and application of ordered mesoporous carbons with a variety of structures, e.g., CMK-1, CMK-3, and CMK-5, have attracted considerable attention. These ordered mesoporous carbons have been synthesized by carbonizing mesoporous silica materials, such as MCM-48, SBA-15, and KIT-6, and then by removing the silica template. Ordered mesoporous carbon is expected to have extensive potential in a range of applications because of the uniform pore size, large specific surface area, and large pore volume. These materials are considered to have a potential for applications to other fields, such as heterogeneous catalysis and host-guest chemistry. In particular, CMK-3, based on SBA-15, which is easy to synthesize, is expected to be useful not only as an adsorbent but also as a catalyst substrate [51].

1.4.2. Biochars: A cost-effective technology for air/water treatment

Biochar, a stable carbon-rich by-product synthesized through carbonization of biomass in an oxygen-limited environment has been recognized as a multifunctional material for energy and environmental applications. Bio-char is currently being used as a soil amendment and to sequester carbon in the soil [52]. Furthermore, biochar can also be used as an efficient adsorbent for environmental-contaminant removal [53]. The chemical and physical properties of biochar mainly depend on feedstock types and pyrolysis conditions i.e., residence time, temperature, heating rate, and reactor type [54]. Conventional carbonization (i.e. slow pyrolysis), fast pyrolysis, flash carbonization, and gasification are the main thermochemical processes that are widely employed for biochar production. In general, biochar produced at high temperatures (600-700 °C) shows a highly aromatic nature with well-organized C layers but has fewer H and O functional groups due to dehydration and deoxygenation of the biomass potentially with lower ion exchange capacities. On the other hand, biochar produced at lower temperatures (300-400 °C) has more diversified organic characters, including aliphatic and cellulose type structures, and contains more C=O and C-H functional groups.

The complex and heterogeneous chemical and physical composition of biochar provides an excellent platform for contaminants removal through sorption. In spite of considerable scientific work on the uses of biochar for environmental uses, extensive attention has recently been focused on the modification of biochar with novel structures and surface properties in order to enhance its remediation efficacy and environmental benefits [55].

Producing activated carbon from lignocellulosic biomass has many advantages: the precursors are diverse, abundant, and renewable; the synthesis is a process relatively simple due to the high reactivity of the biomass, and it contributes to decreasing costs of waste disposal and the negative impact to the environment.

1.4.3. Activated carbons

Activated carbon (AC) is a traditional carbonaceous material widely used in many fields for its high surface area, excellent porous structure, tunable surface property, and low cost [56, 57]. Activated carbon is known as a black solid containing a major portion of fixed carbon content, and other minor contents such as ash, moisture, and volatile matter; it also has physical characteristics such as density, surface area, and pore volume. AC is produced from carbon-rich materials such as coal [58], acid-char [59], agricultural residue [60], peat, lignite, petroleum pitch, wood, nutshells, biodiesel solid [61], etc. by the processes of carbonization and activation.

The traditional activated carbons, however, suffer from limited interconnectivity between micropores and irregular and defective pore structures which serves to inhibit mass transfer efficiency and limit diffusion kinetics, ultimately restricting molecular access to the adsorbent surface. Nowadays, novelty functionalized adsorbents such as MCs achieved wide increasing attention for the burgeoning technology like adsorption.

Basically, there are two different processes for the preparation of activated carbon, physical and chemical activation.

In physical activation, the first step is the carbonization of the raw material. After carbonization, the charcoal obtained will be activated using oxidizing gases at high temperatures (commonly, 500 ºC to 1000 ºC). In activation process, the oxidizing gas removes more reactive carbon species forming pores and vessels.

In general, the formation of pores by activating gas consists of three phases which are opening of previously inaccessible pores, new pore formation and lastly broadening of existing pores. Below are the reactions that might take place during the activation using different types of activating agent:

Oxygen:

$$C + O_2 \rightarrow CO_2$$

$$2C + O_2 \rightarrow 2CO$$

Carbon dioxide:

$$C + CO_2 \rightarrow 2CO$$

Steam activation is obtained when the initial pyrolysis reactions, occurring in an oxygen-free atmosphere at moderate temperatures (400-800 ºC), are complemented by a second stage in which the resulting biochar is subjected to partial gasification with steam. This promotes partial devolatilization and crystalline-C formation in biochar. Steam application may change the properties of biochar by removing the trapped products of incomplete combustion during thermal treatment. Typical reactions of the steam activation involve an initial exchange of oxygen from the water molecule to the carbon surface site C(f) to create a surface oxide C(O) and H_2 gas, and the produced H_2 may react with the C surface to form surface hydrogen (H) complexes [C(H)]:

$$C(f) + H_2O \rightarrow C(O) + H_2$$

$$2\ C(f) + H_2 \rightarrow 2\ C(H)$$

$$CO + H_2O \rightarrow CO_2 + H_2$$

Steam oxidizes the C surface sites generating H_2 and CO_2 which may activate the surface of biochar and inhibit the gasification reaction of C sites.

Additional syngas in biochar after pyrolysis may be liberated during the steam activation process in the form of H_2 increasing the surface area and pore volume. The steam activation process increases the sorption capacity by increasing the surface area of the biochar.

The chemical modification process involves both a one-step modification and a two-step modification process. The carbonization and activation steps are achieved simultaneously during one-step chemical activation in the presence of an activating chemical agent. Two-step chemical activation involves carbonization of raw feedstock followed by activation of the carbonized product by mixing with a chemical agent or pretreatment of precursors before the carbonization process.

In chemical activation, the starting material is impregnated with a chemical agent, and the impregnated material is heated for carbonization in an inert atmosphere. The chemical agents help to develop the activated carbon porosity using dehydration and degradation. After impregnating the

precursor by chemical agent and heat treat-men to the mixture, the impregnating agent and its salts are removed by washing with acid/base and water, which makes the pore structure available in activated carbon. The advantages of the chemical activation process are lower activation temperatures (lower operating and energy costs), shorter activation times, a single activation step (simultaneous carbonization-activation), higher activated carbon yields, a large surface area, and well-developed microporosity. Among the disadvantages are the cost of the activating agents, the need for intense washing to remove process-generated impurities, and general process corrosiveness [62].

Treatment by chemical modification is generally carried out by the addition of acids or bases. In addition, intentional oxidation using hydrogen peroxide (H_2O_2), potassium permanganate ($KMnO_4$), ammonium persulfate [$(NH_4)_2S_2O_8$] and ozone (O_3) has been used to modify surface functional groups.

Phosphoric acid is one of the most commonly used activating agents for chemical modification and is more environmental-friendly than other corrosive and hazardous reagents. Phosphoric acid can decompose lignocellulosic, aliphatic, and aromatic materials while forming phosphate and polyphosphate cross bridges to avoid shrinkage or contraction during porosity development.

Other mineral acids, such as HNO_3, H_2SO_4, or HCl, have also been widely used for the modification of carbon materials. The oxidation with HNO_3 treatment has been shown to cause degradation of the micropore wall due to its erosive nature, resulting in a decrease in total surface area. Similarly, H_2SO_4 treatment resulted in a decrease in the porosity of biochar from 10 to 40% and improved the size distribution of heterogeneous micropores. Dehydration of H_2SO_4 during pyrolysis could be detrimental to the development of surface area due to excess water vapor movement towards the surface structure.

The dissociation of HNO_3 forms highly active intermediate nitronium ions that react with the aromatic rings and turn into nitrated products ($-NO_2$) on the biochar surface. Since the nitration of aromatic surfaces is limited by the slow rate of nitration and small quantities of NO_2^+, simultaneous addition of concentrated H_2SO_4 is necessary to facilitate the formation of nitronium ions. The nitration is believed to take place via electrophilic aromatic substitution which introduces nitrogen groups on aromatic rings in biochar. The nitro-groups are subsequently reduced to amino groups on the surface by using sodium dithionite ($N_2S_2O_4$) as a reducing agent. Surface amination results introduction of amino groups which provide basic properties and strong affinities to pollutants [63].

Organic acids such as oxalic enhance the sorption of pollutants through ligand- and proton-promoted processes. Although pretreatment with 10% H_2SO_4 at 60 ºC was observed to impose a little effect on C and O contents, a combined treatment of 30% H_2SO_4 and oxalic acid demonstrated a 250-fold increase of surface area compared to the unmodified biochar [64]. Also reported that the modification of wheat straw-derived biochar with HCl introduced more heterogeneous pores than the unmodified ones [65].

In general, it is recognized that treatment with strong acids can introduce acidic functional groups such as amine, carboxylic groups onto the carbonized surface.

Alkali activation of biochar using potassium hydroxide (KOH) or sodium hydroxide (NaOH) can increase the O content and surface basicity while dissolving ash and condensed organic matter (e.g., lignin and celluloses) to facilitate subsequent activation (Figure 3) [66]. A two-stage KOH activation process of precarbonized precursors could produce a larger surface area with additional surface hydroxyl groups.

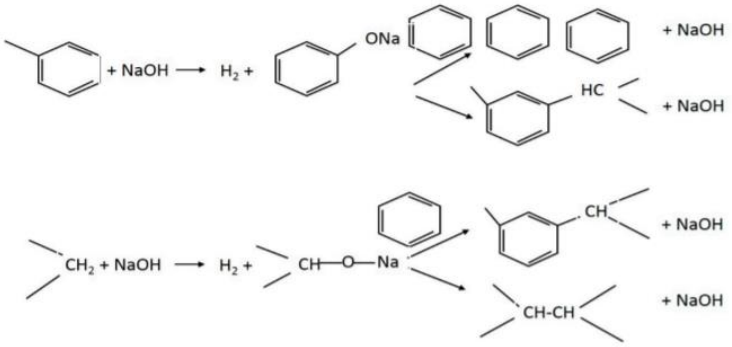

Fig. 3. Scheme of carbon activation by sodium hydroxide [67].

Potassium species (K_2O, K_2CO_3) may be formed during activation as a result of K^+ intercalation in the layers of the crystallites that form the condensed C structure. These species may diffuse into the internal structure of the biochar matrix widening existing pores and creates new pores of the product [68].

H_2O_2 oxidation has been increased the amount of carboxyl groups on biochar surfaces and provided an additional cation exchange site for surface complexation with metals.

Carboxylic group modifications can also be accomplished by using water-soluble carbodiimides and esterification via acidic methanol. The use of acidified methanol for carboxylic modification is inexpensive. The chemical reactions involved in methanol modification are esterification and then direct reaction between the carbonyl groups of biochar with methanol [69].

Generally, chemical oxidation using HNO_3, $KMnO_4$, H_2O_2, H_3PO_4, or HNO_3/H_2SO_4 mixture can introduce acidic functional groups such as carboxylic, carbonyl, lactonic, and phenolic groups on the C surface at relatively low temperatures.

Chemical modification of biochar may enhance its contaminant sorption ability by creating additional and abundant sorption sites on increased surface areas, rendering biochar surface more conducive to electrostatic attraction, surface complexation, and/or surface precipitation, as well as enabling greater sorption affinity through stronger interactions with specific surface functional groups. In general, physical modification methods are usually simple and economically feasible but are less effective than chemical modification methods.

1.4. Magnetic nanomaterials as adsorbents

Magnetic nanoparticles (MNPs) such as zero-valent nanoparticles, magnetite (Fe_3O_4), maghemite (γ-Fe_2O_3), or cobalt oxide (Co_3O_4) are of the most popular materials in analytical chemistry, medicine, removal of inorganic and organic compounds, and biotechnology due to the advantages of easy control and simple separation [70]. Although pure metals nanoparticles have favourable magnetic properties, their high toxicity and oxidative sensitivity make them unsuitable for aggressive medium and biotechnology (Fig. 4). It is believed that MNPs exhibit the finite-size effect or high ratio of surface-to-volume, resulting in a higher adsorption capacity for metal adsorption [71].

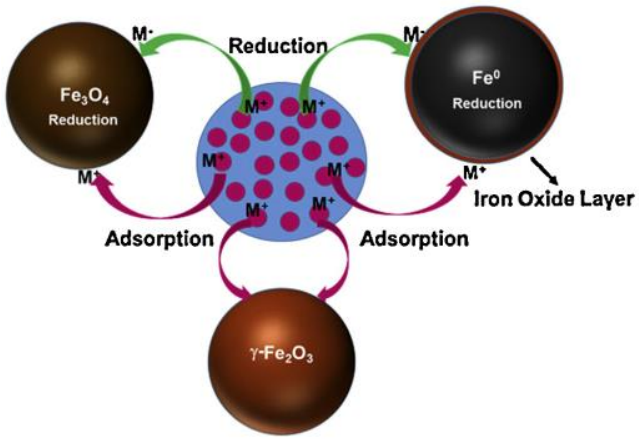

Fig. 4. Adsorption and reduction potential toward pollutants of the MNPs [71].

According to their different magnetic properties, materials are divided into three types: paramagnetic, antimagnetic, and ferromagnetic. Paramagnetic materials, whose magnetization

intensity is proportional to the exterior magnetic field and their susceptibility is a positive value. Antimagnetic materials, whose magnetization intensity also is proportional to the exterior magnetic field, but their susceptibility is a negative value. The magnetization intensity of ferromagnetic materials increases with the strengthening of the exterior magnetic field observably at the beginning, but when the exterior magnetic field intensity increases to a value, their magnetization intensity will not continue to increase, which is the saturation phenomenon (Fig. 5). Also, some particles have the phenomenon of superparamagnetism (on the application of an external magnetic field, they become magnetized up to their saturation magnetization, and on the removal of the magnetic field, they no longer exhibit any residual magnetic interaction) [72, 73].

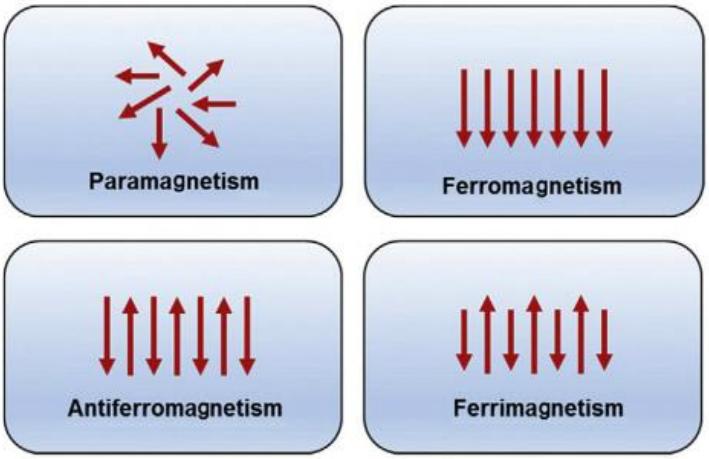

Fig. 5. Schematic illustrating the dominant magnetic moment in MNPs [70].

Fe_3O_4 nanoparticles have attracted particular interest in separation science as adsorbent because they can be easily isolated using an external magnetic field placed outside of the extraction container [74, 75]. Fe_3O_4, an MNPs has the cubic inverse spinal structure (with ratio Fe^{3+}: Fe^{2+}=2 : 1) in which oxygen forms a face-centered cubic closed-pack structure [12]. It is an important class of half-metallic materials, as electrons hop between Fe^{2+} and Fe^{3+} [76]. Fe_2O_3 possesses ferrimagnetic properties in bulk with high magnetization saturation (Ms) of 92 $emu \cdot g^{-1}$ at room temperature and high Curie temperature (Tc) of 577 °C. The particle size and its effect on the specific surface area greatly influence the physical and chemical characteristics of the magnetic particles. Decreasing the particle size to the nanoscale increases its active sites and consequently reduces the total mass required for treatment [77, 78]. The magnetic properties of nanoparticles are governed by their particle size. When the size of ferrimagnetic Fe_3O_4 nanoparticles is sufficiently small, they possess superparamagnetic properties with a large response to the applied magnetic field. In general, Fe_3O_4

nanoparticles with a diameter below the threshold of 20 nm exhibit superparamagnetic properties, and the name is superparamagnetic iron oxide nanoparticles (SPIONs) [79]. At a 10-20 nm size, the nanoparticles do not exhibit multiple domains as in large magnets. They become a single magnetic domain and act as a "single super spin" that exhibits high magnetic susceptibility [80]. Compared with atomic or larger-scale systems, nanoscale materials have shown better physical and chemical properties due to their mesoscopic effect, small object effect, quantum size effect, surface effect, etc. [81, 82]. It was shown that the removal capacity of 8 nm magnetite nanoparticles was about seven times higher than that of 50 nm particles [78]. In the study [83], the reactivity of iron nanoparticles increased by 50–90 times when the particle size was reduced from 500 to 100 nm. Although effective removal capacity can be achieved using porous structures particles with large surface [84].

1.5.1. Methods for the preparation of magnetic nanoparticles

In the last time, a significant amount of researches has been devoted to synthesize Fe_3O_4 nanoparticles in order to achieve proper control over their particle size, shape, crystallinity, as well as magnetic properties (Fig. 6) [85]. The magnetic particles have been synthesized via three categories of methods: physical, chemical, and biological methods. The biological methods have good reproducibility and high yield, but through their slow and laborious use rarely [86]. The physical methods belong to such methods as the aerosol-based synthesis [87], laser induced pyrolysis method for manufacturing Fe-based nanoparticles [88], electron beam lithography for synthesizing cylindrical nanoparticles [89], and ball milling method for the synthesis of iron nanoparticles [90]. In general, physical methods are exact and easy to execute. However, these methods are incapable of controlling the particle size within the nanoscale or require expensive and highly complex machines.

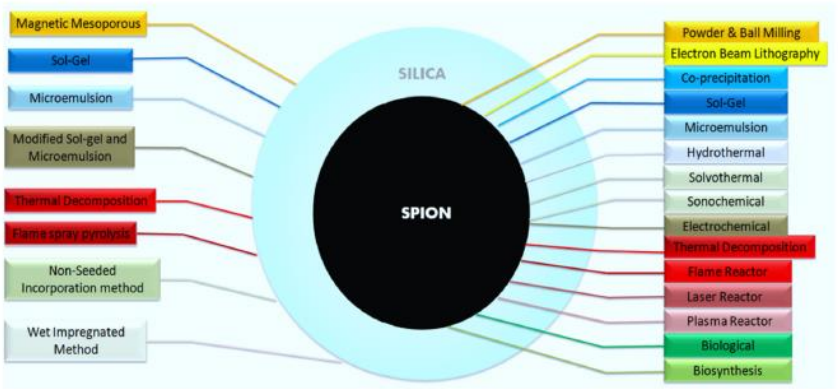

Fig. 6. The various methods of producing superparamagnetic iron oxide nanoparticles (SPIONs) and its surface modification with silica layer [91].

Compared to physical and biological ways, chemical way has the advantages in synthesizing new materials with better chemical homogeneity by modifying the combination of precursor, and well controlling the size, shape and composition of nanoparticles. In addition, the chemical route is a time-saving, simple, reproducible, and cost-effective technique for synthesizing nanoparticles as it does not require expensive equipment and chemicals. However, there are some drawbacks such as the formation of surplus intermediates and impurities, as well as the risk of colloidal agglomeration happening during the synthesis process. Nowadays, there are various chemical methods for the synthesis of MNPs [92].

Pyrolysis method. Magnetic micro/nanoparticles can also be prepared by the thermal decomposition of precursors such as metal compounds ($FeAc_3$, $Fe(CO)_5$, $Co_2(CO)_8$; where Ac are acetyl acetone) at high temperature and high pressure. Then they are further oxidized to magnetic metal oxide nanoparticles. The method has the advantages of high nanoparticle crystallinity, tunable size, and narrow diameter distribution.

Hydrothermal method. The hydrothermal method is that under high temperature and pressure conditions of autoclave, with water as reaction medium, those substances, which are usually sparingly soluble and insoluble, are dissolved and react, then recrystallize, thus getting the ideal product. High temperature is beneficial to improve magnetism, and high pressure is good to improve product purity. The hydrothermal method can control the size and shape of particles effectively, and particles seldom agglomerate. Besides, the particles have good dispersibility and uniform size distribution.

Solvent-thermal method. The solvent-thermal method is similar to the hydrothermal method, except the solvent of the former is a non-aqueous solution.

Sol-gel method. The sol-gel method is frequently performed by preparing sol with a metal-organic compound solution or metal inorganic compound at first, and then the sol is dehydrated under certain conditions (heating) to get gel, at last, the nano-scale product is prepared with the gel after drying and roasting. This method has the advantages of mild reaction conditions, high product purity, accurate stoichiometry, simple process, and a short reaction period, and usually used to prepare the core-shell SiO_2 magnetic composites.

Micro-emulsion method. The micro-emulsion method has been developed into an effective method of preparing magnetic microparticles. The micro-emulsions are transparent, isotropic, and low viscosity thermodynamic stability system, which is made from oil (hydrocarbon), water (electrolyte aqueous solution), and surfactant (sometimes with alcohols as cosurfactant.). They are divided into the water in oil type (W/O) and oil in a water type (O/W). The droplet size of them is nanometer and the droplet separates from each other. The reaction space is limited to this micro-reactor – droplet. This method can make particles avoid agglomerating effectively, so it is easy to prepare magnetic microparticles with a narrow particle size distribution, regular shape, and good dispersion property.

Sonochemical method. The ultrasonic vaporization bubble produced by an ultrasonic wave can make local high temperature and high-pressure environment come into being and has micro-jet with strong impulsive force, which promotes oxidation reaction, reduction reaction, decomposition reaction, hydrolysis reaction, and so on for preparing micro/nanoparticles. The application of ultrasonic technology, there not being special requirements to the properties of this system, only requests for liquid medium for energy transmission and has strong universality to all kinds of the reaction medium. Compared with conventional stirring technology, the ultrasonic cavitational effect produces shear action on agglomeration, which is beneficial to form small particles, and it makes the uniform mixing of medium easier to be realized, avoiding inhomogeneous local concentration, improving reaction rate.

Emulsion polymerization. Emulsion polymerization is that with mechanical stirring, monomers disperse in water to become emulsion under the effects of emulsifier, then polymerize initiated by initiator. At least, the emulsion polymerization system is composed of monomer, initiator, emulsifier, and water [74].

Co-precipitation method. Co-precipitation method is one of the most widely used and cited methods. In this method, alkaline solution (ammonia, sodium, hydroxide solution) is added into metallic salt solution as precipitant, making metal ions precipitate from the solution:

$$Fe^{2+} + 2\ Fe^{3+} + 8\ OH^{-} \rightarrow Fe_3O_4\downarrow + 4\ H_2O$$

This method has the advantages of shorter process, simple reaction conditions and higher product purity. But the agglomeration phenomenon of product will happen easily during washing, filtering and drying [93].

1.5.2. Surface modification of magnetic nanoparticles

MNPs utilization for practical application still requires rectification of several parameters, broadly categorized into three main class: (a) their tendency to get aggregate in order to reduce their surface energy and (b) their ability to get oxidize easily, and (c) their non-selectivity. The aforementioned parameters can hamper their interfacial area, thereby hindering their magnetism and dispensability [94]. MNPs are extremely reactive with oxidizing agents, particularly with air. For the complete and permanent protection from oxidizing, each MNP is covered with a thin covering that has little or no impact on the magnetic property of MNPs, different coating materials are used for this purpose, i.e., gold and silica, but these coatings weaken the magnetic properties. However, it is often necessary to coat the particles with another material or embed them in a magnetic matrix, in order to prevent their agglomeration, sedimentation, and selectivity, to make them useful for MSPE applications.

A modification to the MNPs can prevent agglomeration, thus increasing its dispersion and protection from oxidizing resulting in broader opportunities for application. The magnetic cores are usually coated with inorganic materials, polymers, and/or functionalised with organic and biological molecules [95]. Modified MNPs have been proven to possess unprecedented advantages over traditional nanoformulations and the fabrication is simple, scalable, cost-effective, and controllable.

The silica has allocated a special place to itself because of its unique properties such as chemical stability, biocompatibility, strong affinity toward magnetite, and reactivity with various coupling agents [96]. Thanks to the flexible processing of silica chemistry, the surface of MNPs modified with different functional groups, such as hydroxyl (OH), carboxyl (COOH), phosphonate (CH_3HPO_2), poly(ethyleneglycol) (PEG), and amine (NH_2), can be easily prepared via silane chemistry. The surface functionalization endows the MSNs with different charges and shows great influences on their colloidal behaviors [97].

In the case of surface modification by polymers there is two techniques of functionalization by coating: one-step and multistep coatings. The first technique involves the coating of NPs during the synthesis and the multi-step coating consists on attaching the polymer onto the IONP surface after its synthesis. From the literature, the commonly used polymers are polyvinylpyrrolidone (PVP), chitosan, cetyltrimethylammonium bromide, and tri-sodium citrate. These polymers differ in terms of molecule length, as well as polar head group and charge [98].

1.5.3. Magnetic mesoporous carbons

Polymerization using Co, Ni, and Fe compounds is particularly attractive because these metal elements can be incorporated in the final MCs, thus affording the possibility to prepare MC

materials containing magnetizable metal nanoparticles. On one side, the carbon coating could protect the magnetic nanoparticles, for another, the magnetization parameters can be adjusted by the content of the magnetic source and the carbonization temperatures. These materials containing such magnetic nanoparticles have suitable applications for the development of heterogeneous catalysts and adsorbents that can be separated by a magnetic field after use in the liquid phase. Up to date, there are generally two routes to insert metal nanoparticles into the MCs. One route is incorporating metal nanoparticles into the pre-synthesized MCs using the incipient-wetness impregnation procedure. Another route is infiltration of an appropriate carbon precursor and metal source (Fe, Co, Ni compounds) into the mesopores of the silica template, followed by thermal polymerization, carbonization, and subsequent removal of the silica framework with HF or NaOH solutions. However, these traditional methods are time-consuming and high-cost multi-step synthesis procedures, including repeated impregnation with carbon and metal precursors and the removal of hard templates, which severely hamper the broad applications of the magnetic composite materials.

In the work of [99] has been prepared magnetic mesoporous carbon (Ni-CMK-3) and has been studied its performance for adsorption of an aromatic sulfur compound from liquid samples. The adsorbent was prepared by synthesis of the SBA-15 template, followed by pore-filling with the carbon precursor, carbonization, removing the silica template, and deposition of Ni nanoparticles by impregnation. Adsorption of DBT onto Ni-CMK-3 was found to be suitable at 20% Ni loading, at which the adsorbent retained its mesoporosity and morphology. The adsorbent is easily attracted by a magnet and can be separated from the liquid medium. The kinetic survey suggests that the pseudo-second-order adsorption mechanism is predominant. Langmuir isotherm best represented the equilibrium adsorption data (q_{max} = 62.0 $mg \cdot g^{-1}$). The value of ΔG^o was calculated to be $-18.0\ kJ \cdot mol^{-1}$, indicating that the DBT adsorption by Ni-CMK-3 is a spontaneous and favorable process. This, together with the endothermic nature of the process, gives a positive ΔS^o confirming a high preference of DBT molecules for the adsorbent surface. The spent adsorbent can be reused after regeneration by solvent extraction with toluene.

In the work, the co-precipitation of iron salts onto a mesoporous activated carbon, with NaOH and/or NH_4OH as precipitating agents as well as impregnation of activated carbon with magnetic nanoparticles, led to the preparation of non-magnetic or of a very low magnetic mesoporous activated carbon. For this sample, magnetic activated carbon was successfully synthesized by impregnation with magnetite nanoparticles via sonication. The resulting materials were used for the adsorption of the Reactive Black dye. Equilibrium experiments show that magnetic modification

decreases the adsorption capacity. The data of adsorption isotherms and kinetics were better fitted by the Freundlich isotherm model and the pseudo-second-order kinetic model, respectively. An increase in of temperature increased the adsorption capacity for all impregnated carbons. Thermodynamic analysis revealed that all adsorbents presented negative ΔG^o values showing, positive ΔH^o values indicating the endothermic nature of the process, and positive values of ΔS^o indicating the affinity of the adsorbent towards the adsorbate species. Used carbon samples can be regenerated by thermal treatment [100].

1. Objectives

The principal objective of the present Ph.D. Thesis is to develop methods for the synthesis of materials for removal and pre-concentration of organic contaminants in air/water, with the possibility of using adsorbents in different sample preparation approaches, and compare their effective with commercial sorbents. In order to reach the established goals, the following specific objectives are proposed:

- Synthesis and characterization of new ***magnetic nanocomposites*** combining superparamagnetic Fe_3O_4 nanoparticles functionalized by hydrophobic groups by core-shell structure.

(1) Optimization of key factors on the adsorption efficiency of magnetic nanoadsorbent for organic compounds in aqueous solution.

(2) Experimental design of nanoadsorbent for purification stage of sample preparation procedure (extraction and elution solvents and their volume, sample weight, contact time, comparison with other cleanup adsorbents, reusability (inter- and intraday precision, matrix effect), application of the developed procedure in real matrices).

- Synthesis of granular ***mesoporous ordered carbons*** (MCs) with combination mesoporous silica (MCM-48, SBA-15) as template and sucrose/polystyrene as a carbonaous precursor.

(1) Physical (steam-pyrolysis) and chemical (H_2O_2, HNO_3, etc.) activation of MCs.

(2) Adsorption performance of mesoporous AC towards pharmaceuticals (pH, kinetics, isotherms), regeneration of adsorbents.

- Synthesis and characterization of ***mesoporous spherical carbons*** with combination mesoporous silica (MCM-48) and divinylbenzene/polystyrene as carbon source.

(1) Removal of air pollutants with spherical MCs (extraction solvents and their volume, extraction time, comparison with commercial adsorbents, sorption in dynamic and static modes.

(2) Application as fillers for a smoking room, regeneration of carbon materials.

- Low-cost synthesis and characterization of ***activated carbons*** from low-cost biowaste by-products as raw materials.

(1) Sunflower seed husks by-products generated in power plant industry tested as raw material for ACs;(2) pre-treatment stage (organic solvents, HNO_3, NaOH, etc.) and carbonization procedures for raw materials.

(3) Chemical (HNO_3, NaOH, etc.) activation of carbon materials.

(4) Adsorption performance of low-cost ACs towards dyes in water solutions (adsorption capacities, kinetics, isotherms, pH, and regeneration).

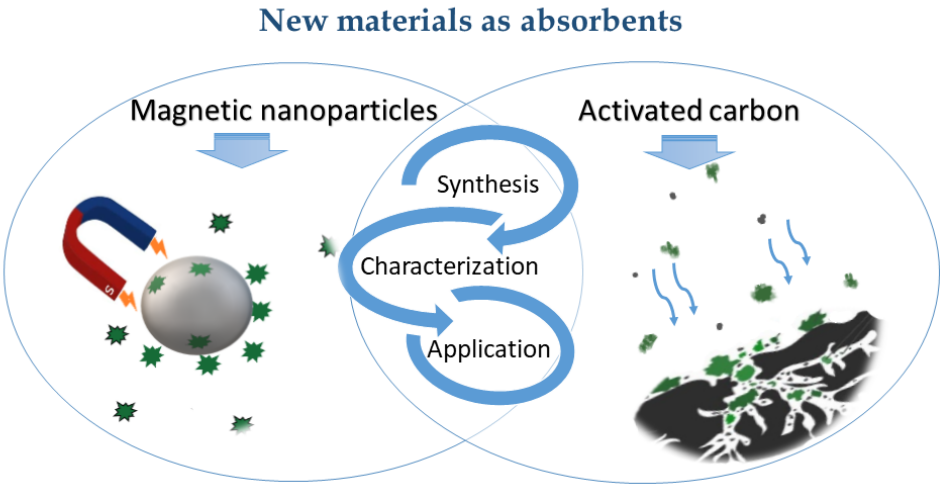

Objetivos

El objetivo principal de la presente Tesis Doctoral es desarrollar métodos de síntesis de materiales para la remoción y preconcentración de contaminantes orgánicos en aire y agua, con la posibilidad de utilizar adsorbentes en diferentes enfoques de preparación de muestras, y comparar su efectividad con sorbentes comerciales. Para alcanzar las metas establecidas se proponen los siguientes objetivos específicos:

- Síntesis y caracterización de nuevos ***nanocompuestos magnéticos*** que combinan nanopartículas superparamagnéticas de Fe_3O_4 funcionalizadas por grupos hidrófobos mediante estructura núcleo-capa.

(1) Optimización de factores clave sobre la eficiencia de adsorción de nanoadsorbentes magnéticos para compuestos orgánicos en disolución acuosa.

(2) Diseño experimental de nanoadsorbentes para la etapa de purificación del procedimiento de preparación de la muestra (disolventes de extracción y elución y su volumen, peso de la muestra, tiempo de contacto, comparación con otros adsorbentes de limpieza, reutilización (precisión inter e intradiaria, efecto matriz), aplicación del procedimiento desarrollado en matrices reales).

- Síntesis de ***carbones ordenados mesoporosos granulares*** (MC) con una combinación de sílice mesoporosa (MCM-48, SBA-15) como plantilla y sacarosa / poliestireno como precursor carbonoso.

(1) Activación física (pirólisis de vapor) y química (H_2O_2, HNO_3, etc.) de los MC.

(2) Rendimiento de adsorción de AC mesoporoso hacia productos farmacéuticos (pH, cinética, isotermas), regeneración de adsorbentes.

- Síntesis y caracterización de ***carbones esféricos mesoporosos*** con combinación de sílice mesoporosa (MCM-48) y divinilbenceno / poliestireno como fuente de carbono.

(1) Eliminación de contaminantes del aire con MC esféricos (disolventes de extracción y su volumen, tiempo de extracción, comparación con adsorbentes comerciales, sorción en modos dinámicos y estáticos).

(2) Aplicación como rellenos para salas de fumadores, regeneración de materiales carbonosos.

- Síntesis y caracterización de bajo costo de ***carbones activados*** a partir de subproductos de residuos biológicos de bajo costo como materia prima.

(1) Subproductos de cáscara de semillas de girasol generados en la industria de centrales eléctricas probados como materia prima para AC.

(2) Etapa de pretratamiento (solventes orgánicos, HNO_3, NaOH, etc.) y procedimientos de carbonización de materias primas.

(3) Activación química (HNO_3, NaOH, etc.) de materiales de carbono.

(4) Rendimiento de adsorción de ACs de bajo costo hacia colorantes en soluciones acuosas (capacidades de adsorción, cinética, isotermas, pH y regeneración).

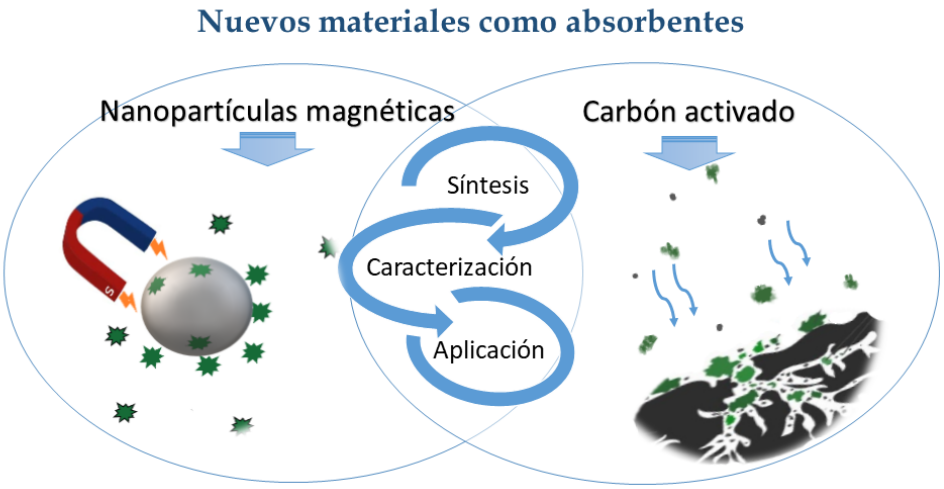

3. Materials and method of characterization

3.1. Chemicals.

Reagents. Tetraethoxysilane (TEOS) and 3-glycidyloxypropyl silane (GTMS) purchased from Aldrich. The Triton X-100 (Merck) in was used as for hydrophobic surface (Fig. 7).

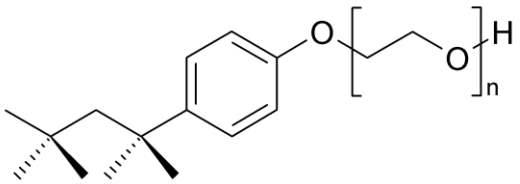

Fig. 7. Chemical formula of Triton X-100 (p-tert-octylphenoxy polyethylene (9.5) ether).

Sodium hydroxide, sulfuric acid 95 wt%, and sucrose 95.5% were purchased from VWR Chemicals. Hydrogen peroxide 30 wt. % and HNO_3 63 wt. % waters solutions were obtained from Aldrich. Divinylbenzene, and ammonium hydroxide (25 %) were obtained from Merck. For strong binding has been used polystyrene (Alfa Aesar, MW-192,000 $g \cdot mol^{-1}$). Inorganic salts such as sodium acetate (NaAc), magnesium sulfate ($MgSO_4$, anhydrous), $FeCl_2 \cdot H_2O$, and $FeCl_3$(anhydrous) were purchased in Sigma-Aldrich.

Solvents. HPLC grade methanol and acetonitrile (MeCN), hexane, ethyl acetate (EtAc), chloroform, acetone, and CH_2Cl_2 were acquired from Sigma-Aldrich.

Analytes. The adsorption properties of the obtained materials were studied using various analytes (Fig. 8). The standard solutions of the pharmaceuticals (tetracycline, oxytetracycline, chlortetracycline, and doxycycline) were purchased from Aldrich.

The standards of pesticides were provided via the Supelco EPA Pesticide Mix (aldrin, α-BHC, β-BHC, γ-BHC, 4,4′-DDD, 4,4′-DDE, 4,4′-DDT, α-endosulfan, β-endosulfan, endosulfan sulfate, dieldrin, endrin, endrin aldehyde, heptachlor, heptachlor epoxide Isomer B) in MeOH/CH_2Cl_2 (98:2) and the EPA 8080 Pesticide Mix (aldrin, α-BHC, β-BHC, γ-BHC, 4,4′-DDT, 4,4′-DDD, 4,4′-DDE, endosulfan α, endosulfan β, endosulfan sulfate, endrin, endrin aldehyde, dieldrin, heptachlor epoxide Isomer B, heptachlor, methoxychlor) in toluene/hexane (50:50).

Octafluoronaphthalene (OFN) and 4,4′- DDT-d8 were both used as internal standards and obtained in Sigma-Aldrich.

Methylene blue (MB) was supplied by Panreac Quimica S.L.U. (Spain).

Organochlorine pesticides

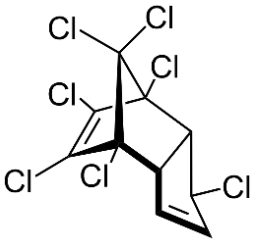

Heptachlor

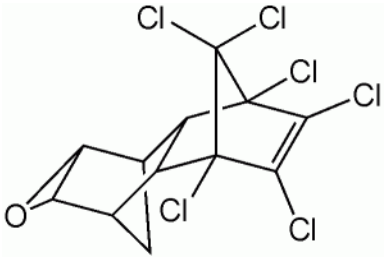

Dieldrin

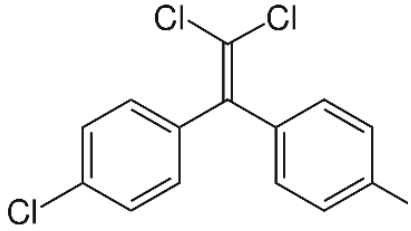

p,p'-DDE

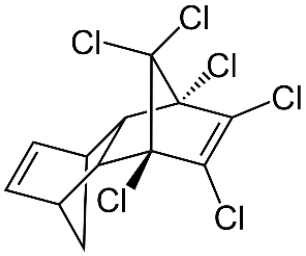

Aldrin

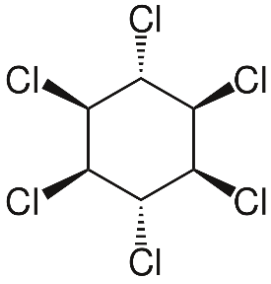

Lindane

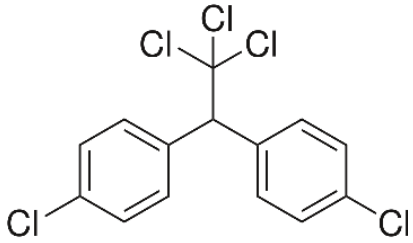

p,p'-DDT

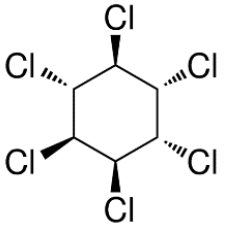

α-HCH

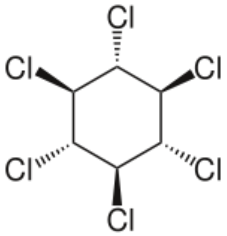

β-HCH

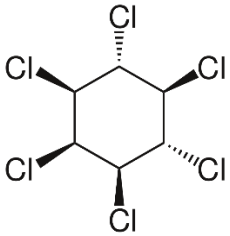

δ-HCH

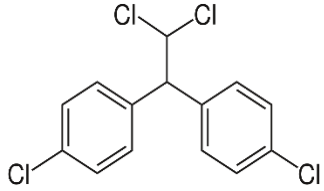

4,4'-DDD

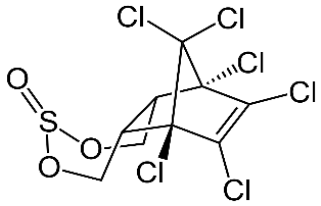

Endosulfan (alpha)

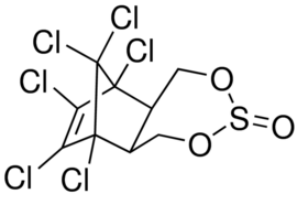

Endosulfan (beta)

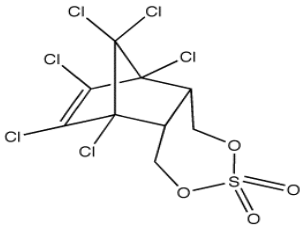

Endosulfan sulphate

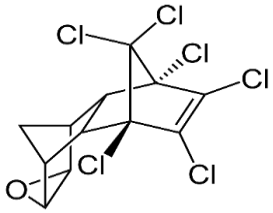

Endrin

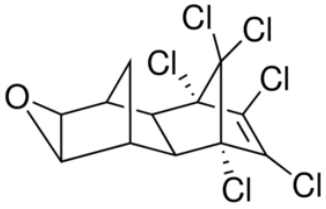

Endrin aldehyde

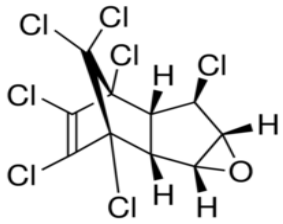

Heptachlor epoxide

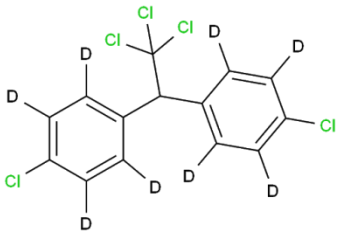

4,4′- DDT-d8

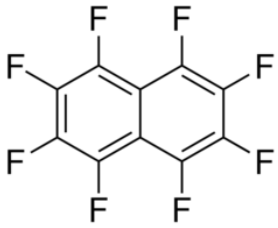

Octafluoronaphthalene

Gaseous pollutants

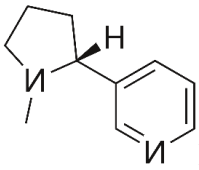

Nicotine

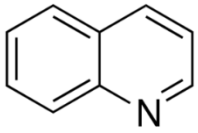

Quinoline

Pharmaceuticals

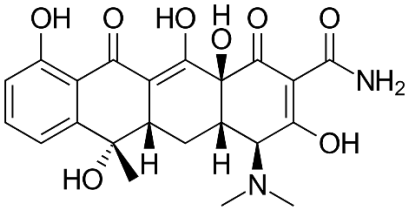

Tetracycline

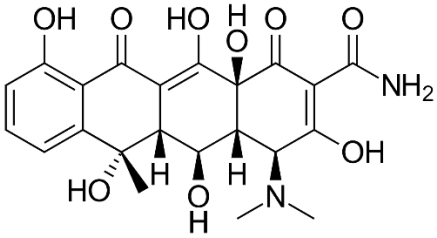

Oxytetracycline

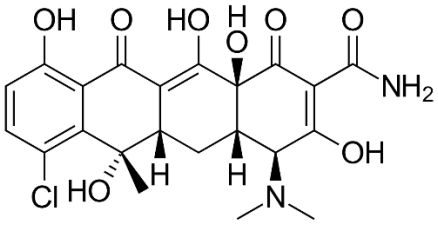

Chlortetracycline

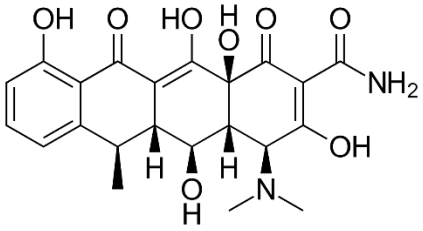

Doxycycline

Organic dyes

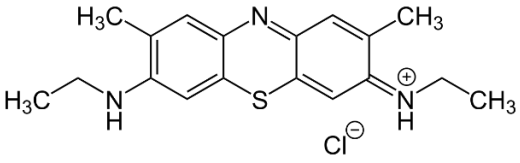

Methylene blue

Fig. 8. Structural formula of studied analytes.

3.2. Materials.

Silica. The series of mesoporous carbons were derived using two mesoporous forms of silica: MCM-48 and SBA-15 sieves (Fig. 9). The MCM-48 and SBA-15 have been preparing via hydrothermal synthesis using TEOS (Aldrich) as the silica source [101].

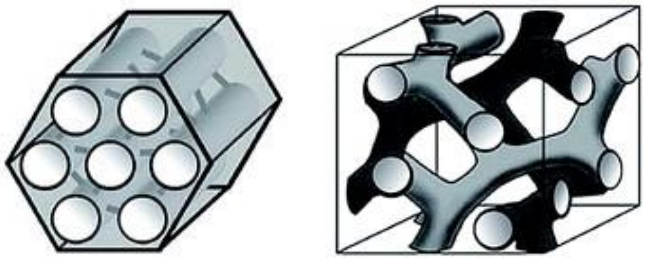

Fig. 9. SBA-15 (a) and MCM-48 (b) silica.

Activated carbons (ACs). The chemical activation of surface carbonous samples has been done in autoclave Fig. 10a. After synthesis and removing the template of mesoporous carbonous materials has been placed in the Teflon part of the autoclave, then mixed with activation agents. The final step of the activation procedure was carried with purified nitrogen in stainless steel reactor that was placed inside a graphite furnace Fig. 10b.

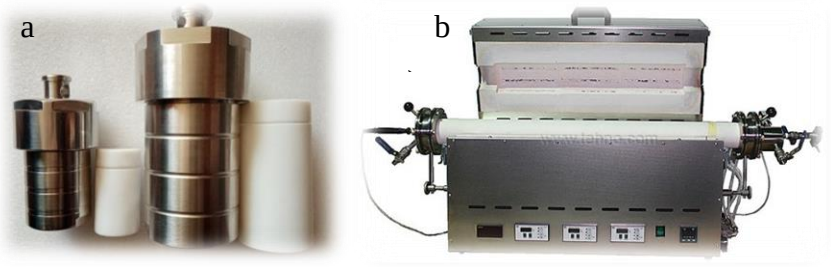

Fig. 10. Activation of mesoporous carbonous materials (a) autoclaves and (b) graphite furnace.

Synthesis of bare magnetite. The MNPs were prepared by the modified co-precipitation method. Typically, 2.83 g of anhydrous $FeCl_3$ was dissolved in 80 mL of deionized water in the tree-necked flask. Water was previously deoxygenated by streaming nitrogen gas for 20 min. Then, 1.72 g of $FeCl_2 \cdot 4H_2O$ was added and thoroughly mixed at 600 rpm in a water bath at 35 °C. When the temperature of the mixture became 60°C, 10 mL of NH_4OH solution (25 wt%) was drop wise added and mixed at 800 rpm. Upon ammonia addition, the solution turned black. Then, the black mixture was aged in a water bath at 60 ◦C for 30 min under continuous stirring.

Synthesis of core-shell modified MNPs. The magnetic **Fe_3O_4/GTMO** nanoparticles were prepared in a three-neck flaskby by one-pot hydrolysis of TEOS and GTMS using the sol–gel process (Fig. 11). First, the suspension of the MNPs in ethanol solution (near 1.8 g of Fe_3O_4 was mixed with 400 mL of ethanol) was added to 10 mL of ultra-pure water and sonicated for 15 min, then 2.0 mL of ammonium hydroxide (25%) was introduced. Subsequently, the mixture of 5.0 mL of TEOS and 3.0 mL of GTMS in 10.0 ml of EtOH was added to it in portions (36 times by 0.5 ml every 10 min). The suspension was then mechanically stirred at 50°C in an oil bath under a nitrogen atmosphere. After

approximately 1 h, the flask was removed from the bath and allowed to cool down to room temperature following by 5 h of mechanical stirring.

Fig. 11. Synthesis of epoxy-derived samples (Fe_3O_4/GTMO).

A 1.8 g of Fe_3O_4/GTMO was suspended in 250 ml of MeCN and stirred at room temperature in a 500 mL three-neck round bottom flask equipped with a reflux condenser. Then, 10 ml of MeCN containing 0.25 g of Triton X-100 was added to the reaction mixture and the reaction was carried out under N_2 atmosphere and mechanical stirring for 30 min. The reaction continued overnight at a constant temperature while stirred. The total schema obtained Fe_3O_4/Triton material was shown in Fig. 12.

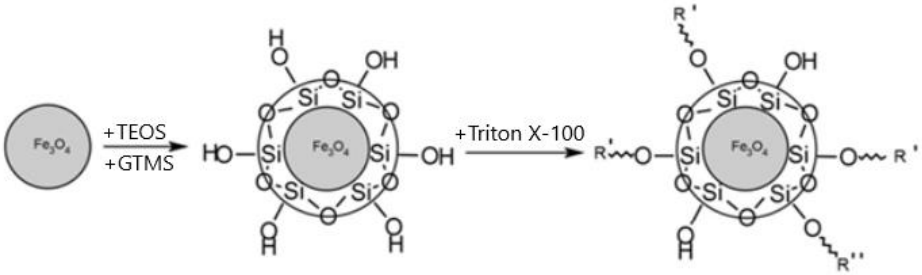

Fig. 12. Scheme of formation of the magnetic Fe_3O_4/Triton nanocomposite (R' = Triton X-100, R" $–CH_3$)

Commercial materials. To compare the properties of the synthesized adsorbents with the commercial products were used activated wood charcoal (Filtroc), this applied in filters for smoking rooms, activated carbon (untreated, Fluka (CAS:7440-44-0)) and Cartridge Varian SPE Bulk Packing (C18 phase, polymeric bonded) (Sigma-Aldrich).

Sample preparation. The modified QuEChERS extraction procedure was performed to pretreatment samples for study sorption efficiency of magnetic adsorbents (as bare Fe_3O_4, Fe_3O_4@Triton, GCB, and C18). Figure 13 shows a scheme for the experimental procedure. The vegetables and fruits were crushed to achieve homogeneousness. Then, samples were placed in a centrifuge tube and pesticide standards and MeCN were also added. Thereupon the mixture was shacked and $MgSO_4$ (anhydrous) was added. Then, the tube was agitated and centrifuged. The upper layer of the MeCN extracts was transferred in an Eppendorf vial containing a certain amount of Fe_3O_4@Triton (0.05 g), C18 (0.05 g), or GCB (0.05 g), and 0.15 g $MgSO_4$ for clean-up (optimized condition). The samples were agitated and then magnetically separated by a NdFeB magnet. The obtained solution was injected into the GC-MS.

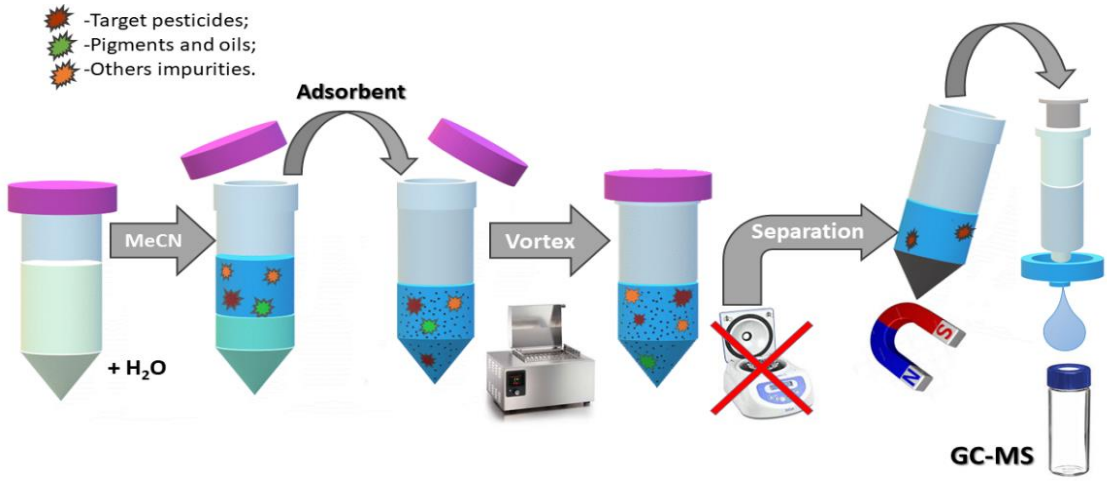

Fig. 13. Scheme of developed sample preparation for fruits and vegetables.

Preconcentration of main smoking products. The preconcentration of the cigarette smoke has been performed in machines simulated actual conditions of cigarette smoking (Fig. 14). This instrument was very similar to the industrial smoking machines used at routine testing of cigarettes.

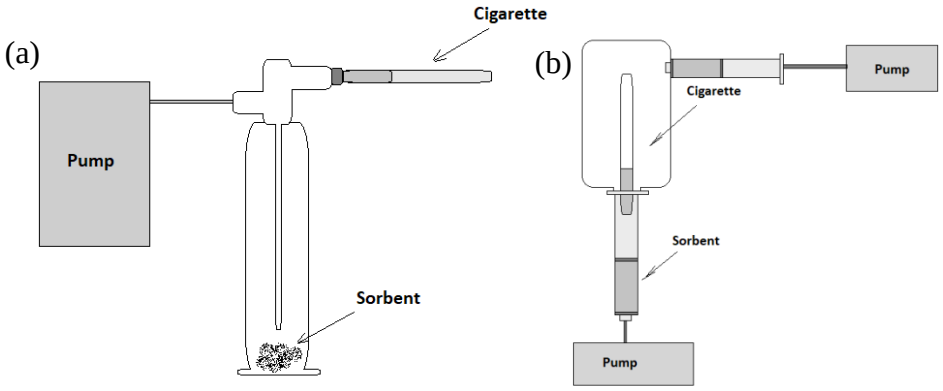

Fig 14. Scheme of the cigarette smoke adsorption in static (a) and dynamic (b) conditions.

The smoking machine Fig. 14a has been used for concentration cigarette smoke in static mode. The sample of adsorbent was placed on the bottom of a glass bulb, a cigarette was inserted, a pump was turned on for developed a thrust, and then the cigarette was burned. Whereas a smoking machine Fig. 14b has been worked in dynamic mode and allowed to simultaneously sample mainstream and second-hand cigarette smoke and easily replace cartridges with adsorbents for adsorption measurements.

3.3. Characterization of materials.

The prepared solids and raw materials were characterized by using various techniques. Each analysis technique typically discovers only a particular aspect of the material and, therefore, a combination of methods was necessary to obtain a complete samples description of the raw, intermediate and final materials. This is very important to use and improve material preparation conditions for a specific application.

Powder X-ray diffraction (XRD) analysis. The crystalline phase identification of the prepared materials has been determined using the powder XRD technique. Also, the small-angle X-ray scattering (SAXS) technique was used to estimate the ordered structure of mesoporous silica samples. Powder XRD data were obtained at room temperature using a PAN Analytical X'Pert Pro highr-esolution diffractometer with Ni-filtered CuKα (λ = 1.5406 Å) radiation. The results of crystalline patterns were compared with the patterns database supplied by the International Centre for Diffraction Data (ICDD).

The crystallite sizes were calculated by applying the Scherrer equation [102]:

$$B(2\theta) = \frac{K\lambda}{Lcos\theta} \quad (13)$$

where $B(2\theta)$ is the mean size of the ordered (crystalline) domains, which may be smaller or equal to the grain size, which may be smaller or equal to the particle size; K is a dimensionless shape factor, with a value close to unity. The shape factor has a typical value of about 0.9, but varies with the actual shape of the crystallite; is the X-ray wavelength; is the line broadening at half the maximum intensity (FWHM), after subtracting the instrumental line broadening, in radians. This quantity is also sometimes denoted as Δ 2(θ); θ is the Bragg angle.

X-ray photoelectron spectroscopy (XPS). The surface elemental composition of obtained samples has been studied by XPS analysis. The XPS spectra were recorded by using a Kratos Analytical

Series-800 unit equipped with a Hemispherical Phoibos analyser operating in constant pass energy, using MgK_{α} radiation (1253.6 eV). The surface elemental composition of the studied materials was estimated using Casa XPS software. Overview spectra in the 0–800 eV range were recorded.

Transmission electron microscopy (TEM). The particle size distribution and morphology of the samples were determined by the TEM technique. TEM images were performed on a JEOL JEM-2100F instrument operating at 200 kV. The samples for TEM measurement were dispersed in alcohol, sonicated and sprayed on a holey carbon film-coated copper grid, and then allowed to air-dry.

Scanning electron microscopy (SEM). The surface texture, structure, and arrangements of the pores of prepared samples were studied by SEM (JEOL JSM-7001F) equipped with an EDX detector. The EDX analysis was mainly used to confirm the semi-quantitative elemental composition of the samples. The surface of the samples was coated with gold film before SEM measurements.

Elemental analysis. The macro elemental content of materials has been determined and controlled by a Vario Macro CNHS/O Analyser. This method allows determining the simultaneous carbon, hydrogen, nitrogen, and sulfur content with high precision and accuracy without any matrix dependency.

Thermogravimetric analysis. Thermal analysis measurements were performed on a Mettler-Toledo TGA/SDTA851 combined with Pfeifer Vacuum Thermostar GSD301T.

Porosity measurements. The surface area, pore volume, and pore diameter of the prepared adsorbents were measured by ASAP 2020 Micromeritics (USA). Before measurement the N_2 gas adsorption-desorption isotherms at 77 K, the samples were outgassed under vacuum at 120 °C for 12 hours to remove any moisture content from the solid surface. The surface area of obtained materials was calculated by the BET method [103]. The pore size distribution was determined using the Barrett, Joyner, and Halenda (BJH) method [104] by the software (Micropore, version 2.26) of the instrument.

Fourier transforms infrared (FTIR) spectroscopy is an essential tool to chemical analysis surface functional groups of obtained materials. The dried adsorbent samples were ground to fine a powder in the agate mortar. The sample and KBr were used in a 1:10 ratio and with the aid of a manual bench press, translucent tablets were prepared. The spectra were measured from 400 to 4000 cm^{-1} (Perkin Elmer FTIR-2000 (USA), Nexus Thermo Nicolet 470, and Varian 620-IR spectrometers) with 4 cm^{-1} resolution and 32 scans.

Magnetization measurement. Magnetic properties of the Fe_3O_4 samples were measured by a vibrating sample magnetometer (EV9 VSM with PPMS-14T system) at room temperature using 100 Oe/s magnetic fields in a driving mode with Nb_3Sn magnet between +22 to -22 kOe longitudes at 300 K with the sensitivity of 10^{-5} emu and 0.5% precision. The samples were compressed inside the sample-holder that consisted of a quartz cylinder of 3 mm inner diameter and stuck every rod to each cylinder by alumina cement. The vertical hall cells were designed using the data of an initial test carried out with the pristine sample.

Titration analysis. The "one weight sample" method was applied for conductometric and potentiometric titration of samples. Briefly, a weighted sample was added to bidistilled water for 12-24 hours. The prepared suspension was titrated by the solution of sodium hydroxide (0.01-0.05 mol/L) in a thermostatic container, with simultaneous measurement of the specific electroconductivity and pH (Mettler Toledo MPC227). The suspension of samples during titration was stirring by a magnetic stirrer (Mettler Toledo™ EL3). In the case when the only pH of the suspension was measured using an I-160M ionomer with a combined glass electrode.

3.2. Methods investigation of adsorption properties.

Chromatography analysis is a method of separation and quantitative determination of substance in mixtures with high sensitivity. Gas chromatography and methods were selected to study the adsorption performance of the obtained materials. Gas chromatography methods employed for the analysis of volatile and semi-volatile organic compounds. Liquid chromatography was used for non-volatile and thermally labile organic compounds at trace concentration level. UV Vis spectrophotometry was used to determine the concentration of organic compounds in solution with a concentration of $\geq 10^{-5}$ M.

Gas chromatography with a flame ionization detector (GC-FID) was used for the analysis of nicotine and quinoline. Gas chromatography analyzes were performed using Agilent 6890 equipment with an HP-5 capillary column of 30 m × 0.25 mm × 0.25 μm. The gas carrier was helium (purity ≥ 99.999%) with a flow rate was 2.0 mL/min. The heating rate of the furnace from 50 °C to 200 °C was 10 °C/min. The temperatures of the injector and the detector were 270 and 350 °C, respectively. The aliquot volume was 1.0 μL. The samples were injected in splitless mode.

Gas chromatography-mass spectrometry (GC-MS) was chosen for analysis of pesticides on the ppb level. Both gas chromatography and mass spectrometry with Isq LT single quadrupole combined in one as GC-MS were from Thermo Fisher Scientific (USA). The autosampler 6890

series was used to inject sample extracts and standards into the GC-MS. The column was an HP-Ultra-1MS capillary column of 60 m × 0.25 mm × 0.25 μm film thickness. The oven temperature was initially held at 85 °C and then increased to 150 °C at a rate of 10 °C·min^{-1}. The temperature was subsequently increased to 350 °C at a rate of 5 °C/min and was finally held at 350 °C for 5.0 min. Helium gas (purity ≥ 99.999%) was the carrier mobile phase with a constant flow at 1.0 mL/min. The injection volume was 2.0 μL in split mode. The total time of analysis based on these settings was 45.0 min. Selective ion monitoring (SIM) mode was adopted for the quantitative analysis of pesticides. The initial identification of a pesticide in the sample was based on the detection of its characteristic ion peaks and their relative abundances as well as the comparison of its retention time with those observed in the analytical standard.

High performance liquid chromatography (HPLC). The determination of tetracycline antibiotics was conducted using a system (Agilent 1260) with UV–Vis detector at wavelength 230–290 nm. The Discovery C18 column (150 mm × 4.6 mm × 5 μm) was used for the separation of the analyte. The column temperature was maintained at 30 °C. The mobile phase consisted of 25 mM KH_2PO_4 at pH 3.0 (40%) and acetonitrile (60%). The mobile phase solution was filtered by 47 mm (diameter), 0.2 μm (pore size) Pall Nylaflo(Nylon) Membranes Filters, and degassed by ultrasonication for 20 min. The eluent flow rate was 1.0 mL/min. A sample injection volume of 100 μL was used.

UV spectrophotometry determines the concentration of specific analytes in a sample based on their absorption of radiation in the visible range. The concentration of the MB was measured at 660 nm using Thermo Scientific Evolution 600 UV-Vis spectrophotometer. Experiments were performed at controlled pH. The concentration of analytes in solution was calculated by the calibration plot: $A_{660} = f(C_{MB})$.

4. Results and discussion

In order to analyze samples via chromatographic instrumentation, sample pre-treatment is often required. Issues necessitating pretreatment include enrichment of analyte concentration to allow for the detection of compounds present at trace levels, or the removal of substances that may interfere with the analysis. Another commonly encountered issue requiring pre-treatment of the sample is a lack of compatibility between the sample matrix and the chromatographic platform. Analysis of aqueous matrices directly by gas chromatography is a greater challenge. Direct injection of these matrices onto the instrument is problematic or impossible, while the properties of both water and the analytes it may contain make an evaporation/solvent exchange procedure prohibitively difficult. Thus, other approaches are required.

The most common techniques for the preparation of aqueous samples for analysis by gas chromatography in wide use today are liquid/liquid extraction (LLE), static or dynamic headspace extraction, solid or liquid micro-extraction, and SPE. After considering the advantages/disadvantages of each technique, it was hypothesized that a sample preparation method using SPE would provide an optimal approach for the analysis of aqueous samples generated during an extractable survey for analysis by gas chromatography/mass spectrometry (GC/MS). A review of the current literature was performed to determine if this has been explored previously. Although this review did yield a significant amount of information on the use of SPE for the analysis of a wide range of compounds from aqueous matrices, a minimal amount of information on its use for extractable surveys was found [105].

However, VOCs are very complex and the target analytes are often present at low concentrations in these samples. Therefore, sample preparation methods are usually required to extract, isolate, fractionate, and/or concentrate the target analytes from the complex matrices. These steps are both time-consuming and labor-intensive, and may greatly influence the reliable and accurate analysis of these materials [106].

4.1 Carbon-based materials for removal of organic compounds

In this chapter, various methods of synthesis of activated carbon from different raw materials for different practical applications based on the adsorption process. The possibility of using the obtained samples of activated carbon of different genesis to study the efficiency of determination and

removal of organic pollutants in air and water medium is considered. All developed adsorbents were tested for the possibility of regeneration for multiple uses.

4.1.1. Mesoporous activated carbon for removal of organic compounds in atmospheric air

Large amounts of volatile organic compounds (VOCs) are emitted into the atmosphere by industrial sources each year. Many of these VOCs are hazardous to human health and the environment. To identify and determine volatile organic compounds in the air, a prerequisite is to bring the substance to its original form before instrumental analysis. Sampling and extraction of toxic volatile organic compounds from the air, including nicotine, is the most important analytical procedure for the quantification of contaminants. It is with incorrect sampling that the largest numbers of possible errors in the results of the analysis of volatile organic compounds are associated.

One of the most significant sources of environmental exposure to many toxic compounds is environmental tobacco smoke. Nicotine and its derivatives [107] are the main compounds in air the of cigarette smoke include chewing tobacco, cigars, cigarettes, e-cigarettes [108], snuff, pipe tobacco, and snus. Nicotine is an easily volatile organic compound with an evaporation temperature at 244 °C. Therefore, it is better to use the gas chromatography method for determination. A very low nicotine concentration in the exhaust air is expensive to treat. For many low-concentration situations, it is possible to use adsorption to increase the concentration to a level at which it is more feasible to clean up the air. In the chromatographic determination of nicotine in air, it is most often captured from the air in concentration tubes with sorbents (activated carbon and other carbonaceous sorbents, silica gel, etc.) are used. Among various adsorbents, carbon materials are widely used for their stable physical and chemical properties, high surface area, porosity, and regenerability [109]. VOCs are removed from the inlet air by physical adsorption onto the surface of the carbon. Such adsorbents can be used in special smoking booths necessary for the organization of comfortable and isolated places of smoking in public places and airports. To minimize the effects of cigarette smoke on reducing air emissions.

In recent years, new adsorbent materials and sorption methods have been actively studied for efficient separation of VOCs from polluted air streams [110]. In our study work, we devoted a new generation of the most attractive mesoporous adsorbents for VOCs. The spherical microporous adsorbents exhibit superior VOC adsorption ability for their pore sizes are close to the nicotine molecule sizes. In addition, usually published in the literature developed carbon adsorbents are

microporous, and then even with an increasing affinity for nicotine, they cannot be regenerated (or it is not easy to do). Spherical ordered mesoporous carbon with relatively large pore size successfully overcome this drawback, and the adsorbed VOCs can be easily desorbed. Our results of nicotine in indoor air confirm that the compounds of interest occur at significant levels in location where people smoke cigarettes, and using selective adsorbent can be significantly decreased their level.

Article I

"*Spherical mesoporous carbon adsorbents for sorption, concentration, and extraction of nicotine and other components of cigarette smoke*"

Protection of Metals and Physical Chemistry of Surfaces

55 (423–432)

Year 2019

DOI: 10.1134/S2070205119030171

Impact Index: 0.985

Article II

"*Efficient adsorption of pharmaceutical drugs from aqueous solution using a mesoporous activated carbon*"

Adsorption

26 (251–266)

Year 2020

DOI: 10.1007/s10450-019-00143-0

Impact Factor: 1.949

Article III

"*Sunflower Biomass Power Plant Wastes: Properties and Its Potential to Respect the Water Purification of Organic Pollutants*"

Journal of Analytical and applied pyrolysis

Accepted

Year 2021

Impact Factor: 3.905

Journal of Analytical and Applied Pyrolysis 157 (2021) 105237

Contents lists available at ScienceDirect

Journal of Analytical and Applied Pyrolysis

journal homepage: www.elsevier.com/locate/jaap

Sunflower biomass power plant by-products: Properties and its potential for water purification of organic pollutants

Tetiana S. Hubetska [a], Natalia G. Kobylinska [b,*], José R. García [a]

[a] University of Oviedo-CINN, Avda. Julián Clavería, 8, 33006 Oviedo, Spain
[b] Taras Shevchenko National University of Kyiv, 64 Volodymyrska Str, 01601 Kyiv, Ukraine

ARTICLE INFO

Keywords:
Waste management
Biowaste of energy pyrolysis plant
Chemical activation
Organic pollutants removal
Water treatment

ABSTRACT

The present study explores possibility of using sunflower seed husk agricultural biowastes from industrial pyrolysis power plant as a feedstock for preparation of activated carbon (AC). Sunflower biomass by-products contain up to 70 % of carbon with residual seed husk components, have low specific surface area (less than 21 $m^2 g^{-1}$) and smaller number of oxygen-containing groups in comparison with wood-based biochars. The main process parameters of AC preparation, namely a type of an activation agent (organic solvent, HNO_3, NaOH), temperature and duration of the carbonization step, were optimized in respect to adsorption efficiency. We found that simple pre-treatment of sunflower biomass with tetrahydrofuran easily converts it into biochar precursor having large number of carbonyl and hydroxyl groups. Further thermal and chemical activation of the biochar precursor results in formation of AC products with specific surface area in the range from 625 to 980 $m^2 g^{-1}$ and from 1000 to 1755 $m^2 g^{-1}$, respectively. Methylene blue (MB) was used as a test molecule for characterization of adsorption properties of the obtained AC. Kinetics studies showed that MB adsorption on AC is fast and follows pseudo-second-order model. MB adsorption on biochar and AC is well described by Langmuir isotherm, assuming monolayer formation of MB on the surface of adsorbents via chemical interactions. Adsorption capacity of AC towards MB achieved by nitric acid activation is higher (379.0 mg g^{-1}) than capacity of benchmark commercial activated carbon from Norit. The study opens up possibilities for the development of by-product-based adsorbents via the straightforward, eco-friendly approach, with specific focus on the economic effect achieved with these materials.

1. Introduction

Adsorption is one of the most efficient methods for separation of gases and liquids from a wide variety of pollutants [1], and activated carbons (AC) are the most widely used adsorbents [2]. World demand for AC grows rapidly (5.5 % annually in the past decade) and according to the forecast this trend will remain in the future. The right choice of feedstock is an important factor in the production of activated carbons effecting on both cost and adsorption performance. This use of low-cost feedstocks from biowaste [3,4], food [5] and municipal wastes [6–8] becomes more and more attractive for making low-cost adsorbents [9,10] for cleansing liquid streams and wastes of heavy metals [11], organics [5], dyes [6], pesticides, antibiotics, etc. Among agricultural waste sources, woody materials are regarded as the most promising precursors for AC manufacturing due to their textural characteristics favourable for the porosity development [12]. However, sugar cane bagasse, sunflower seed hull [13], coconut shell [14], corn stalk [15], oil palm shell, tobacco stems, flower [16], walnut shell, chickpea, wood and rice husks [17], jackfruit peel [18] and tea waste [19] are also widely used as the feedstock for preparation of activated carbons [10]. AC manufacturing process from industrial and biowastes includes stage of their pyrolysis leading to the formation of biochars. Biochar is an intermediate product but in some cases it can serve as an inexpensive alternative to AC [11,17]. For example, it was shown that specific surface area of cork-based biochar prepared by pyrolysis at 750 °C is 392.5 m^2/g, and adsorption capacity towards Cu(II) is 18.5 mg/g [11]. Indeed, the sorption capacity of biochar is less than of commercial AC due the undeveloped pore network in absence of an activation process but that is becoming reasonable and substantiated for practical applications.

Applicability of biowaste sources as feedstock for making AC for the water treatment depends strongly on their type and origin. Wastes from municipal incinerators are not good for this purpose because of

* Corresponding author.
E-mail address: kobilinskaya@univ.kiev.ua (N.G. Kobylinska).

https://doi.org/10.1016/j.jaap.2021.105237
Received 18 January 2021; Received in revised form 15 May 2021; Accepted 9 June 2021
Available online 12 June 2021

irreproducibility of their composition, properties [20], and high content of heavy metals [21]. On the other hand, sunflower seeds look like a promising feedstock for making low-cost activated carbons. As an example to this, AC is reported [4] with developed specific surface area (~2000 m^2/g), high pore volume (1.6 cm^3/g) and affinity to Cr (VI) ions. B.S. Girgis and co-workers [22] presented results how chemical activation of various seed shells rich in lignocellulose affects AC textural and adsorption properties. After activation, surface area increased from 437 to 1022 m^2/g, and pore volume rose from 0.444 to 0.809 cm^3/g. Porous AC from sunflower seed hulls with a surface area of 1411 m^2/g was prepared by a microwave-assisted K_2CO_3 activation process [23]. Li et al. used KOH as an activation agent and succeeded in making AC with extremely high specific surface area (2584 m^2/g) and pore volume (1.41 cm^3/g) [24]. This illustrates the point that the search for new sources of carbon-based materials and efficient routes of their activation is important and continues.

World production of sunflower (*Helianthus annuus*) exceeds 700,000 million seeds per year [25]. The largest producers are Ukraine, Russian Federation, Argentina, and China. On average, a 400 tons/day sunflower oil production plant leaves almost 100 tons of seed husks waste. So far only a fraction of such bio-wastes is utilized [4,24,26]. National Renewable Energy Action Plans of the EU Member States give special significance to the use of agricultural biomass wastes in novel environmentally-friendly technologies [27]. Residual biomass from the sunflower oil industry could be used for biofuels production or generating heat energy via pyrolysis [28,29]. During pyrolysis, the decomposition of carbohydrates from biomass takes place [30] leaving carbon-rich solid residue [31], which is inexpensive renewable carbon precursor for activated carbons production. Currently, several thermal power plants fuelled with agricultural wastes are in operation in different countries [32]. However, only few studies about application of by-products generated in power plants in adsorption or catalysis have been reported [33]. The higher value product could be obtained by converting biomass into efficient adsorbent for environmental pollutant removal [1,33]. Therefore, an inexpensive by-product management technology is needed. Meanwhile, it is also important to obtain carbon adsorbents in cost-effective processes, which depend on two factors: low-cost precursors and low-cost schemes of preparation.

In the present work, sunflower seed husks by-products generated in power plant industry are tested as materials for adsorption. They are subjected to three subsequent treatment processes under optimized conditions: 1) acid-alkali (traditional) and organic solvents (novel) pretreatment technologies, 2) simple carbonization at 600 °C, and 3) chemical activation by HNO_3 or NaOH. This aims to demonstrate many aspects:

(1) the suitability of these by-products to obtain materials for water treatment,
(2) the best scheme to develop products with enhanced surface area and porosity characteristics,
(3) adsorption capacity of the obtained carbon adsorbents for the efficient uptake of organic pollutants (e.g. methylene blue) from aqueous solution,
(4) the eff ;ect of porosity and heteroatom functionalities on adsorption performance (efficient uptake, shorter adsorption time and maximum capacity, capability to be regenerated),
(5) the most feasible technologies for producing efficient adsorbents with enhanced features.

In addition, this would help to realize two environmental aspects: the economic disposal and utilization of undesirable residues, and to produce an industrially valuable substance for water treatment and other applications.

2. Experimental part

2.1. Sunflower husk-based by-product feedstock

The sunflower seed husks by-products from the industrial biowaste power plant in Kyiv region (Ukraine): small (*SF-Small*) and striped (*SF-Huge*) were used in this study as feedstock. They were collected at the bottom of the fluidizing bed reactor and then separated from sand by sieving.

2.2. Sample's preparation

2.2.1. Preparation of odourless biochar

To prepare odourless biochar, sunflower feedstocks were thermally treated in a furnace. Samples were placed into open vessels and then heated at 80 °C for 1−2 h. The experiments were conducted at atmospheric pressure in air. Additionally, sunflower by-products were heated in a tube oven: quartz tube (Ø2.6 cm), 5 cm from the inlet; heating ramp 10 °C min^{-1}, constant nitrogen flow (50 mL min^{-1}), atmospheric pressure. To determine the time of exposure to the heat source, initially, 4 crucibles were placed in the quartz tube and heated, at a temperature of 180−200 °C, for 30, 60, 120 and 180 min.

2.2.2. Preparation of pre-treated samples

Three process routes were used for treatment of sunflower husk-based solids: 1) acid-alkali and 2) organic solvents pre-treatments with 3) a subsequent carbonization. *Acid-alkali pre-treatment*: The dark solid matter (2 g) was mixed with HNO_3 (65 %) or NaOH (50 %) solution overnight. Acid/base treated materials were filtered and thoroughly washed with distilled water until reaching pH ~6 in eluate. After that, materials were dried at 50 °C for 12 h. This resulted in two types of carbons with different degree of wettability. *Solvent pre-treatment*: 2 g portions of dark solid were brought into contact with 50 mL of organic solvent (tetrahydrofuran (THF) or dichloromethane (CH_2Cl_2)) under constant stirring and room temperature for overnight. Then solids were separated by centrifugation, washed with diethyl ether and oven dried at 50 °C for 1 h. *Carbonization stage:* Carbonization was performed in a quartz tube (horizontal oven, Nabertherm, model RD30/200/11) at 600 °C (ramp 10 °C min^{-1}) for 2 h under inert atmosphere (N_2 or Ar flow). After that, materials were cooled down to room temperature under a constant flow of inert gas. Carbonized samples were washed with distilled water until neutral pH, dried at 100 °C overnight and finally crushed to a fine powder.

2.2.3. Preparation of activated carbon

The activation process was based on pre-treatment of samples by solvent (or acid-alkali) or conventional heating. First, a feedstock sample (2 g) was soaked in 10 mL of HNO_3 (or NaOH) solution in a quartz crucible at room temperature for 12 h. At the next step, crucibles with the feedstock were placed inside the oven, heated to 600 °C and incubated for 2 h. After cooling to room temperature samples, were washed with diluted HCl and then with deionized water to neutral pH to remove all admixtures. Finally, moist materials were dried at 80 °C for 1 h.

The samples in this study were named according to the feedstock type (*SF-Small* and *SF-Huge*) and their treatment sequence in the following way: name of husks feedstock/pretreatment/heating/activation agent. The subscripts "THF" and "NaOH" represent pre-treatment by washing biochar with THF or NaOH, respectively. The number "600" indicates temperature of the thermal treatment. As an example, the biochars prepared by only thermal treatment at 600 °C are labelled *SF-Huge/600* and *SF-Small/600*, respectively. *SF-Huge/HNO_3/600/NaOH* means that AC was prepared via HNO_3 pre-treatment of *SF-Huge* biochar and that feed biochar was first thermally activated at 600 °C with subsequent chemical activation with a concentrated solution of NaOH.

2.3. Characterization of the materials

The N_2 adsorption/desorption isotherms at 77 K were determined using a KELVIN 1042 BET-Sorptometer (Costech International). Prior to adsorption measurements, the samples (50 mg) were outgassed at 110 °C for 4 h under a vacuum above 10^2 Pa. The microporosity of the samples was analysed by applying the α_s-method [34]. The pore size distribution of samples was calculated by using the Non-local Density Functional Theory (NLDFT) and Barrett, Joyner and Halenda (BJH) methods. Powder XRD data were obtained using a PAN Analytical X'Pert PRO apparatus equipped with an X'Celerator detector with automatic data acquisition (X'Pert Data Collector (v2.0b) software) using monochromatized Cu Kα ($\lambda = 1.5406$ Å) radiation. Studies of particle size and morphology of samples were conducted on the JSM-6100 (JEOL, Japan) scanning electron microscope (SEM) equipped with an Oxford Instruments INCA energy-dispersive X-ray spectrometer (EDX).

Fourier transform infrared (FTIR) spectra were recorded from the samples pressed into pellets with KBr using a Nicolet Nexus 470 (Thermo, USA) spectrometer. Thermal analysis measurements were performed on a Mettler-Toledo TGA/SDTA851 (N_2 atmosphere, 10 °C min^{-1}). The chemical composition of samples was obtained by elemental analysis (C, H, N, S) using LECO CHNS-932.

2.4. Determination of the point of zero charge pH

The point of zero charge (pH_{PZC}) of the carbon samples was determined using 100 mL of NaCl solution (0.1 M) placed in vials kept at room temperature. The pH was adjusted to values between 2 and 10 by adding HCl (0.1 M) or NaOH (0.1 M). The carbon sample (100 mg) was added to the solution and pH values were measured against the initial pH ($pH_{initial}$). The obtained suspension was stirred for 12 h. Then, the final pH (pH_{final}) of suspension was measured. The pH_{PZC} value was obtained by analyzing plot $\Delta pH = f(pH_{initial})$, where $\Delta pH = |pH_{final} - pH_{initial}|$.

2.5. Batch of adsorption assays (screening tests)

Methylene blue (MB) was supplied by Panreac Quimica S.L.U. (Spain). The working solutions were prepared by dilution of a stock solution of MB (1000 mg L^{-1}) to target concentration (10−50 mg L^{-1}). The adsorption experiments were conducted by mixing 50 mg of the sample with 15 mL of 10 mg L^{-1} MB solution (neutral pH). After shaking for 60 min, solids were separated by centrifugation (5000 rpm for 1 min). The suspension was then filtered and the MB residual concentration was measured at 660 nm using a UV–vis spectrophotometer (Thermo Scientific Evolution 600). Experiments were performed at controlled pH using NaOH and HNO_3. The pH of the solutions was checked regularly. The adsorption experiments were performed in triplicates and mean values were used for calculations.

Commercial activated carbon (Norit SAE Super 8044-0, from the Netherlands) was used as a benchmark.

2.6. Effect of a contact time

For kinetics study, a test sample (50 mg) was added to 25 mL of 1000 mg L^{-1} MB solution (at pH = 6.0) and mixed for different periods of time from 1 min to 45 min. Change of MB concentration in solution after adsorption was determined by the spectrophotometric method. Peak absorbance of the solution was detected with a maximum at 665 nm.

2.7. Reusability of the adsorbents

The MB-loaded AC sample was dispersed in 10 mL of 1 mmol L^{-1} HCl solution and stirred for 60 min. After that adsorbent was separated from the acid solution and washed with several portions of deionized water until the eluate became neutral. Finally, carbonization at 300 °C for 1 h was applied to obtain new adsorbent. After regeneration, the adsorbent was analyzed on MB content by FTIR. Adsorption/regeneration experiment has been repeated in three consecutive cycles.

3. Results and discussion

In order to define the most efficient strategies for the development of carbon-based adsorbents from sunflower seed husks by-products, composition, textural features, thermal stability, surface area and porosity of the feedstock and synthesized activated carbons were studied.

3.1. Feedstock and derivative carbon samples

The sunflower seed husks by-product formed after pyrolysis is a black powder with a foul smell and low wettability (Fig. S1). A possible reason for the biochar odor could be presence of partially decomposed sunflower oil [35]. This odor is not stable and easily disappears after sample heating at 80 °C for 2 h in static air or after 1 h under air flow. By another way, after air streaming through the sample during 1 h at 80 °C, the smell diminishes to its complete disappearance. It is possible to obtain a similar effect by thermal treatment in inert atmosphere during 2 h at 180 °C, but this method is pretty more expensive in comparison with the two previous methods. Thus, the high temperature (up to 180 °C) is not necessary for disappearance of the smell. Therefore, low-temperature processing (up to 80 °C) of the raw materials was used for smell removal.

Chemical composition of the initial two sunflower seed husks by-products was determinedby semi-quantitative elemental analysis (Fig. S2, Table 1).

Sunflower by-products have pretty complex composition and low content of toxic element impurities (Table 1). Predominant elements are unburned carbon and oxygen. Both feedstock samples are rich in carbon (~80 %) and contain various admixtures including transition elements. Unexpectedly, silica content in the sunflower by-products is extremely low. Typically, ash from biowaste power plants contains large quantities of alkali-earth metals and crystalline silica, sometimes as 5−10 μm spheres [36,37]. This means that sunflower husks composition is more similar to contaminated biochar than to biomass ash [38].

To improve the wettability and adsorptive performance of contaminated biochars, low-cost pretreatment methods were applied at the initial stage of the sample preparation process (Scheme 1). This stage is based on pretreatment with organic solvent and acid-alkali of feedstock. Concentrated nitric acid reacts with biochar aggressively and the solution colour changes to brown in less than 1 h. As a result of such treatment, a large number of oxygen-containing functional groups are formed at the surface resulting in improved biochar hydrophilicity and wettability [7]. A similar effect can be achieved by treatment with concentrated NaOH for longer time (3 h and more). The silica reacts with NaOH (forming Na_2SiO_3), and then is removed by water washing and filtration. Biochar treatment with THF changes solution colour to extremely dark. These could be a result of extraction into organic phase of oil and other organic impurities from the material. It is worth to note that the THF treatment significantly improves biochar wettability but makes it more fragile. An attempt to do pre-treatment with CH_2Cl_2 resulted in only marginal improvement in the material wettability. The sample has a specific smell and wettability slightly increased compared to the non-treated feedstock, indicating that this pre-treatment was not successful.

As seen from Table 1, feedstock samples have relatively low content of metallic and non-metallic impurities (Mg, Ca, Fe, Na, P, Cl, K, Cu). The amount of these elements is clearly reduced after the pre-treatment stages (Fig. 1). Pre-treatment of samples with organic solvents (*SF-Huge/THF* and *SF-Huge/CH_2Cl_2*) does not significantly change content of the metallic admixtures, which is expected since they are not soluble neither in THF, nor CH_2Cl_2. Treatment with HNO_3 gives different results.

Table 1
Elemental analysis data of the feedstocks according to EDX method (wt. %).

Elements	C	O	Na	Mg	Si	P	Cl	K	Ca	Cu	Total
SF-Small											
1 point	79.77	14.01	0.07	1.62	0.02	0.29	0.22	2.02	1.79	0.20	100.00
2 point	79.17	14.23	0.13	1.78	0.06	0.39	0.12	2.00	1.71	0.42	100.00
Mean	79.47	14.12	0.10	1.70	0.04	0.34	0.17	2.01	1.75	0.31	100.00
SF-Huge											
1 point	88.82	9.11	0.03	0.21	–	–	–	1.17	0.21	0.44	100.00
2 point	80.14	14.45	0.15	0.79	–	–	–	1.33	2.45	0.70	100.00
Mean	84.48	11.78	0.09	0.50	–	–	–	1.25	1.33	0.57	100.00

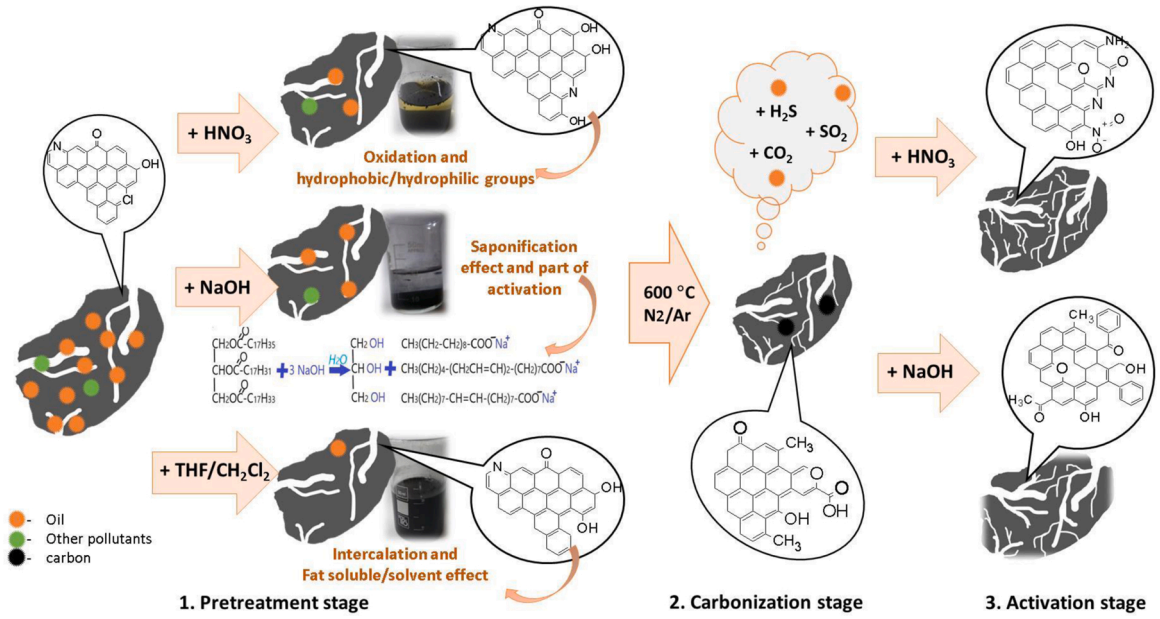

Scheme 1. Schematic representation of sunflower biowaste by-products treatment stages.

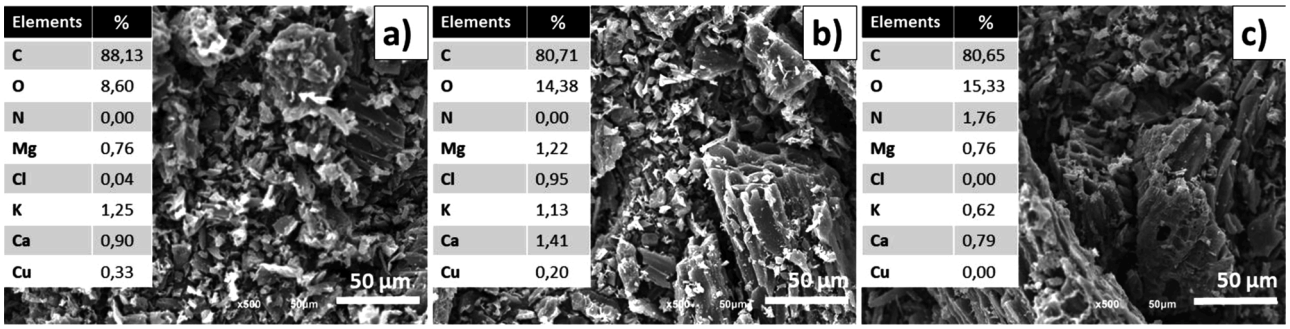

Fig. 1. SEM images, EDX elemental analysis data (mean value of triplicate experimental data) of *SF-Huge/THF* (a), *SF-Huge/CH_2Cl_2* (b), *SF-Huge/HNO_3 (c)* samples.

Fraction of cation species reduces, and Cu (II) disappears completely. At the same time, EDX results show incorporation of nitrogen into biochar matrix (Fig. 1c).

The thermal decomposition route of the biochars was studied thermogravimetrically under N_2 flow (Fig. 2). Decomposition products of the samples were further studied using mass spectrometric control in a simultaneous TGA-MS experiment (Fig. S3).

Thermal decomposition of by-products takes place in several stages: at low temperature (50−100 °C), moderate temperature (300−600 °C) and high temperature (≥ 600 °C). A minor weight loss (5–15 %) observed in both feedstocks at low temperatures is related to release of physically bound water and volatile contaminants. Such low temperature water loss (~80 °C) is a result of feedstocks hydrophobicity and poor wettability (Fig. S1). Practically, no weight changes occur in the temperature range 100−300 °C. Thermal stability of *SF-Small* biochar is higher than that of *SF-Huge* (Fig. 2). The second step of thermal decomposition of *SF-Small* biochar results in a weight loss of 3.57 % and takes place at 329 °C. *SF-Huge* sample loses almost 45 % of weight in two overlapping steps at 337 °C and 374 °C (Fig. 2b), and this relates to organic matter decomposition from sunflower husk [7]. In this temperature range, rearrangement of biochar atomic structure takes place with decrease of aliphatic and increase of aromatic function in the matrix. This is accompanied also by biochar volume expansion and porosity increase. Similar behaviour is observed during thermolysis of

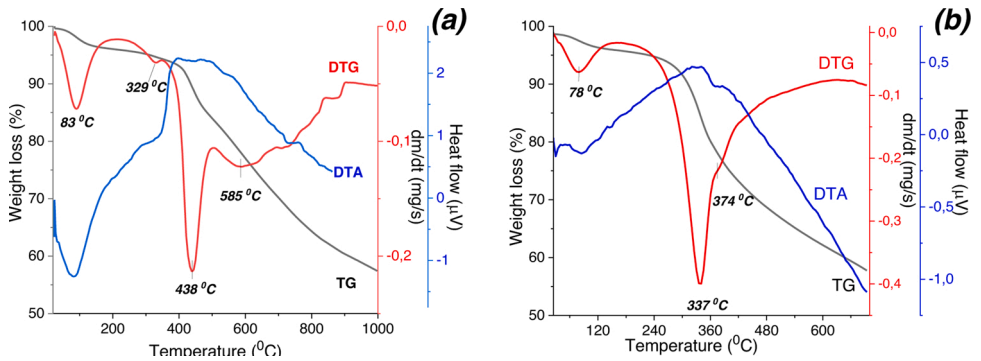

Fig. 2. TGA curves of initial by-products: SF-Small (a) and SF-Huge (b).

lignocellulosic matter [29,39], which is a major constituent of sunflower seeds [28]. This indicates that complete pyrolysis of sunflower biomass does not take place under conditions used in industry.

During the TGA-MS measurements, release of following gases was monitored: H_2O (*m/z* 18), SO_3 (*m/z* 80), CO_2 (*m/z* 44), NO_2 (*m/z* 46), SO_2 (*m/z* 64) and SO (*m/z* 48). Water release occurs throughout the whole process (at 83 °C, 439 °C, 585 °C) and as trace amounts at high temperature. The peak release of NO_2 and SO_3 takes place at 439 °C. Simultaneous release of CO_2 and H_2O gases occurs at 550−650 °C (Fig. S3a). Formation of these gases is a result of sunflower oil decomposition, which is the main impurity in biochars and leads to the formation of dark spots on the wall of a test quartz tube. This is stage in which the feedstock decomposes and the wettability of the samples increases. Intensive decomposition of feedstock ends mainly at 600−650 °C, though some weight loss continues up to 1000 °C (Fig. 2) [40]. So, it is not an energy-friendly technique for waste management. Considering this, the activation temperature was set at 600 °C in all carbonization experiments.

Morphology of initial feedstocks and corresponding carbonized samples from different sunflower precursors was studied by scanning electron microscopy (Fig. 3).

The initial *SF-Small* biochar consists of non-porous irregular shaped particles of different size ranging from 0.5 to 60.0 μm (Fig. 3a). At the same time, the *SF-Huge* biochar contained interconnected ordered inclusions of a different nature than carbon, with an average particle size of around 0.3–200.0 μm (Fig. 3b). The largest particle sizes are often attributed to organic, unburned carbon fraction [37]. Morphology of *SF-Huge* biochar (Fig. 3b) is different and has features typical for a wood-derived material [12]: elongated fibrous shaped particles with a capillary structure and fibrous-like pores. SEM images confirm that cellulose is the major constituent of biochars, especially of the *SF-Huge* by-product, and that type of sunflower waste has a significant effect on their morphology. According to SEM, biochar carbonization produces carbon-based materials with smaller particle size than in the initial feedstocks (Fig. 3c, d). Carbonized samples' particles are non-porous and irregular shaped in the case of *SF-Small* and have dendrite-like structures in the case of *SF-Huge*.

Some valuable information about presence of different crystalline phases in sunflower feedstocks and products of their treatment was obtained from powder XRD measurements (Fig. 4).

Two broad halos seen in XRD pattern (Fig. 4) at 2θ 20–30 degrees and 40–50 degrees are characteristic to amorphous carbon, with

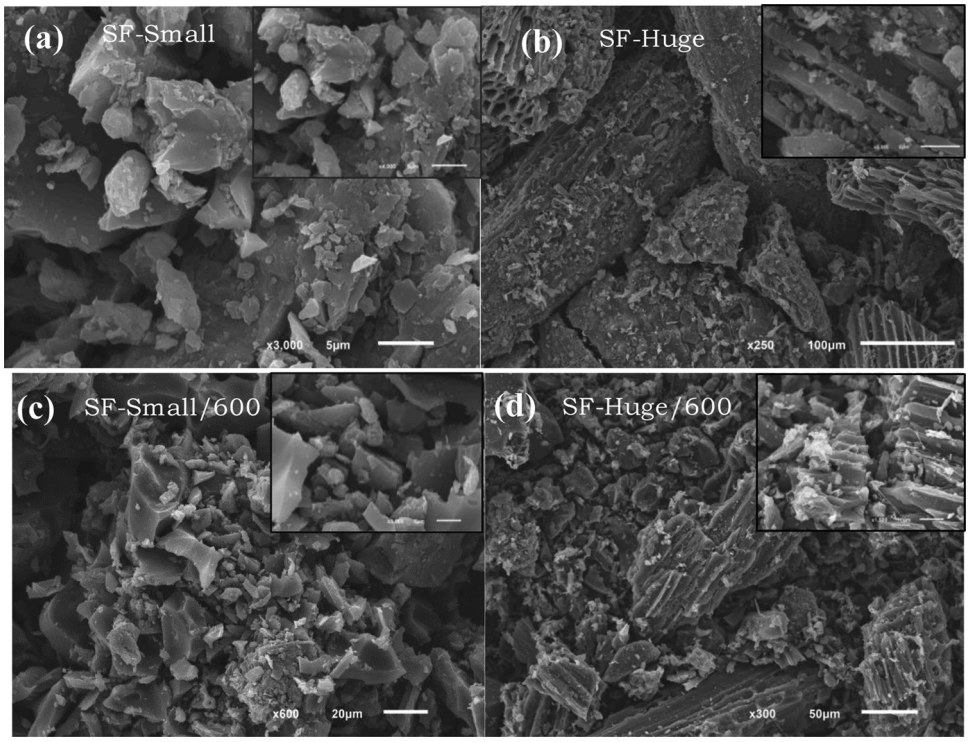

Fig. 3. SEM images of the two types of initial biochars ((a) *SF-Small*, (b) *SF-Huge*), and (c, d) after carbonization at 600 °C at different magnifications.

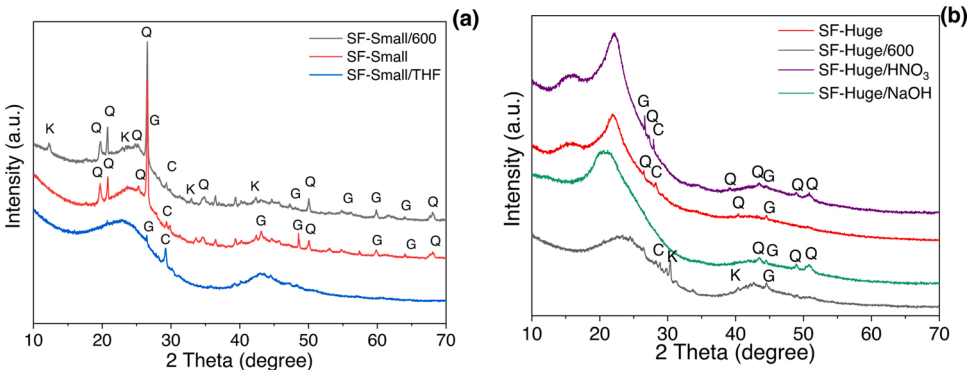

Fig. 4. Powder XRD patterns of the *SF-Small* (a) and *SF-Huge* (b) and products of their treatment (*Q* – quartz, *G* – graphite, *K* – kalicinite and *C* – calcite).

randomly oriented aromatic moieties, mixed with small quantities of graphite (JCPDS Card N⁰ 26-1080). Sharp peaks observed at 2θ = 12.3, 19.7, 20.7, 26.5, 29.3, 34.9, 50.0, 59.9 and 68.0 degrees in the XRD patterns of *SF-Small* indicate the presence of miscellaneous inorganic compounds, mainly quartz (JCPDS Card N⁰ 80-2147; Card N⁰ 88-2487) and a lesser amount of $CaCO_3$ (JCPDS Card N⁰ 47-1743). Multiple peaks with low intensity are related to different impurities existing in the biomass waste (such as TiO_2, Fe_2O_3 etc.). Additionally, new crystalline phase of kalicinite ($K_2O + 2CO_2 + H_2O \xrightarrow{600\ ^\circ C} 2KHCO_3$) (JCPDS Card N⁰ 1-976) was detected in the carbonized *SF-Small* sample. Pre-treatment of biochar with THF (*SF-Small/THF*) results in a significant reduction of the peak intensities or even in a disappearance of some of them, thus confirming removal/washing out of most of the ash and inorganic components. A rather narrow halo at 2θ = 15–20 in the XRD pattern of *SF-Huge* (Fig. 4b) indicates presence of another amorphous phase, which disappears after the thermal treatment at 600 °C. Thus, XRD analysis of sunflower feedstocks confirmed presence of carbon as amorphous phase, graphite, quartz, and some other crystalline impurities, previously detected by the EDX analysis (Table 1).

Quantitative elemental analysis data of feedstock pre-treated and carbonized samples are summarized in the Table 2. C, H, S and N content in the two biochars is very similar. High carbon content in both biochars, in combination with S and N impurities, makes these precursors promising for preparation of adsorbents with good performance. Carbon content in the initial feedstocks is close to 70 % and it increases to 82 % after the thermal treatment at 600 °C for 2 h. The alkali treatment leads only to a marginal increase of the carbon content and some decrease of nitrogen. On the other hand, the pre-treatment with nitric acid results in enrichment of the products with nitrogen. This phenomenon could be related to nitrogen incorporation into the lattice with formation of different nitrogen-containing groups, which is in a good agreement with TGA-MS and EDX analyses data (Figs. 1 and S3). Change of the sulphur content in the materials after different treatments is negligible. However, a distinctive H_2S odour is present during carbonization.

Materials' textural properties were determined by analysis of low temperature N_2 adsorption/desorption isotherms (Fig. 5).As seen from Fig. 5(a), both feedstocks show very low nitrogen uptake at low relative pressures, and there is only a slight increase at p/p_0 values close to saturation, which indicates a poorly developed porosity with low contribution of mesoporosity. According to the IUPAC classification, the feedstock isotherms belong to the type II [41]. Type II isotherms are characteristic for materials with a broad pore size distribution. In contrast, N_2 isotherms for acid/alkali treated and carbonized samples belong to the type I (Fig. 5b), for which N_2 uptake at low p/p_0 and a lack of hysteresis at high p/p_0 is typical, indicating N_2 adsorption in micropores comparable by size with adsorbate molecules. Specific surface area (S_{BET}), pore diameter (D_{pore}, nm) and micropores volume (V_{micro}, $cm^3\ g^{-1}$) were determined from isotherms using DFT method (Table 2). Both feedstock materials have low specific surface area (7−21 $m^2\ g^{-1}$)

Table 2
Elemental composition and textural parameters of feedstock and derivative carbon samples.

Sample	Elemental analysis				Textural parameters		
	C (%)	H (%)	S (%)	N (%)	S_{BET} ($m^2\ g^{-1}$)	D_{pore} (nm)	V_{micro} ($cm^3 \cdot g^{-1}$)
Feedstock							
SF-Small	73.3	3.2	1.3	1.4	7.18	0.02	0.04
SF-Huge	75.5	4.6	0.9	1.3	21.15	0.03	0.03
Solvent and acid-alkali pre-treated samples							
SF-Huge/THF	79.2	6.8	1.1	1.4	279	0.9	0.22
SF-Huge/THF/HNO_3	79.0	6.7	1.0	1.9	355	1.0	0.24
SF-Huge/CH_2Cl_2	81.0	6.8	0.7	1.4	223	0.8	0.18
SF-Huge/HNO_3	75.7	4.8	1.1	2.6	143	0.6	0.15
SF-Huge/NaOH	77.8	5.9	1.3	0.8	200	0.9	0.20
Carbonized samples							
SF-Small/600	79.0	1.6	1.1	1.3	434	0.7	0.23
SF-Huge/600	82.6	1.5	1.1	1.7	438	0.9	0.21
SF-Huge/HNO_3/600	83.2	2.4	2.1	2.7	614	1.1	0.35
SF-Huge/NaOH/600	–	–	–	–	555	1.3	0.39

and low pore volume of 0.03−0.04 $cm^3\ g^{-1}$. This can be related to pores blockage with sunflower oil unburnt during pyrolysis. Despite similarities in texture of feedstocks, there are big differences in porosity of solvent and acid/alkali treated samples. Pore volume of carbons made by treatment of *SF-Huge* biochar (*SF-Huge/NaOH* and *SF-Huge/HNO_3*) is more than 3 times higher than PV of the initial feedstock. Washing with tetrahydrofuran (*SF-Huge/THF*) results in material with the highest S_{BET} (279 $m^2 \cdot g^{-1}$), which is more than 10 times higher than S_{BET} of the feedstock material. S_{BET} of the material made via caustic treatment is somewhat lower, but still very high: 200 $m^2 \cdot g^{-1}$. Such a significant effect is due to the removal of impurities blocking the pores [42]. The newly formed or unblocked pores are micropores with the average pore diameter equal to 0.6−0.9 nm. The data show that NaOH is the most efficient agent for removal of sunflower oil residue via the saponification reaction as shown in Scheme 1. Further development of material's porosity can be achieved via thermal activation resulting in generation of cracks, crevices, defects, voids, and new pores, including mesopores, in the carbon matrix [43]. However, such thermal activation is energy consuming, whereas alkali washing treatment is less costly and gives

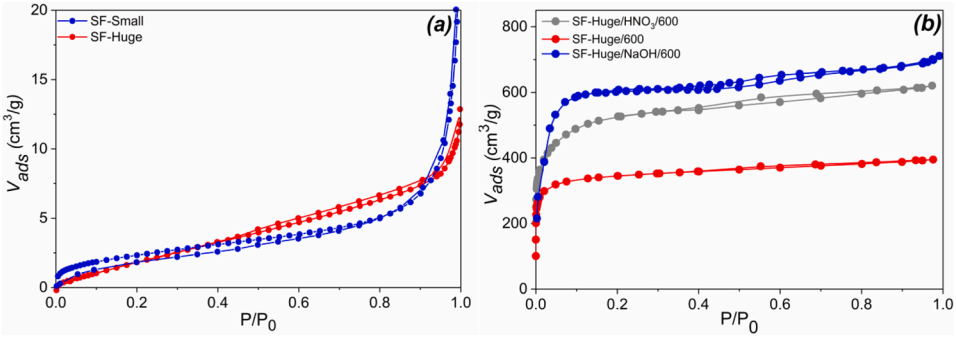

Fig. 5. N_2 adsorption/desorption isotherms at 77 K of (a) the feedstocks and (b) the products after treatments.

products with sufficiently developed porosity, a trend which is usual for carbon samples prepared under similar conditions in the lab [43].

Thermal carbonization and activation by HNO_3 (Fig. 6) result in products with the type I isotherm (microporous materials with pore fillings at very low relative pressure). Like the alkali pre-treated samples, the carbons possess a combination of the type I and type II isotherms. However, considering that plateaus at intermediate p/p_0 are not clearly defined and that there are some low hysteresis loops, materials contain also some mesopores besides predominant micropores.

The effects of chemical activation on the BET surface area, micropores volume (V_{micro}), mesopores volume (V_{meso}) and total pore volume ($V_{total} \approx V_{meso}+V_{micro}$) are summarized in Table 3. The V_{total} value was calculated from N_2 adsorption data as the volume of N_2 at a $p/p_0 = 0.99$. The V_{micro} value was determined by the NLDFT method, while the V_{meso} was obtained by the BJH method.

Activated carbons made via carbonization without any pre-treatment have relatively low specific surface area and low porosity. Pre-treatment with NaOH (*SF-Small/600/NaOH*, *SF-Huge/600/NaOH* and *SF-Huge/NaOH/600/NaOH*) significantly improves material's specific surface area (810–1290 m^2/g) and PV (0.42–0.68 cc/g). These materials are microporous with some fraction of mesopores. Nitric acid activation with subsequent carbonization allows making AC with the highest S_{BET} (up to 1755 $m^2 \cdot g^{-1}$) and porosity (up to 1.06 $cm^3\ g^{-1}$). The predominant pore size is from 1.4 to 1.9 nm, although ultramicropores (0.4–0.9 nm) are also present (Fig. 6b). In the case of NaOH activation, pore fraction with a size ~ 2 nm (mesopores) is higher than in the case of activation with nitric acid, and the predominant pore diameter shifts to 1.4–1.6 nm. Thus, alkali treatment has a double positive effect due to improving biochar wettability (Fig. S1b) and significantly increasing the average pore size of the activated carbons (Table 3). A similar effect was reported in the work [13] for activated carbon made by H_3PO_3 activation and NaOH-treatment.

Chemical composition of raw materials, pre-treated, and carbonized samples was characterized also by FTIR (Fig. 7).

As seen, all spectra have strong, broad absorption band at 3600–3300 cm^{-1} and several narrow peaks at around 3415, 3472 and 3550 cm^{-1}. The position of the broad band is characteristic to stretching vibration of hydroxyl (O—H) groups, while narrow peaks are indicative of the existence of hydrogen bonding in functional groups [22]. There is a small peak at 3230 cm^{-1} in the feedstock sample and this peak can be associated with isolated O—H groups, probably, phenolic type. This data are in an agreement with feedstock low hydrophilicity. The peaks at 2850, 2920 and 1451 cm^{-1} are attributed to CH-stretching. The band at 1616 cm^{-1} is attributed to aromatic ring vibrations: and the one at 1465 cm^{-1} - to symmetric angular deformation on the plane of the methylene groups. Peaks at 1376 and 1330 cm^{-1} are due to O—H angular deformation and C═O axial deformation, respectively [44]. The band at 1087 cm^{-1} is assigned to C—O—C asymmetric axial deformation of ether groups or C—(C═O)—C axial and angular deformation of ketones (typical position at 1300–1100 cm^{-1}). The presence of hydroxyl, carbonyl, ethers groups and aromatic compounds provides an evidence of the lignocellulosic structure of the seed husk biowastes. The feedstock spectrum is similar to one of lignocellulose materials, such as Tunisian olive-waste cakes [42], jackfruit peel waste [18], or other biochars. During carbonization, some bands disappear or broaden, indicating weak bonds breaking. Broaden bands are observed at 3430 and 1096 cm^{-1}. According to Silverstein [44], these bands can be assigned to O—H bonds and symmetric and asymmetric C—O—C stretching vibration of ether groups, respectively. Thus, acid treatment and carbonization increase the amount of oxygen-containing functional groups, especially hydrogen bonded OH groups (at 3430 cm^{-1}). Also, it is worth noting the appearance of a new band at 1736 cm^{-1}. This band is characteristic for the C═O vibration of carboxylic groups. However, it can be seen that this band is much more prominent for carbon samples produced by heating at 600 °C than for the initial by-products, also, a result that may be due to the increased amount of oxygen in the samples.

3.2. Adsorption properties of activated carbons

Typically, solutions containing specific model substances (analytes)

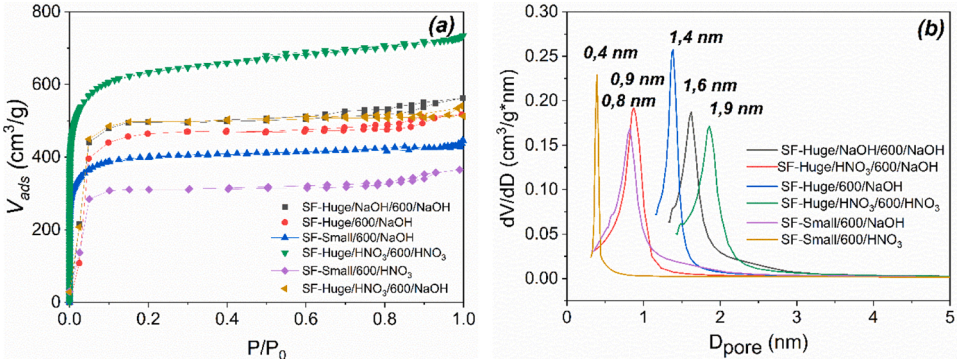

Fig. 6. (a) N_2 Adsorption-desorption isotherms at 77 K and (b) pore distribution by DFT analysis for AC samples.

Table 3
Elemental composition and textural parameters of AC prepared under various conditions.

Sample	Elemental analysis				Textural parameters			
	C (%)	H (%)	S (%)	N (%)	S_{BET} (m^2/g)	V_{total} (cm^3/g)	V_{micro} (cm^3/g)	V_{meso} (cm^3/g)
SF-Small/600/HNO_3	75.3	1.6	1.0	2.5	620	0.303	0.201	0.102
SF-Small/600/NaOH	72.8	1.5	0.7	3.6	810	0.421	0.301	0.120
SF-Huge/600/NaOH	–	–	–	–	907	0.524	0.400	0.124
SF-Small/HNO_3/600/HNO_3	75.8	1.7	–	2.6	1579	0.752	0.191	0.561
SF-Huge/600/HNO_3	77.7	1.8	–	2.1	–	–	–	–
SF-Huge/HNO_3/600/NaOH	–	–	–	–	1718	1.063	0.428	0.635
SF-Huge/NaOH/600/NaOH	–	–	–	–	1078	0.603	0.454	0.159
SF-Huge/HNO_3/600/HNO_3	74.6	1.7	–	3.8	1755	0.687	0.449	0.238
SF-Huge/NaOH/600/NaOH	81.4	1.7	–	1.1	1290	0.674	0.458	0.216

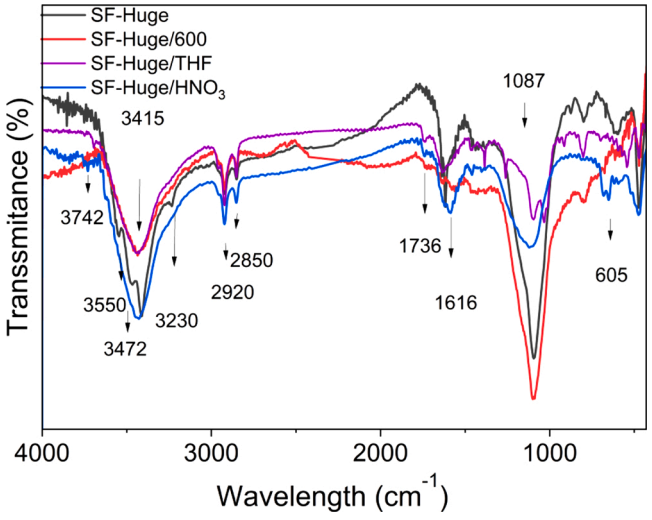

Fig. 7. FTIR spectra of the feedstocks and derivates samples.

with well researched properties are used in adsorption tests of novel materials. A number of test molecules can be applied: for instance, phenol, iodine and methylene blue are commonly used as model compounds. All adsorption experiments were carried out with Methylene Blue as adsorbate. MB is a cationic thiazine dye. MB properties are well known, and MB is widely used as a probe molecule for porous materials characterization [45]. Also, MB is an organic pollutant of industrial genesis being toxic for human and aquatic life [46]. Consequently, there is a need for the adsorption removal of such dyes from wastewater for environment protection.

3.2.1. Adsorption capacities and removal efficiency

The maximum adsorption capacity (q_e (mg g^{-1})) is an important parameter for comparison of adsorbents, as well as for evaluation of materials cost efficiency in industrial applications. Methylene blue adsorption capacities of the tested materials in comparison with the benchmark AC from Norit are presented graphically in Fig. 8. Specific surface areas of all materials are plotted in the graph also.

The experimental data show that MB uptake on activated carbons is significantly higher than on pre-treated or carbonized samples (Fig. 8). A possible reason for this could be presence in AC of oxygen-containing functional groups providing high affinity to the hydrophilic thiazine dye. The *SF-Huge/600* and *SF-Huge/NaOH* samples achieved similar MB removal efficiencies near 100 mg g^{-1} range, as opposed to the low uptake by the *SF-Small/600*. Adsorption of MB on carbon-based samples is in the range from 70 to 370 mg g^{-1} and changes in the following order: *SF-Small/600* < *SF-Huge/600* < SF-Small/600/HNO_3 < *SF-Huge/THF* < *SF-Huge/600/NaOH* ≈ *SF-Huge/THF/HNO_3* < *SF-Huge/NaOH/600/HNO_3* < *SF-Huge/NaOH/600/NaOH* < *SF-Huge/HNO_3/600/HNO_3*. Low capacities of *SF-Huge/600, SF-Small/600 and SF-Huge/NaOH* directly relate to their poor textural properties (low specific surface area/pore volume) (Table 2). These materials have been removed from further studies. The highest adsorption is shown by the sample *SF-Huge/HNO_3/600/HNO_3* (Fig. S4), having also the highest specific surface area and a significant fraction of mesopores (Table 3). High specific surface area and mesoporosity are beneficial factors for sorption of organic dyes [47, 48]. *SF-Huge/THF and SF-Huge/THF/HNO_3* show unexpectedly high MB uptake despite relatively low specific surface area (Fig. 8). This phenomenon can be related to intercalation of MB, having molecular diameter 0.8 nm (size 1.43 × 0.61 × 0.40 nm), in-between layers of adsorbent (0.9 nm openings, Table 2). Additional activation of the sample with nitric acid (*SF-Huge/THF/HNO_3*) results in a marginal increase of adsorption capacity from 247.1 mg g^{-1} to 255.2 mg g^{-1}, but in a significant increase of the specific surface area from 272 m^2 g^{-1} to 355 m^2 g^{-1}. These data suggest that activation of the surface of the adsorbent increases the affinity towards the adsorbate. Since, the surface area is insufficient to significantly increase the adsorption capacity of the adsorbent was increased because of added other mechanism of MB extraction due to polymolecular adsorption effect in the high interplanar

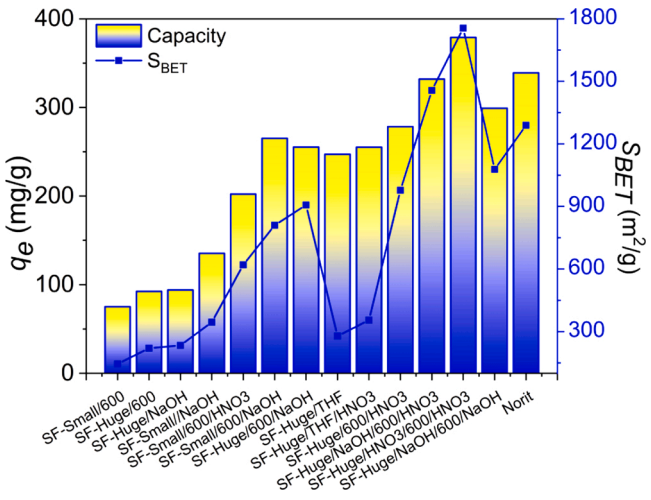

Fig. 8. Relation between specific surface areas and maximum adsorption capacity of carbon-based materials (Experimental conditions: initial MB concentration = 15 mg L^{-1}, contact time = overnight, pH = 6.0).

distance in *SF-Huge/THF/HNO$_3$*. These results confirm the role of intercalation in MB adsorption.

The data presented in Fig. 8 show that sunflower agricultural biowastes can be converted into activated carbons possessing high adsorption capacity towards MB (370 mg· g^{-1}), which is comparable to adsorption capacity of benchmark AC from company *Norit* and superior with respect to some other commercial materials such as *Filtrasorb 400* and *Picacarb* (adsorption capacity 319 ± 14 and 260 ± 6 mg g^{-1}, respectively) [43,45].

Adsorption of cationic dyes, including MB, on activated carbons is driven by electrostatic attraction and π−π stacking interactions between the aromatic rings of the carbon adsorbent and the adsorbate molecules [49]. This means that such factors as adsorbent surface area charge and solution pH should have a significant impact on the dyes adsorption. Low-cost AC materials from sunflower wastes can be efficient adsorbents for removal of organic pollutants from neutral aqueous solutions. Based on screening test, four samples (*SF-Huge/THF*, *SF-Huge/600/HNO$_3$*, *SF-Huge/NaOH/600/NaOH* and *SF-HugeHNO$_3$/600/HNO$_3$*) were selected as the most promising for further evaluation.

3.2.2. Adsorption kinetics

The adsorption kinetics was studied to determine the time required to achieve equilibrium. Kinetics of Methylene blue adsorption on three samples is presented in Fig. 9.

The data show that MB removal by *SF-HugeHNO$_3$/600/HNO$_3$* takes place extremely fast in the first 5 min of contact and then process slows down until reaching equilibrium (in ~15 min). High adsorption rate on the initial stage is due to higher MB concentration gradient and availability of larger number of active sites on the carbon adsorbent [50]. In the cases of *SF-Huge/HNO$_3$/600* and *SF-Huge/NaOH/600/NaOH* samples, the first stage removal rate is not as fast, but the rate of MB uptake gradually increases until reaching equilibrium (~30 min). Lagergren pseudo-first-order [51] and pseudo-second-order [52] models were used for evaluation of the MB adsorption kinetics on the tested AC samples (Table 4).

Pseudo-first order model does not give a good prediction of the MB adsorption on ACs, as evidenced by the poor linear fitting to the experimental data. The correlation coefficient (R^2) for the pseudo-second-order adsorption model for the AC samples (*SF-Huge/NaOH/600/NaOH* and *SF-HugeHNO$_3$/600/HNO$_3$)* is very close to 1 (Table 4). Calculated equilibrium adsorption concentrations (q_e, mg g^{-1}) are in a good agreement with the experimental data. This indicates that the pseudo-second-order adsorption mechanism is predominant and that the overall rate of MB adsorption process is controlled by chemisorption. On other hand, the adsorption kinetics for *SF-Huge/HNO$_3$/600* follows to some extent the pseudo-fist-order model.

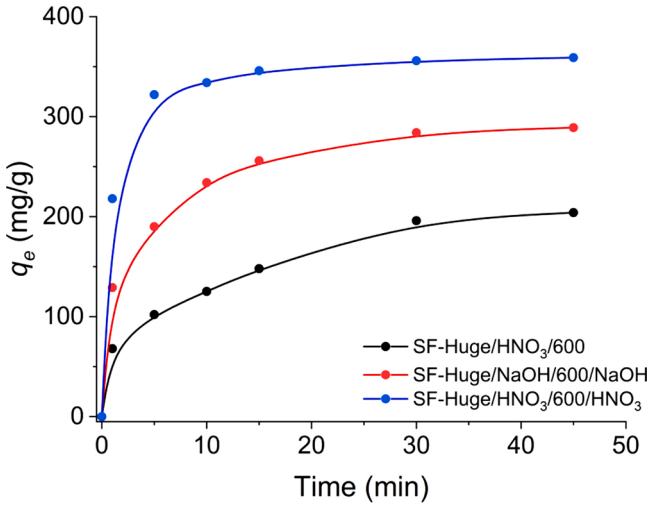

Fig. 9. Effect of contact time on MB removal (Experimental conditions: solution volume 25 mL, initial solution concentration 1000 mg L^{-1}, adsorbent weight 0.05 g, pH = 6.0, ambient temperature).

3.2.3. Adsorption isotherms

Equilibrium data, commonly known as adsorption isotherms, describe how adsorbate (MB) interacts with the surface of adsorbents, and give a comprehensive understanding of the mechanism of these interactions. Such understanding is important for optimization of adsorbent preparation (Fig. 10).

The data show that adsorption capacity increases in all cases with an increase of MB equilibrium concentration. Langmuir and Freundlich models were used for analysis of the equilibrium data in this study [53]. The parameters obtained from the different models are summarized in Table 5. The individual linearized forms of adsorption isotherms are presented in Fig. S5.

Langmuir R_L^2 values for active carbons and biochar are >0.99, which is significantly higher than the corresponding Freundlich R_F^2 values 0.57−0.82 (Table 5). This suggests that Langmuir model describes experimental data better, and that MB uptake is predominantly a chemisorption within the monolayer. Authors in [53] came to a similar conclusion on Langmuir model applicability. On the other hand, the R_F^2 values from the Freundlich model for *SF-Huge/600/HNO$_3$* and *SF-Huge/THF* samples are sufficiently high (0.750 and 0.818) thus suggesting some contribution of physical adsorption. These can be attributed to the heterogeneous nature of biochar surfaces.

3.2.4. Effect of various factors on MB removal efficiency and adsorption mechanism

Adsorption of cationic dyes, including MB, is controlled by electrostatic interaction with functional groups on the surface of adsorbent [49]. As a result, surface charge has a significant effect on dyes adsorption. Adsorbent surface charge can be predicted for different solutions by knowing the point of zero charge (PZC). In general, adsorption of cationic dyes is favoured when the solution pH is higher than the pH_{PZC} and media surface is charged negatively, while adsorption of anionic organic molecules takes place in solutions with pH < pH_{PZC}, where media surface is charged positively. This is valid also for adsorption of metal cations and inorganic anions by activated carbons. The pH_{PZC} values for *SF-Huge/HNO$_3$/600/HNO$_3$* and *SF-Huge/NaOH/600/NaOH* samples are 6.32 and 6.59, respectively (Fig. 11).

This difference in pH_{PZC} values is not significant and can be explained by higher content of oxygen-containing functional groups in *SF-Huge/HNO$_3$/600/HNO$_3$* sample. MB adsorption on *SF-Huge/HNO$_3$/600/HNO$_3$* and *SF-Huge/NaOH/600/NaOH* samples is low under acidic conditions (pH < pH_{PZC}) due to surface protonation leading to dye repulsion. Furthermore, the H^+ ions available in the aqueous solution may interfere with the adsorption sites in ACs.

The effect of the surface chemistry of the carbon materials on the adsorption process with MB was studied with FTIR spectroscopy (Fig. 12).

MB sorption on activated carbons makes multiple changes in FTIR spectra (Fig. 12) in comparison with the spectra of the initial samples (Fig. 7). Namely, a large number of new absorption peaks appears, which suggests materials complexity. The most intensive bands are present at 3420, 2920, 2850, 1715, 1610, 1487, 1140, 1070 and 883 cm^{-1}. The weak band at 2710 cm^{-1} shows C-N-group, two weak peaks at 3043 and 2960 cm^{-1} represent the stretching vibrations of —CH— aromatic and —CH$_3$ methyl groups of the MB dye. The intensive band at 1310 cm^{-1} is due to valence oscillations of C—S bonds of the dye [44]. After adsorption of Methylene blue, peaks assigned to the stretch vibration of hydroxyl groups participating in hydrogen bonds and C═C stretch vibrations of aromatic rings shift from 3430 cm^{-1} and 1630 cm^{-1} to 3420 cm^{-1} and 1610 cm^{-1}, respectively. This is a result of electrostatic interactions surface-adsorbate and π−π stacking interactions between MB and the carbon matrix, respectively. Moreover, intensities of

Table 4
Experimental (q_{exp}) and calculated kinetic parameters for the removal of MB.

Sample	*q_{exp}, mg g^{-1}	Pseudo-first-order model			Pseudo-second-order model		
		q_e, mg g^{-1}	K_1, min^{-1}	R^2	q_e, mg g^{-1}	K_2, g mg^{-1} min^{-1}	R^2
SF-Huge/HNO₃/600	204.05	209.18	0.11	0.9802	217.39	0.0012	0.9746
SF-Huge/NaOH/600/NaOH	289.06	206.91	0.12	0.9931	294.12	0.0020	0.9964
SF-Huge/HNO₃/600/HNO₃	369.20	128.38	0.12	0.9149	367.14	0.0052	0.9997

Notes. *-from data of Fig. 8.

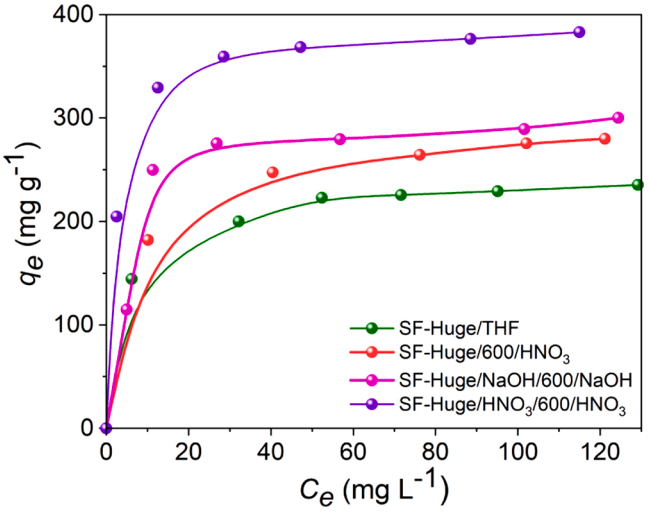

Fig. 10. MB adsorption isotherms on carbon-based materials. Experimental conditions: solution volume 25 mL, solution concentration 100–1000 mg L^{-1}, adsorbent weight 0.05 g, contact time – 1 h, pH = 6.0, ambient temperature.

Table 5
Langmuir and Freundlich models summary of equilibrium isotherm parameters.

Sample	q_{exp}, (mg g^{-1})	Model Langmuir $\frac{C_e}{q_e}=\frac{C_e}{q_m}+\frac{1}{K_L q_m}$			Model Freundlich $logq_e = logK_F + \frac{1}{n} logC_e$		
		q_m, (mg g^{-1})	K_L, (L μg^{-1})	R_L^2	K_F, (mg g^{-1})	N	R_F^2
SF-Huge/THF	235.35	238.10	1.000	0.998	3.691	0.997	0.750
SF-Huge/600/HNO₃	279.90	285.71	1.000	0.998	2.606	1.103	0.818
SF-Huge/NaOH/600/NaOH	300.02	303.03	1.000	0.997	5.846	0.987	0.680
SF-Huge/HNO₃/600/HNO₃	382.90	384.62	1.000	0.999	10.394	0.926	0.574

the three bands attributed to the adsorbed dye in spectrum of the *SF-Huge/HNO₃/600/HNO₃* sample are somewhat stronger in comparison with the *SF-Huge/HNO₃/600* sample, and this is a direct result of higher dye uptake by *SF-Huge/HNO₃/600/HNO₃*.

3.2.5. Regeneration of adsorbents

Possibility of spent media regeneration is important for cost-efficient use of adsorbent in multiple sorption-desorption cycles, as well as for estimation of adsorbate binding strength. It is well known that mineral acids can be used for efficient removal of cationic species from spent media. In this case, fast desorption was observed using 1 mol L^{-1} HCl solution (Fig. 13).

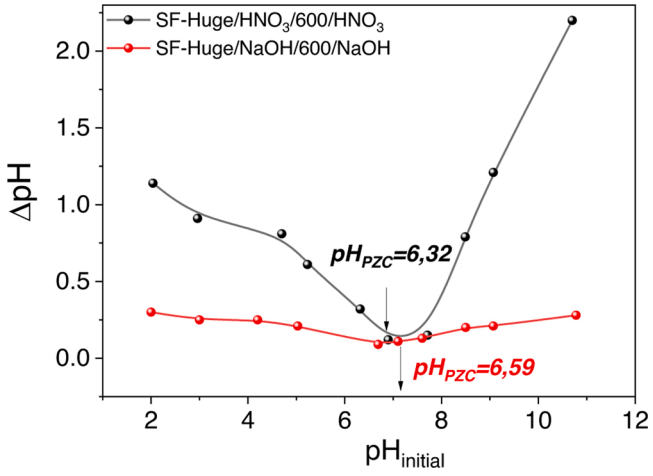

Fig. 11. PZC of the *SF-Huge/NaOH/600/NaOH* and *SF-Huge/HNO₃/600/HNO₃* samples.

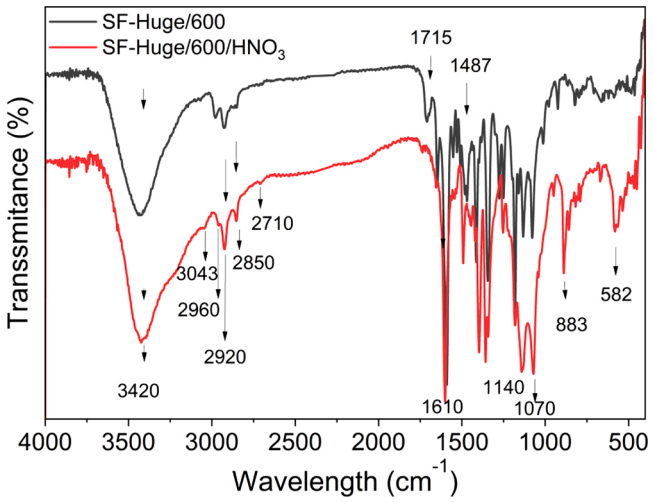

Fig. 12. FTIR spectra of MB-loaded adsorbents.

The data presented in Fig. 13 indicate that the adsorption capacity towards MB decreases only marginally after the first 3 regeneration cycles. Thus, all tested materials can be used in multiple sorption/desorption cycles. However, acid regeneration of spent media, especially in the case of a high affinity to adsorbate, is not always the best route due to generation of a large volume of liquid wastes. Thermal regeneration of adsorbents to remove adsorbed organics is another promising route. Heat treatment of MB-loaded carbon samples at 300 °C for 1 h was carried out. According to FTIR, all peaks assigned to the adsorbed MB disappeared, indicating a high efficiency of this approach.

In economic terms, the solvent, acid-alkali and carbonization pre-treated samples are a good choice for use as adsorbents for removal of

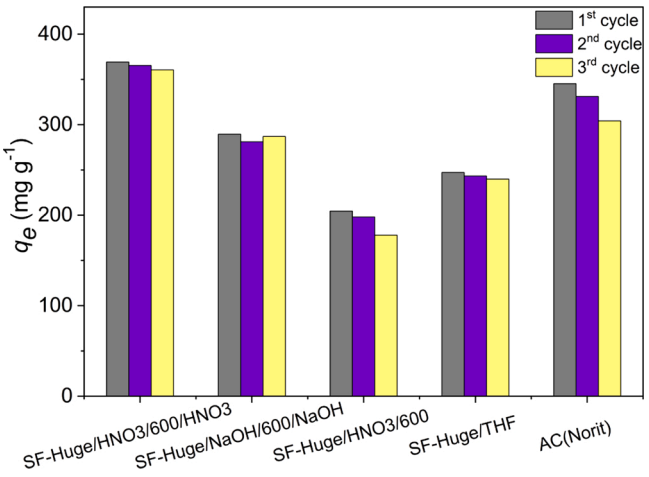

Fig. 13. MB adsorption capacity in three consecutive adsorption/regeneration cycles (Experimental conditions: C_{HCl} = 1 mol L^{-1}, total volume 10 mL, adsorbent weight 50 mg, contact time = 1 h, ambient temperature).

organic pollutants due to their low cost compared to activated carbon with high adsorption parameters (*SF-Huge/NaOH/600/NaOH* and *SF-Huge/HNO_3/600/HNO_3*), which is usually more expensive. Tetrahydrofuran pre-treatement processes do not only reduce the preparation time but successfully produce well-developed porous structures with good adsorption capacity. In environmental terms, commercial preparation of AC is regarded pretty toxic, whereas the biochar can be considered a 'green' material since it is nontoxic and produced from a secondary natural resource.

The obtained ACs can be economically beneficial when applied for adsorption of organic dyes from aqueous solutions. Thus, a straightforward, effective procedure for the preparation of a series of carbon materials from sunflower biomass by-products was developed that has a variety of water treatment and agricultural applications.

4. Conclusions

Sunflower biomass by-products from power plant are abundant and low-cost materials. Sunflower biomass was used as feedstock in preparation of biochar and activated carbons. Three different approaches: solvent, acid-alkali and carbonization pre-treatment processes were used for preparation of low-cost carbon-based materials for sorption applications. It was found that the solvent pre-treatment provides materials with superior textural (high fraction of mesopores) and adsorption properties in comparison with carbons made via the acid-alkali pretreatment route. Pre-treatment with tetrahydrofuran significantly reduces preparation time and overall cost and allows manufacturing of materials with well-developed porosity. Carbonization or thermal activation of sunflower by-products was performed in the presence of HNO_3 and/or NaOH at 600 °C. Experimental data show that: 1) untreated sunflower feedstock has low surface area and poor developed porosity; 2) feedstock treatment/activation with HNO_3 (65 %) and NaOH (50 %) yields biochars with better textural and sorption properties than of the biochars prepared by the heat treatment at 600 °C; 3) the acid activation of the biochars produces activated carbons basic in nature with oxygen-containing functional groups on the surface; 4) the activated carbons prepared via the HNO_3 activation route have superior textural properties (specific surface area/pore volume) in comparison with the materials prepared by the NaOH activation. However, both activating agents yield ACs with high adsorption capacity. High affinity of the adsorbents towards Methylene blue dye relates to their porous structure and presence of a variety of functional groups on the surface, which makes such ACs promising for water purification and cleansing waste waters of organics. Thus, sunflower biomass by-products from power plants have excellent application prospects because of their abundant feedstock, low cost and low environmental impact.

Author statement

Tatiana S. Hubetska: Formal analysis, Investigation, Data curation, Writing - original draft. **Natalia G. Kobylinska**: Conceptualization, Methodology, Formal analysis, Investigation, Data curation, Resources, Writing - review & editing, Supervision. **José R. García**: Conceptualization, Resources, Writing - review & editing, Supervision, Project administration, Funding acquisition.

Declaration of Competing Interest

The authors report no declarations of interest.

Acknowledgements

The University of Oviedo is grateful for financial support from Spain's Ministry for the Economy and Business - MINECO (MAT2016-78155-C2-1-R).

Appendix A. Supplementary data

Supplementary material related to this article can be found, in the online version, at doi:https://doi.org/10.1016/j.jaap.2021.105237.

References

[1] J.M.D. Tascón, Novel Carbon Adsorbents, 1st ed., Elsevier, 2012.
[2] J.C. Moreno-Piraján, L. Giraldo, Activated carbon obtained by pyrolysis of potato peel for the removal of heavy metal copper (II) from aqueous solutions, J. Anal. Appl. Pyrolysis 90 (2011) 42–47, https://doi.org/10.1016/j.jaap.2010.10.004.
[3] L. Singh, V.C. Kalia, Waste biomass management - a holistic approach. Waste Biomass Manag. - A Holist. Approach, 2017, pp. 1–392, https://doi.org/10.1007/978-3-319-49595-8.
[4] Z. Zou, Y. Tang, C. Jiang, J. Zhang, Efficient adsorption of Cr(VI) on sunflower seed hull derived porous carbon, J. Environ. Chem. Eng. 3 (2015) 898–905, https://doi.org/10.1016/j.jece.2015.02.025.
[5] S. Huang, T. Wang, K. Chen, M. Mei, J. Liu, J. Li, Engineered biochar derived from food waste digestate for activation of peroxymonosulfate to remove organic pollutants, Waste Manag. 107 (2020) 211–218.
[6] D. Angela, D. Genuino, M. Daniel, G. De Luna, S.C. Capareda, Improving the surface properties of municipal solid waste-derived pyrolysis biochar by chemical and thermal activation : optimization of process parameters and environmental application, Waste Manag. 72 (2018) 255–264, https://doi.org/10.1016/j.wasman.2017.11.038.
[7] H. Jin, S. Capareda, Z. Chang, J. Gao, Y. Xu, J. Zhang, Biochar pyrolytically produced from municipal solid wastes for aqueous As(V) removal: adsorption property and its improvement with KOH activation, Bioresour. Technol. 169 (2014) 622–629, https://doi.org/10.1016/j.biortech.2014.06.103.
[8] A.A. Anceschi, F. Guerretta, M. Zanetti, P. Benzi, F. Trotta, F. Caldera, R. Nistic, Sustainable N-containing biochars obtained at low temperatures as sorbing materials for environmental application: municipal biowaste-derived substances and nanosponges case studies, J. Anal. Appl. Pyrolysis 134 (2018) 606–613, https://doi.org/10.1016/j.jaap.2018.08.010.
[9] W.J. Liu, H. Jiang, H.Q. Yu, Development of biochar-based functional materials: toward a sustainable platform carbon material, Chem. Rev. 115 (2015) 12251–12285, https://doi.org/10.1021/acs.chemrev.5b00195.
[10] R. Pietrzak, P. Nowicki, J. Kaźmierczak, I. Kuszyńska, J. Goscianska, J. Przepiórski, Comparison of the effects of different chemical activation methods on properties of carbonaceous adsorbents obtained from cherry stones, Chem. Eng. Res. Des. 92 (2014) 1187–1191, https://doi.org/10.1016/j.cherd.2013.10.005.
[11] Q. Wang, Z. Lai, J. Mu, D. Chu, X. Zang, Converting industrial waste cork to biochar as Cu (II) adsorbent via slow pyrolysis, Waste Manag. 105 (2020) 102–109, https://doi.org/10.1016/j.wasman.2020.01.041.
[12] S. Wang, G. Dai, H. Yang, Z. Luo, Lignocellulosic biomass pyrolysis mechanism: a state-of-the-art review, Prog. Energy Combust. Sci. 62 (2017) 33–86, https://doi.org/10.1016/j.pecs.2017.05.004.
[13] T.H. Liou, Development of mesoporous structure and high adsorption capacity of biomass-based activated carbon by phosphoric acid and zinc chloride activation, Chem. Eng. J. 158 (2010) 129–142, https://doi.org/10.1016/j.cej.2009.12.016.
[14] O. Ioannidou, A. Zabaniotou, Agricultural residues as precursors for activated carbon production-A review, Renew. Sustain. Energy Rev. 11 (2007) 1966–2005, https://doi.org/10.1016/j.rser.2006.03.013.

[15] Z. Wang, J. Wu, T. He, J. Wu, Corn stalks char from fast pyrolysis as precursor material for preparation of activated carbon in fluidized bed reactor, Bioresour. Technol. 167 (2014) 551–554, https://doi.org/10.1016/j.biortech.2014.05.123.
[16] D. Angin, T.E. Köse, U. Selengil, Production and characterization of activated carbon prepared from safflower seed cake biochar and its ability to absorb reactive dyestuff, Appl. Surf. Sci. 280 (2013) 705–710, https://doi.org/10.1016/j.apsusc.2013.05.046.
[17] S. Kizito, S. Wu, W.K. Kirui, M. Lei, Q. Lu, H. Bah, R. Dong, Science of the Total Environment Evaluation of slow pyrolyzed wood and rice husks biochar for adsorption of ammonium nitrogen from piggery manure anaerobic digestate slurry, Sci. Total Environ. 505 (2015) 102–112, https://doi.org/10.1016/j.scitotenv.2014.09.096.
[18] D. Prahas, Y. Kartika, N. Indraswati, S. Ismadji, Activated carbon from jackfruit peel waste by H3PO4 chemical activation: pore structure and surface chemistry characterization, Chem. Eng. J. 140 (2008) 32–42, https://doi.org/10.1016/j.cej.2007.08.032.
[19] I.I. Gurten, M. Ozmak, E. Yagmur, Z. Aktas, Preparation and characterisation of activated carbon from waste tea using K2CO3, Biomass Bioenergy 37 (2012) 73–81, https://doi.org/10.1016/j.biombioe.2011.12.030.
[20] S. De Gisi, G. Lofrano, M. Grassi, M. Notarnicola, Characteristics and adsorption capacities of low-cost sorbents for wastewater treatment : a review, Sustain. Mater. Technol. 9 (2016) 10–40, https://doi.org/10.1016/j.susmat.2016.06.002.
[21] P. Janos, H. Buchtova, M. Ryznarov, Sorption of dyes from aqueous solutions onto fly ash sorption of dyes from aqueous solutions onto fly ash, Water Res. 37 (2003) 4938–4944, https://doi.org/10.1016/j.watres.2003.08.011.
[22] B.S. Girgis, Eksi Sozluk, 52 (2002) 105–117. http://eksisozluk.com.
[23] K.Y. Foo, B.H. Hameed, Preparation and characterization of activated carbon from sunflower seed oil residue via microwave assisted K2CO3 activation, Bioresour. Technol. 102 (2020) 9794–9799, https://doi.org/10.1016/j.biortech.2011.08.007.
[24] X. Li, W. Xing, S. Zhuo, J. Zhou, F. Li, S. Qiao, G. Lu, Preparation of capacitor's electrode from sunflower seed shell, Bioresour. Technol. 102 (2011) 1118–1123, https://doi.org/10.1016/j.biortech.2010.08.110.
[25] M.A. Perea-Moreno, F. Manzano-Agugliaro, A.J. Perea-Moreno, Sustainable energy based on sunflower seed husk boiler for residential buildings, Sustainability 10 (2018), https://doi.org/10.3390/su10103407.
[26] D. Chen, X. Chen, J. Sun, Z. Zheng, K. Fu, Pyrolysis polygeneration of pine nut shell: quality of pyrolysis products and study on the preparation of activated carbon from biochar, Bioresour. Technol. 216 (2016) 629–636, https://doi.org/10.1016/j.biortech.2016.05.107.
[27] N. Scarlat, J.F. Dallemand, F. Monforti-Ferrario, M. Banja, V. Motola, Renewable energy policy framework and bioenergy contribution in the European Union - an overview from National Renewable Energy Action Plans and Progress Reports, Renew. Sustain. Energy Rev. 51 (2015) 969–985, https://doi.org/10.1016/j.rser.2015.06.062.
[28] X. Cui, J. Yang, X. Shi, W. Lei, T. Huang, C. Bai, Pelletization of sunflower seed husks: evaluating and optimizing energy consumption and physical properties by response surface methodology (RSM), Processes 7 (2019), https://doi.org/10.3390/pr7090591.
[29] D.J.M. Hayes, Biomass composition and its relevance to biorefining. The Role of Catalysis for the Sustainable Production of Bio-fuels and Bio-chemicals, Elsevier B. V., 2013, pp. 27–65, https://doi.org/10.1016/B978-0-444-56330-9.00002-4.
[30] J.J. Manyà, Pyrolysis for biochar purposes: a review to establish current knowledge gaps and research needs, Environ. Sci. Technol. 46 (2012) 7939–7954, https://doi.org/10.1021/es301029g.
[31] J. Paz-Ferreiro, A. Nieto, A. Méndez, M.P.J. Askeland, G. Gascó, Biochar from biosolids pyrolysis: A review, Int. J. Environ. Res. Public Health 15 (2018), https://doi.org/10.3390/ijerph15050956.
[32] G.M.J. Herbert, A.U. Krishnan, Quantifying environmental performance of biomass energy, Renew. Sustain. Energy Rev. 59 (2016) 292–308, https://doi.org/10.1016/j.rser.2015.12.254.
[33] S.V. Vassilev, D. Baxter, L.K. Andersen, C.G. Vassileva, An overview of the composition and application of biomass ash. Part 2. Potential utilisation, technological and ecological advantages and challenges, Fuel 105 (2013) 19–39, https://doi.org/10.1016/j.fuel.2012.10.001.
[34] F. Rodriguez-Reinoso, An overview of methods for the characterization of activated carbons, Pure Appl. Chem. 61 (1989) 1859–1866, https://doi.org/10.1351/pac198961111859.
[35] Q. Zhang, J. Chang, T. Wang, Y. Xu, Review of biomass pyrolysis oil properties and upgrading research, Energy Convers. Manage. 48 (2007) 87–92, https://doi.org/10.1016/j.enconman.2006.05.010.
[36] G. Liang, Y. Li, C. Yang, C. Zi, Y. Zhang, X. Hu, Production of biosilica nanoparticles from biomass power plant fly ash, Waste Manag. 105 (2020) 8–17, https://doi.org/10.1016/j.wasman.2020.01.033.
[37] S.V. Vassilev, D. Baxter, L.K. Andersen, C.G. Vassileva, An overview of the composition and application of biomass ash. Part 1. Phase – mineral and chemical composition and classification, Fuel 105 (2013) 40–76, https://doi.org/10.1016/j.fuel.2012.09.041.
[38] I.B.I. IBI, Standardized Product Definition and Product Testing Guidelines for Biochar That Is Used in Soil, Int. Biochar Initiat., 2015, 23.
[39] G. Lv, S. Wu, Analytical pyrolysis studies of corn stalk and its three main components by TG-MS and Py-GC/MS, J. Anal. Appl. Pyrolysis 97 (2012) 11–18, https://doi.org/10.1016/j.jaap.2012.04.010.
[40] A.M.M. Vargas, A.L. Cazetta, C.A. Garcia, J.C.G. Moraes, E.M. Nogami, E. Lenzi, W. F. Costa, V.C. Almeida, Preparation and characterization of activated carbon from a new raw lignocellulosic material: flamboyant (Delonix regia) pods, J. Environ. Manage. 92 (2011) 178–184, https://doi.org/10.1016/j.jenvman.2010.09.013.
[41] M. Thommes, K. Kaneko, A.V. Neimark, J.P. Olivier, F. Rodriguez-Reinoso, J. Rouquerol, K.S.W. Sing, Physisorption of gases, with special reference to the evaluation of surface area and pore size distribution (IUPAC Technical Report), Pure Appl. Chem. 87 (2015) 1051–1069, https://doi.org/10.1515/pac-2014-1117.
[42] U. Iriarte-Velasco, I. Sierra, L. Zudaire, J.L. Ayastuy, Preparation of a porous biochar from the acid activation of pork bones, Food Bioprod. Process. 98 (2016) 341–353, https://doi.org/10.1016/j.fbp.2016.03.003.
[43] Y. Azizi, B. Benhamou, N. Galanis, M. El-ganaoui, Etude De L' Effet Des Forces D' Archimede Sur Les Transferts Couples De Chaleur Et De Masse, Avec Changement De Phase, Dans Un Canal Vertical, J. Chem. Technol. Biotechnol. 88 (2013) 1183–1190, https://doi.org/10.1002/jctb.04028.
[44] R. Silverstein, F. Webster, D. Kiemle, Spectrometric Identification of Organic Compounds, 8th ed., John Wiley & Sons, 2014.
[45] F. Raposo, M.A. De La Rubia, R. Borja, Methylene blue number as useful indicator to evaluate the adsorptive capacity of granular activated carbon in batch mode: influence of adsorbate/adsorbent mass ratio and particle size, J. Hazard. Mater. 165 (2009) 291–299, https://doi.org/10.1016/j.jhazmat.2008.09.106.
[46] P.N. Patel, Methylene blue for management of ifosfamide-induced encephalopathy, Ann. Pharmacother. 40 (2006) 299–303, https://doi.org/10.1345/aph.1G114.
[47] A.M. Dehkhoda, E. Gyenge, N. Ellis, A novel method to tailor the porous structure of KOH-activated biochar and its application in capacitive deionization and energy storage, Biomass Bioenergy 87 (2016) 107–121, https://doi.org/10.1016/j.biombioe.2016.02.023.
[48] S. Yenisoy-Karakaş, A. Aygün, M. Güneş, E. Tahtasakal, Physical and chemical characteristics of polymer-based spherical activated carbon and its ability to adsorb organics, Carbon N. Y. 42 (2004) 477–484, https://doi.org/10.1016/j.carbon.2003.11.019.
[49] K. Gobi, M.D. Mashitah, V.M. Vadivelu, Adsorptive removal of Methylene Blue using novel adsorbent from palm oil mill effluent waste activated sludge: equilibrium, thermodynamics and kinetic studies, Chem. Eng. J. 171 (2011) 1246–1252, https://doi.org/10.1016/j.cej.2011.05.036.
[50] S. Azizian, Kinetic models of sorption: a theoretical analysis, J. Colloid Interface Sci. 276 (2004) 47–52, https://doi.org/10.1016/j.jcis.2004.03.048.
[51] Y.S. Ho, Citation review of Lagergren kinetic rate equation on adsorption reactions, Scientometrics 59 (2004) 171–177, https://doi.org/10.1023/B:SCIE.0000013305.99473.cf.
[52] M.G, Y.S. Ho, Pseudo-second order model for sorption processes, Process Biochem. 34 (1999) 451–465, https://doi.org/10.1016/S0032-9592(98)00112-5.
[53] T. Hubetska, N. Kobylinska, J.R. García, Efficient adsorption of pharmaceutical drugs from aqueous solution using a mesoporous activated carbon, Adsorption 26 (2020) 251–266, https://doi.org/10.1007/s10450-019-00143-0.

Supplementary materials

Sunflower Biomass Power Plant by-products: Properties and Its Potential to Respect the Water Purification of Organic Pollutants

Tatiana S. Hubetska[1], Natalia G. Kobylinska[2], Jose R. García[1]

[1]Faculty of Chemistry, University of Oviedo-CINN, Avda. Julián Clavería, 8, 33006, Oviedo, Spain, kobilinskaya@univ.kiev.ua,
[2]Faculty of Chemistry, Taras Shevchenko National University of Kyiv, 64 Volodymyrska Str, 01601, Kyiv, Ukraine,

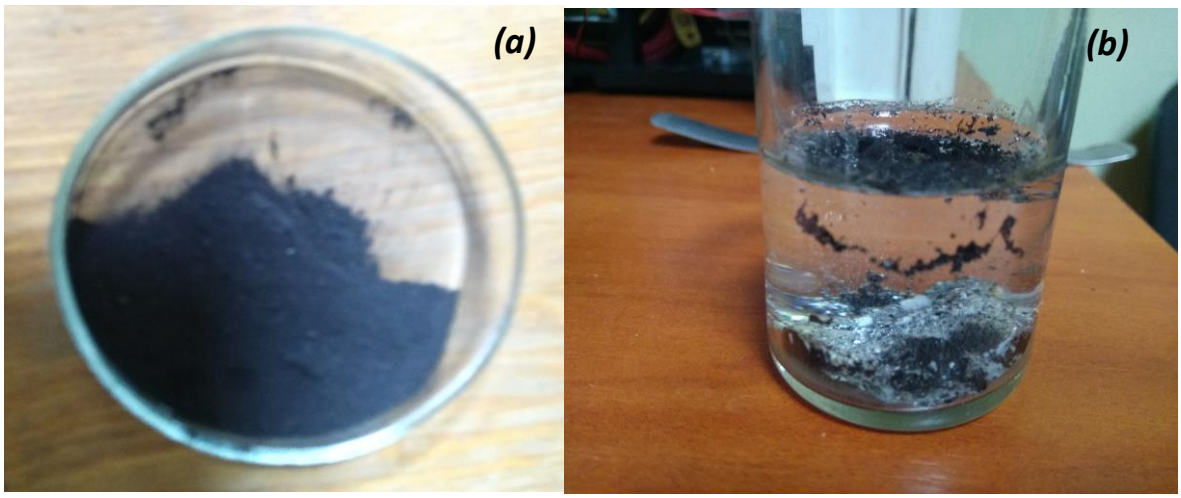

Fig. S1. Images of feedstock (SF-Huge-based): (a) initial sample and (b) its wettability (b).

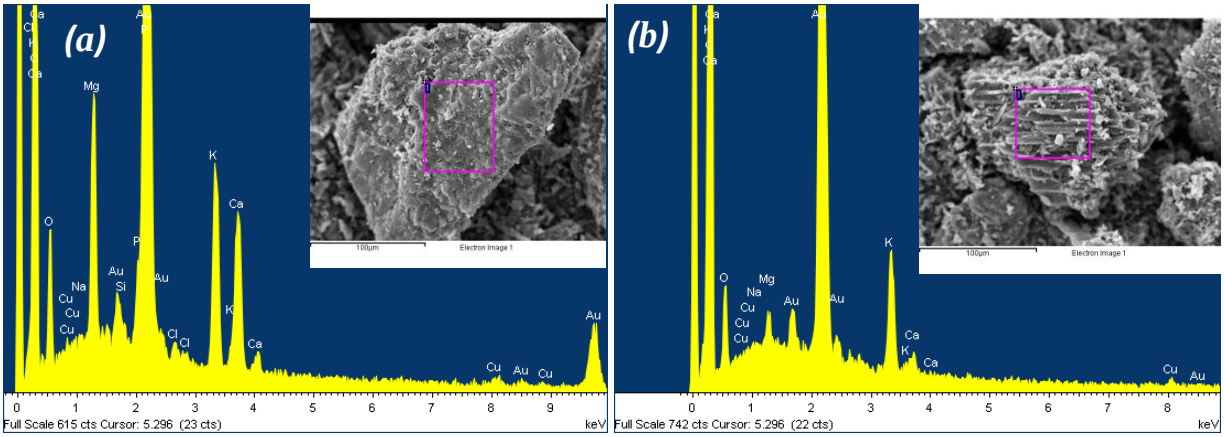

Fig. S2. SEM image ~~(a)~~ and EDX elemental analysis spectra ~~(b)~~ of SF-Small (a) and SF-Huge (b) samples.

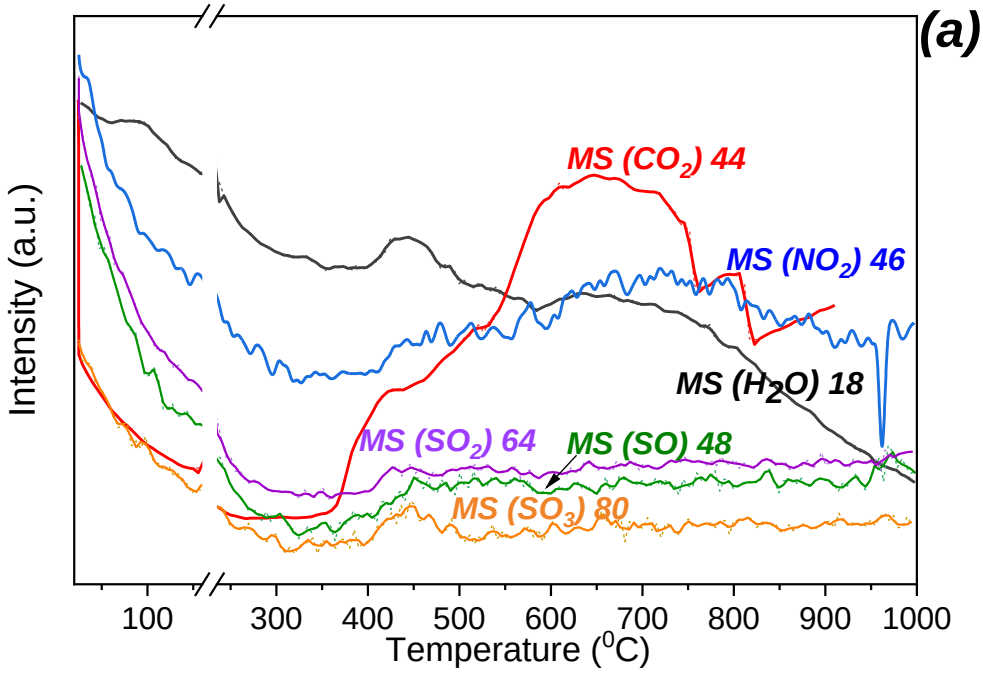

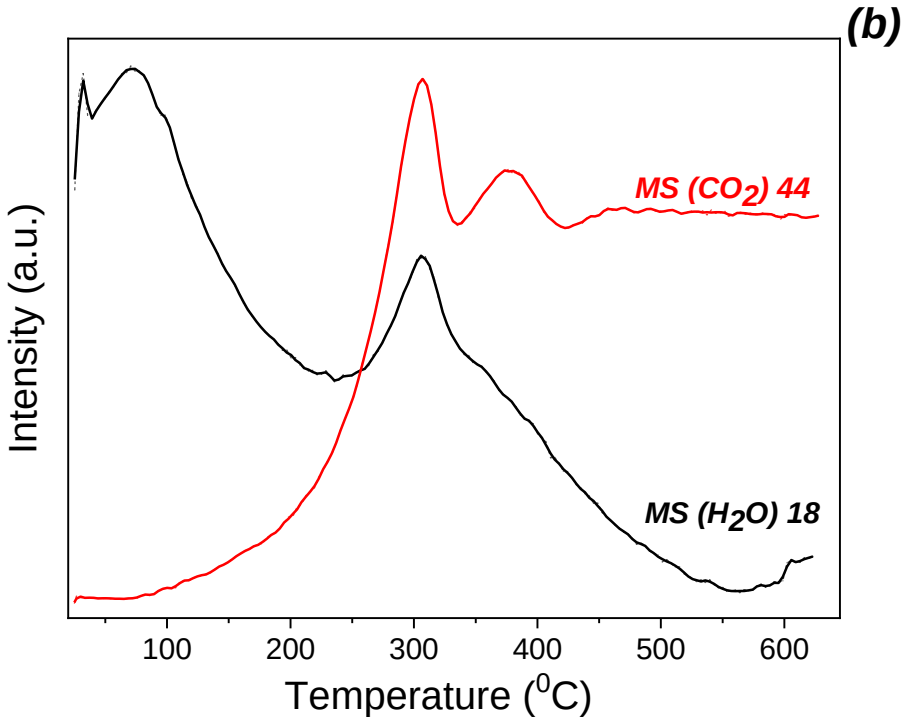

Fig. S3. Selected TGA-MS spectra of *SF-Small* and *SF-Huge* samples.

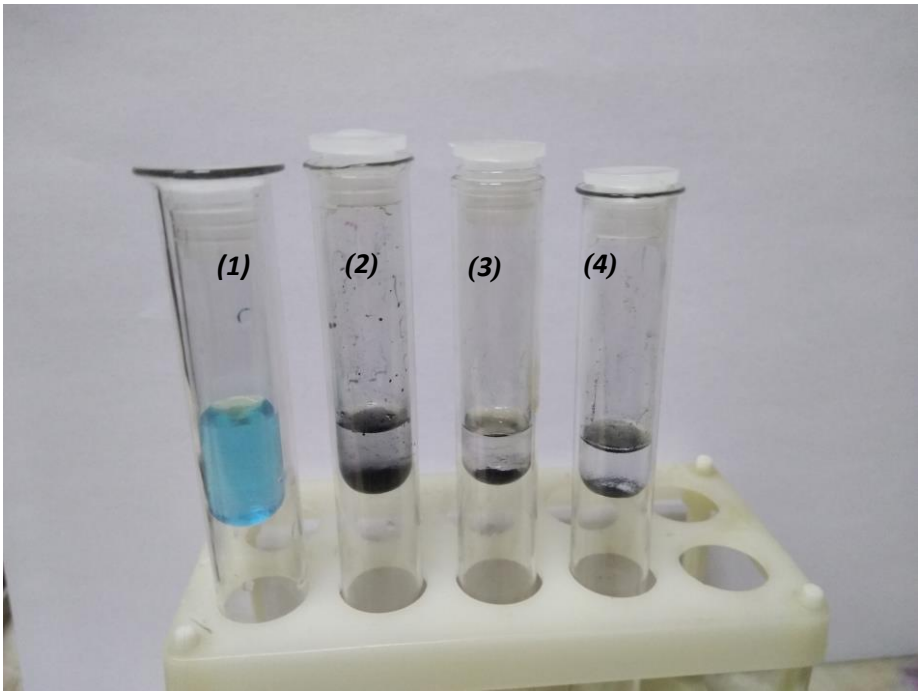

Fig. S4. Visual effect adsorption of Methylene blue on three types of ACs samples: (1) initial MB solution, (2) *SF-Huge/THF*, (3) *SF-Huge/HNO_3/600*, and (4) *SF-Huge/HNO_3/600/HNO_3*, after 3 min of contact time.

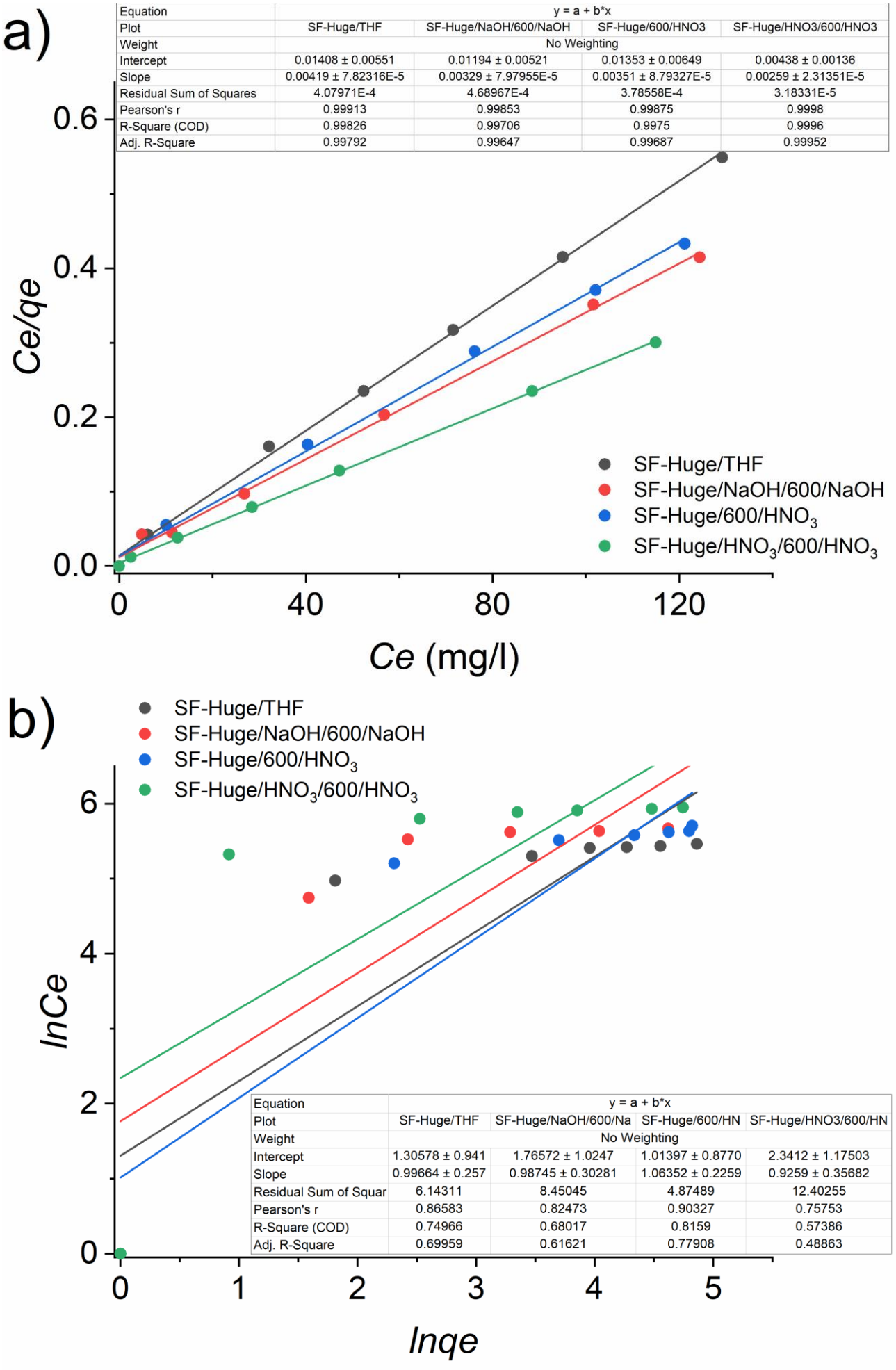

Fig. S5. The linearized forms of adsorption isotherm model Langmuir (a) and Freundlich (b).

4.2. Magnetic materials for effective removal of volatile organic compounds from aqueous and complex

This chapter is devoted to the design of hydrophobically functionalized magnetic nanocomposite for the application as adsorbents of VOCs (as an example, pesticides) in different matrixes. Pesticides (organochlorine) selected as target analytes were chosen among the most widely used in agricultural practices worldwide. Pesticides (fungicides, herbicides, insecticides, etc.) have been widely used in agriculture for the better part of the past century. While they are known to save farmers time and money, negative effects on human health and environmental situation [127] have been well described. National and international bodies have identified diffuse pollution by pesticides as a major concern. However, the actual occurrence and distribution of pesticides in the soil are poorly understood, despite soil's vital role in global biogeochemical cycles. Determination of a wide variety of pesticide residues in the soil on a regional scale has historically been difficult and expensive. In relation to the analytical techniques applied for pesticides in various matrixes, there has been a clear evolution along the time from the first analysis, commonly performed by GC-MS and/or GC-ESI, to the most recent ones, based on GC-MS, which nowadays are the techniques of choice in this field [128].

This first part of the chapter is divided into two sub-chapters addressing the questions of synthesis and characterization of magnetic core-shell nanoparticles with layers of silica and Triton X-100. The magnetic adsorbent was evaluated for the determination of pesticides in an aqueous solution.

The second part proposes a new approach for the application of obtained magnetic adsorbents for QuEChERS extraction of pesticides in food and soil matrixes was developed.

4.2.1. Hydrophobically functionalized magnetic nanocomposite as adsorbents

Usually, organic-mineral materials are used as adsorbents and demonstrate better affinity and selectivity towards target objects, for example, to organic and inorganic pollution in environmental water [129, 130, 131]. Further improvement of the adsorbent properties, such as capacity and adsorption kinetics can be achieved by reducing the particle size [132]. The critical drawback in such an approach is difficulties in phase separation. The fine nanoparticles of the adsorbent can create a stable water suspension, which essentially increases efforts in sample preparation because requires centrifugation or filtration. This drawback can be overcome by the introduction of magnetic adsorbents to sample preparation practice [133]. Because of such improvement, a small amount of

nanosized magnetic adsorbent can be used for dispersive solid-phase extraction (dSPE) of impurities from the higher volume of liquid sample, and then quickly separated from the solution by applying an external magnetic field [134]. Such a combination of dSPE with further magnetic separation is called magnetic solid-phase extraction (MSPE). In contrast to dSPE, MSPE is applied for static conditions, where adsorption equilibrium is reached and thus the results of separation are more predictable and the recovery degree of analytes could be higher than for dynamic SPE. Therefore, the application of MSPE in analytical chemistry and water treatment can receive rapid development in near future. This development is limited by several obstacles: a) size of magnetic adsorbents particles has to be in nanoscale range to ensure high surface area and adsorption capacity; b) they have to be corrosively and oxidatively stable; c) the particle surface has to be modified to increase their affinity towards low-concentration impurities.

Magnetic particles consist of magnetic elements (iron, nickel, cobalt) and exhibit ferromagnetic, paramagnetic, or superparamagnetic properties [135]. However, to be applied for MSPE, magnetic particles should possess superparamagnetic properties: they have to be attracted to a magnetic field, but the magnetic properties of the particles should not remain after the elimination of the magnetic field. Bare magnetite nanoparticles (MNPs) are not suitable for water treatment since they can be quickly oxidized from the surface, demonstrate low affinity to metal ions and bad adsorption kinetics [136]. Core-shell magnetic particles have much better corrosion stability and higher adsorption capacity due to the porous structure of the shell. Different materials were tested as coatings for MNPs, such as carbon nanotubes [137], graphene oxide [138], polymeric films [139], and inorganic oxides include silica, alumina, zirconium [137, 140]. It can hardly be expected that carbon nanotubes or graphene oxide can protect the magnetic core from corrosion. Polymeric films can offer such protection but commonly not a mesoporous structure of the shell. Silica shell can do both: protect the particles from corrosion in a wide range of solution pH (0.5-8.5) and increase the surface area of the particles (and so the adsorbent capacity). Additionally, silica gel shell provides a platform for further immobilization of organic functional groups over silanization reactions [141].

The most significant element to achieve sensitivity and selectivity in MSPE is the choice of the immobilized ligand [141], which provides necessary selectivity and affinity toward target molecules. Up to date, several silica coated-based nanocomposites with covalently immobilized chelating ligands were reported. Among them, MNPs with immobilized S-containing ligands, such as cysteine [142], Schiff base [143], aliphatic [144] amines were studied as adsorbent for organic and inorganic molecules in water, food, and biological samples. In this work, we report a new approach for the

preparation of magnetic nano adsorbent with covalently grafted non-ionic Triton X-100 surfactant. Mesoporous Triton X-100-immobilized magnetic nanoparticles were successfully synthesized by core-shell technology. The produced solid was employed as an adsorbent for the pre-concentration of pesticides present in water medium before analyzing them by gas chromatography coupled with mass spectrometry technique.

Article IV

"*Hydrophobically functionalized magnetic nanocomposite as a new adsorbent for pre-concentration of organochlorine pesticides in water solution*"

IEEE Magnetics Letters

9 (1-5)

Year 2018

DOI: 10.1109/LMAG.2018.2824248

Impact Index: 1.540

Article V

"Application of hydrophobic magnetic nanoparticles as clean-up adsorbent for the pesticides residue analysis in fruits, vegetables and soils"

Journal of Agricultural and Food Chemistry

Year 2020

DOI: 10.1021/acs.jafc.0c00601

Impact factor: 4.192

5. Conclusions

In the present Ph.D. thesis, the morphological, textural, and surface properties of the studies materials (activated carbons and magnetic core-shell nanoparticles) for future using as adsorbents have been tuning. Special attention has been paid to establish the relationship between the structural and surface properties of the obtained materials with their adsorption performance in air and water purification. Also, new materials were performed for the preconcentration and determination of target compounds in a complicated matrix.

➢ New spherical ordered mesoporous carbon materials, with an average diameter of 0.45–0.50 mm, were obtained by carbonization via MCM-48 impregnated with polystyrene and divinylbenzene mixtures.

- Among most common chemical activation agents H_2O_2 solution was found as the optimal choice due to higher yields of high specific surface area (1680 $m^2 \cdot g^{-1}$), narrow pore size distribution (5–9 nm), and active functional groups of surface mesoporous carbons formed at oxidation by that one.
- Oxygen-rich mesoporous activated carbons demonstrate superior adsorption properties toward nicotine than its ones with high specific surface area (the maximum adsorption uptake toward nicotine from the gas phase has been estimated as 9.2 $mmol \cdot g^{-1}$).
- The synthesized mesoporous spherical adsorbents can be applied both in stationary smoking rooms and in spaces equipped with autonomous ventilation, which ones are twice more efficient than industry using granular carbons due to enhanced mass transfer in the adsorption layer of the carbon material.
- The regeneration of the adsorbents has been achieved through extraction by organic solvents or other routes.

➢ The granular mesoporous carbons were prepared via molecular sieves as templates with a solution of polystyrene and sucrose at the hydrothermal conditions. The activation process (steam-pyrolysis at 900 °C and chemical activation) was performed after removing the template. The solutions were used as the chemical activation agents: HNO_3, H_2O_2, and their mixture.

- The treatment of mesoporous carbons by chemical oxidation lead to 2.5 times more in total pore volume compared to the samples treated by steam activation at 900 °C.
- The specific surface areas of the samples initially treated only via pyrolysis are 1720-1800 $m^2 \cdot g^{-1}$ and 1760-2340 $m^2 \cdot g^{-1}$ for the chemical activation samples, respectively.
- The titration analysis indicates that there are significant differences in the surface concentrations of the total acidic functional groups of the pristine and activated carbonous samples. In particular, the concentration of O-containing groups including carboxyl ones is higher after chemical activation.
- The maximum uptake capacity found at 909.2 $mg \cdot g^{-1}$ (at pH 7) for tetracycline as the model analytes for carbon material activated by HNO_3 and H_2O_2.
- The kinetics of tetracycline adsorption fits the pseudo-second-order model better. The adsorption data calculated by Langmuir and Freundlich models indicates that the adsorption was monomolecular.
- The mesoporous carbons after oxidation by a mixture of HNO_3 and H_2O_2 with ration 1:1 exhibited higher adsorptive activity and demonstrated relatively high adsorption after five adsorption/desorption cycles of regeneration.
- The relationship between the adsorption behavior and the surface acid–base properties of the carbonous adsorbents was studied.
- These carbon adsorbents may apply in the removal of different organic compounds from municipal wastewater.

In the second part of this study, a novel functionalized magnetic nanocomposite has been prepared. The magnetic nanocomposite covered with layers of silica and Triton X-100 has been synthesized through a step-by-step “post-synthesis assembly” strategy.

- The powder XRD patterns indicate that the obtained samples Fe_3O_4, Fe_3O_4/GTMO, and Fe_3O_4/Triton have the same set of diffraction maxima implying that the crystal structure of the Fe_3O_4 nanoparticles embedded in SiO_2 remains unchanged with average crystallite sizes are 12.2, 17.9, and 19.6 nm, respectively.
- The initial magnetite sample is non-porous material with superparamagnetic properties. The specific surface area increase in the modified nanocomposites up to 150 $m^2 \cdot g^{-1}$ is due to the porosity silica coat layer.

- Covalent anchoring of MNPs was found to enhance the stability without aggregation effect and increasing adsorption performance. The hyperbranched 4-(1,1,3,3-tetramethylbutyl)-phenyl groups of nanocomposites improve greatly affinity toward pesticides than known several hydrophobic adsorbents. It is a key issue to combine the characteristics and advantages of both the hydrophobic functional groups of nonionic surfactant and magnetic extraction effect.
- The proposed method of OCPs determination in water medium demonstrated good linearity ($R^2 > 0.9915$) in the range of 1–10000 $ng \cdot kg^{-1}$, with the LOD of 0.5-1.0 $ng \cdot kg^{-1}$ at S/N = 3, and precision of RSD was ≤ 11.8 %. The pre-concentration factors obtained under the optimal conditions have been in the range of 2362–10593 for 100 mL water sample solution.
- The hydrophobic MNPs have been applied as an effective cleanup adsorbent in the extract purification of different matrices for the QuEChERS procedure as an alternative cleanup agent comparing to commercial C18, GCB, and bare MNPs. Magnetic Fe_3O_4@Triton adsorbents provided the lowest level of co-extracted interference compounds in the food samples i.e. showed better cleanup performance than C18 and GCB. Compared with the QuEChERS method based on GCB and C18, the present by our method can provide savings in terms of pretreatment time, simplicity, and high throughput.
- The results of the cleanup performance of modified QuEChERS procedure for determination of target OCPs by GC-MS detection showed good linearity ($R^2 \geq 0.9916$) and the average recoveries were considered satisfactory, obtaining values of between 84.0 and 108.0% (71.0−103.0% for soil), an RSD of 2.5−7.8% (1.0−12.0% for soil). LOQ and LOD ranged from 0.11 to 1.85 $\mu g \cdot kg^{-1}$ and from 0.34 to 5.45 $\mu g \cdot kg^{-1}$, respectively.
- The OCPs by modified QuEChERS procedure were detected in strawberry (α-HCH, lindane, 4,4′-DDT, heptachlor), avocado (4,4′-DDD, dieldrin), watermelon (aldrin, lindane, 4,4′-DDE, 4,4′-DDD), radish (α-, β-HCH isomers, 4,4′-DDD), and kiwi flesh (lindane, dieldrin) in the real samples from a supermarket.
- The applicability of the developed procedure to very different soil types as a most complicated matrix for sample preparation by QuEChERS procedure was demonstrated. Matrix effects of soil samples were not very relevant, permitting quantification of the target OCPs using typical organic solvents. In spite of the fact that the soils used in this study have not been applied for agricultural practices for many years, four insecticides (lindane, 4,4′-DDE, 4,4′-DDD, 4,4′-DDT) were detected at low concentrations (mostly below 20 $\mu g \cdot kg^{-1}$).

- Developed a new approach regarding the usability of magnetic core−shell MNPs to remove matrix impurities based on switchable highly hydrophobic functional groups in the QuEChERS procedure, indicating the potential for the development of cleanup materials for the determination of various pesticides in complex matrixes.

Conclusiones

En la presente Tesis Doctoral, se mejoraron las propiedades morfológicas, texturales y superficiales de los materiales estudiados (carbones activados y nanopartículas de núcleo-capa magnética) para su uso futuro como adsorbentes. Se prestó especial atención a interrelacionar las propiedades estructurales y superficiales de estos materiales con su capacidad de adsorción de contaminantes en aire y en procesos de purificación de aguas. Además, se diseñaron nuevos materiales para la preconcentración y determinación de compuestos diana en matrices complejas.

- Se obtuvieron nuevos materiales de carbono mesoporosos ordenados, de forma esférica y diámetro medio de 0.45-0.50 mm, mediante carbonización via MCM-48 impregnado con mezclas de poliestireno y divinilbenceno.
  - Entre los agentes de activación química más comunes, se eligió el uso de disoluciones acuosas de peróxido de hidrógeno, que conduce a áreas superficiales específicas elevadas (1680 $m^2 \cdot g^{-1}$), distribución de tamaños de poro estrechas (5-9 nm), y presencia de grupos funcionales activos en la superficie de los carbones mesoporosos, consecuencia de procesos de oxidación.
  - En la capacidad de adsorción de nicotina en fase gas, la riqueza en grupos oxigenados de los carbones activados mesoporosos estudiados es un factor más decisivo que su área superficial específica (adsorción máxima de los materiales sintetizados = 9.2 $mmol \cdot g^{-1}$).
  - Los resultados obtenidos con los adsorbentes esféricos mesoporosos sintetizados indican que estos materiales podrían ser aplicables tanto en salas estacionarias de fumadores como en espacios equipados con ventilación autónoma.
  - La regeneración de los adsorbentes fue posible mediante extracción con disolventes orgánicos, en adición a otras vías menos eficientes.

- Se prepararon carbones mesoporosos granulares utilizando tamices moleculares como plantilla y disoluciones de poliestireno y sacarosa en condiciones hidrotermales. El proceso de activación se llevó a cabo después de la eliminación de las plantillas. Como agentes de activación química se utilizaron disoluciones acuosas de HNO_3, H_2O_2, y sus mezclas.
  - El tratamiento de los carbones mesoporosos por oxidación química duplicó el volumen de

poro total en comparación con las muestras activadas con vapor a 900 °C.

- Los rangos de áreas superficiales específicas de las muestras obtenidas por pirólisis y activadas químicamente son 1720-1800 $m^2 \cdot g^{-1}$ y 1760-2340 $m^2 \cdot g^{-1}$, respectivamente.
- Existen diferencias significativas entre las concentraciones superficiales de los grupos funcionales ácidos totales de las muestras carbonosas prístinas y activadas, observándose que la concentración de grupos oxigenados, incluyendo los carboxilo, aumenta después de la activación química.
- Se utilizó tetraciclina como especie modelo para determinar las propiedades de adsorción de carbones activados con HNO_3 y H_2O_2, obteniéndose una capacidad máxima de absorción de 909.2 $mg \cdot g^{-1}$ (pH = 7).
- El mejor ajuste de la cinética de la adsorción de tetraciclina corresponde a un modelo de pseudo segundo orden con adsorción monomolecular (Langmuir y Freundlich).
- Los carbones mesoporosos tratados con mezclas de HNO_3 y H_2O_2 (1:1) mantuvieron un buen comportamiento después de la regeneración, al menos en cinco ciclos de adsorción/desorción.
- Se estudió la relación entre el comportamiento de adsorción y las propiedades ácido-base en la superficie de los adsorbentes carbonosos.
- Se propuso el uso de estos adsorbentes carbonosos en la eliminación de compuestos orgánicos en aguas residuales urbanas.

En la segunda parte de esta Tesis, se preparó un nuevo nanocompuesto magnético funcionalizado, constituido por capas de sílice y Triton X-100, sintetizado paso a paso mediante ensamblaje post-síntesis.

- En muestras de Fe_3O_4, Fe_3O_4/GTMO y Fe_3O_4/Triton, la estructura cristalina de las nanopartículas de Fe_3O_4 no sufrió alteraciones apreciables por efecto de la incrustación en SiO_2, con tamaños de cristalito promedio de 12.2, 17.9 y 19.6 nm, respectivamente.
- La magnetita inicial (Fe_3O_4) es no porosa. El área superficial específica de los nanocompuestos modificados, a consecuencia del revestimiento de sílice, aumenta hasta 150 $m^2 \cdot g^{-1}$.
- El anclaje covalente de las nanopartículas metálicas mejoró su estabilidad, no indujo su agregación, y aumentó el rendimiento de adsorción, permitiendo combinar las ventajas de los grupos funcionales hidrófobos de tensioactivos no iónicos con la posibilidad de separación magnética del adsorbente.

- El método propuesto para la determinación de OCPs en medio acuoso demostró buena linealidad ($R^2 > 0.9915$) en un rango amplio (1-10000 $ng \cdot kg^{-1}$), con un LOD de 0.5-1.0 $ng \cdot kg^{-1}$ a S/N = 3, y una precisión RSD ≤ 11.8%, mientras los factores de pre-concentración obtenidos en condiciones óptimas estuvieron en el rango 2362-10593 (100 mL, disolución acuosa).
- Las nanopartículas metálicas hidrófobas se utilizaron como agentes de limpieza eficaces en la purificación de extractos de diferentes matrices para el procedimiento QuEChERS. Los adsorbentes magnéticos Fe_3O_4@Triton mostraron un elevado rendimiento de limpieza, superior al de los mejores compuestos comerciales.
- El procedimiento QuEChERS, modificado para la determinación de OCPs mediante GC-MS, mostró buena linealidad (R2 ≥ 0.9916), con recuperaciones promedio satisfactorias, con valores entre 84.0 y 108.0% (71.0-103.0% para suelo), y una RSD de 2.5-7.8% (1.0-12.0% para suelo). LOQ y LOD variaron de 0.11 a 1.85 $\mu g \cdot kg^{-1}$ y de 0.34 a 5.45 $\mu g \cdot kg^{-1}$, respectivamente.
- Se detectaron OCPs, utilizando el procedimiento QuEChERS modificado, en muestras reales de supermercado: fresa (α-HCH, lindano, 4,4′-DDT, heptacloro), aguacate (4,4′-DDD, dieldrina), sandía (aldrina, lindano, 4,4′-DDE, 4,4′-DDD), rábano (isómeros α-, β-HCH, 4,4′-DDD), y pulpa de kiwi (lindano, dieldrín).
- Se demostró la aplicabilidad del procedimiento desarrollado en diferentes tipos de suelo, a pesar de la dificultad de preparación de muestras mediante QuEChERS. Los efectos de matriz no fueron muy relevantes, lo que permitió la cuantificación de los OCPs objetivo utilizando disolventes orgánicos típicos. A pesar de que los suelos utilizados en este estudio no habían sido dedicados a cultivos agrícolas en los últimos años, se detectaron cuatro insecticidas (lindano, 4,4′-DDE, 4,4′-DDD, 4,4′-DDT) en concentraciones bajas (en su mayoría por debajo de 20 $\mu g \cdot kg^{-1}$).
- Las nanopartículas metálicas de núcleo-capa magnética, con grupos funcionales altamente hidrófobos, intercambiables en QuEChERS, poseen gran potencial para el desarrollo de materiales de limpieza útiles en la determinación de pesticidas en matrices complejas.

6. References

1. B. Alves Rocha, A.R. Moraes de Oliveira, F. Barbosa Jr, A fast and simple air-assisted liquid-liquid microextraction procedure for the simultaneous determination of bisphenols, parabens, benzophenones, triclosan, and triclocarban in human urine by liquid chromatographytandem mass spectrometry, Talanta, 183 (2018) 94–101.

2. D. Megson, E.J. Reiner, K.J. Jobst, F.L. Dorman, M. Robson, J.F. Focant, A review of the determination of persistent organic pollutants for environmental forensics investigations, Analytica Chimica Acta, 941 (2016) 10-25.

3. V. Perez-Fernandez, L.M. Rocca, P. Tomai, S. Fanali, A. Gentili, Recent advancements and future trends in environmental analysis: Sample preparation, liquid chromatography and mass spectrometry, Analytica Chimica Acta, 983 (2017) 9-41.

4. B.H. Tan, T.T. Teng, A.K.M. Omar, Removal of dyes and industrial dye wastes by magnesium chloride, Water Research, 34 (2000) 597–601.

5. S.H. Lin, R.S. Juang, Removal of free and chelated Cu(II) ions from water by a nondispersive solvent extraction process, Water Research, 36 (2002) 3611–3619.

6. B. Bolto, D. Dixon, R. Eldridge, S. King, K. Linge, Removal of natural organic matter by ion exchange, Water Research, 36 (2002) 5057–5065.

7. I. Ali, M. Asim, T.A. Khan, Low cost adsorbents for the removal of organic pollutants from wastewater, Journal of Environmental Management, 113 (2012) 170-183.

8. N. Casado, J. Gañán, S. Morante-Zarcero, I. Sierra, New Advanced Materials and Sorbent-Based Microextraction Techniques as Strategies in Sample Preparation to Improve the Determination of Natural Toxins in Food Samples, MDPI molecules, (2020) 1-31.

9. E. Boyacı, Á.Rodríguez-Lafuente, K.Gorynski, F.Mirnaghi, É.A. Souza-Silva, D.Hein, J. Pawliszyn, Sample preparation with solid phase microextraction and exhaustive extraction approaches: Comparison for challenging cases, Analytica Chimica Acta, 873 (2015) 14–30.

10. R. Ambashta, M. Sillanpaa, Water purification using magnetic assistance: a review, Journal of Hazardous Materials,180 (2010) 38–49.

11. C. Herrero-Latorre, J. Barciela-García, S. García-Martín, R.M. Pena-Crecente,J. Otarola-Jimenez,, Magnetic solid-phase extraction using carbon nanotubes as sorbents: A review. Analytica Chimica Acta, 892 (2015)10–26.

12. G. Tchobanoglous, F.L. Burton, D.H. Stensel, Wastewater Engineering: Treatment, And Reuse, 4th ed., Metcalf and Eddy, Inc., McGraw-Hill Book Company, New York, NY (2003)

13. S. Lagergren, Zur theorie der sogenannten adsorption gelo¨sterstoffe. Kungliga Svenska Vetenskapsakademiens. Handlingar, 24 (4) (1898) 1–39.

14. Y.S. Ho, G. McKay, Pseudo-second order model for sorption processes. Process Biochemistry 34 (1999) 451–465.

15. W.J. Weber, J.C. Morris, Kinetics of adsorption on carbon from solution. Journal of the Sanitary Engineering Division, 89 (1963) 31–59.

16. A.O. Okewale, K.A. Babayemi, A.P. Olalekan, Adsorption isotherms and kinetics models of starchy adsorbents on uptake of water from ethanol–water systems. International Journal of Applied Science and Technology, 3 (1) (2013) 35–42.

17. S.H. Chien, W.R. Clayton, Aplication of elovich equation to the kinetics of phosphate release and sorption in soil. Soil Science Society of America Journal, 44 (1980) 265.

18. K.L. Tan, B.H. Hameed, Insight into the adsorption kinetics models for the removal of contaminants from aqueous solutions. Journal of the Taiwan Institute of Chemical Engineers, 74 (2017) 25-48.

19. W. Rudzinski, W. Plazinski, Studies of the Kinetics of Solute Adsorption at Solid/Solution Interfaces: On the Possibility of Distinguishing between the Diffusional and the Surface Reaction Kinetic Models by Studying the Pseudo-First-order Kinetics. The Journal of Physical Chemistry C, 111 (2007) 15100 – 15110.

20. S. Azizian, Kinetic models of sorption: a theoretical analysis, Journal of Colloid and Interface Science, 276 (2004) 47–52.

21. A.M. Hubbe, S. Azizian, S.Douven, Implications of Apparent Pseudo-Second-Order Adsorption Kinetics onto Cellulosic Materials: A Review, BioResources, 14(3) (2019) 7582-7626.

22. G. W. Kajjumba, S. Emik, A. Öngen, H. Kurtulus Özcan,S. Aydın, Modelling of Adsorption Kinetic Processes—Errors, Theory and Application, DOI: 10.5772/intechopen.80495

23. Z. Aksu, Biosorption of reactive dyes by dried activated sludge: equilibrium and kinetic modelling. Biochemical Engineering Journal,7 (2001) 79–84.

24. I. Langmuir, Journal of the American Chemical Society 40 (1918) 1361–1403.

25. M. El-Naas, Modelling of adsorption processes, ISBN: 978-1-61209-651-3, 1-23

26. J. Fang, B. Gao, A. Mosa, L. Zhan, Chemical activation of hickory and peanut hull hydrochars for removal of lead and methylene blue from aqueous solutions, Chemical Speciation and Bioavailability, 29:1 (2017) 197-204.

27. J. Reungoat, J.S. Pic M.H. Manéro H. Debellefontaine, Adsorption of Nitrobenzene from Water onto High Silica Zeolites and Regeneration by Ozone, Separation Science and Technology, 42:7 (2007) 1447 – 1463.

29. D.D. Do, Adsorption Analysis: Equilibria and Kinetics. Imperial College Press, Queensland, (1998) 50–51.

30. Z. Maderova1, E. Baldikova, K. Pospiskova, I. Safarik, M. Safarikova, Removal of dyes by adsorption on magnetically modified activated sludge, International Journal of Environmental Science and Technology, 13 (2016) 1653–1664.

31. B.Y. Zhang Hiew, L.Y. Lee, K.C.Lai, S. Gan, S. Thangalazhy-Gopakumar, G.T. Pan, T. Chung-Kuang Yang, Adsorptive decontamination of diclofenac by three-dimensional graphenebased adsorbent: Response surface methodology, adsorption equilibrium, kinetic and thermodynamic studies, Environmental Research, 168 (2019) 241–253.

32. A. Kotoulas, D. Agathou, I.E. Triantaphyllidou, T.I. Tatoulis, C.S. Akratos, A.G. Tekerlekopoulou, D.V. Vayenas, Zeolite as a Potential Medium for Ammonium Recovery and Second Cheese Whey Treatment, MDPI Water (2019) 1-23.

33. X. Zhao, S. Liu, Z. Tang, H. Niu, Y. Cai, W. Meng, F. Wu, J.P. Giesy, Synthesis of magnetic metal-organic framework (MOF) for efficient removal of organic dyes from water, Scientific Reports, 5 (2015) 11849.

34. M.J. Temkin, V. Pyzhev, Acta Physiochim. USSR 12 (1940) 217–222.

35. A. V. Borhade, A. S. Kale, Calcined eggshell as a cost effective material for removal of dyes from aqueous solution, Applied Water Science, 7(2017) 4255–4268.

36. A.A. Ujile, Adsorption, 1-24

37. C.B. Vidal, G.S.C. Raulino, A.L. Barros, A.C.A. Lima, J.P. Ribeiro, M.J.R. Pires, R.F. Nascimento, BTEX removal from aqueous solutions by HDTMA-modified Y zeolite, Journal of Environmental Management, 112 (2012) 178-185.

38. H.M.H. Gad, N. S. Awwad, Factors Affecting on the Sorption/Desorption of Eu (III) using Activated Carbon, Separation Science and Technology, 42(16) (2007) 3657-3680.

39. J. Fan, J. Zhang, C. Zhang, L. Ren, Q. Shi, Adsorption of 2,4,6 trichlorophenol from aqueous solution onto activated carbon derived from loosestrife, Desalination 267 (2011) 139–146.

40. K.K. Kennedy, K.J. Maseka, M. Mbulo, Selected Adsorbents for Removal of Contaminants from Wastewater: Towards Engineering Clay Minerals, Open Journal of Applied Sciences, 8 (2018) 355-369.

41. A. Buekens, N.N. Zyaykina, Adsobents and adsorption processes for pollution control. Pollution Control Technologies, 2 1-10

42. S. Wang, Y. Peng, Natural zeolites as effective adsorbents in water and wastewater treatment. Chemical Engineering Journal 156 (2010) 11 – 24

43. S. Kubilay, R. Gurkan, A. Savran, T. Sahan, Removal of Cu(II), Zn(II) and Co(II) ions from aqueous solutions by adsorption onto natural bentonite. Adsorption, 13 (2007) 41–51.

44. M. Citraningrum, N. Gunawan Indraswati, S. Ismadji, Improved adsorption capacity of commercially available activated carbon Norit Row 0.8 Supra with thermal treatment for phenol removal. Journal of Environmental Protection Science, 1 (2007) 62–74.

45. I.A. Baciogliu, M. Otker, Treatment of pharmaceutical wastewater containing antibiotics by O3 and O3 /H2O2 processes. Chemosphere, 50 (2003) 85–95.

46. A. Shaikjee, N.J. Coville, The synthesis, properties and uses of carbon materials with helical morphology, Journal of Advanced Research, 3 (2012) 195–223.

47. W. Zou, B. Gao, Y. Sik Ok, L. Dong, Integrated adsorption and photocatalytic degradation of volatile organic compounds (VOCs) using carbon-based nanocomposites: A critical review. Chemosphere, 218 (2019) 845-859.

48. E.M. Calvo-Muñoz, F.J. García-Mateos, J.M. Rosas, J. Rodríguez-Mirasol, T. Cordero, Biomass Waste carbon Materials as adsorbents for CO_2 capture under Post-combustion conditions. Frontiers in Materials, (2016) 1-14.

49. R. Ryoo, S.H. Joo, S. Jun, Synthesis of highly ordered carbon molecular sievesvia template-mediated structural transformation, Journal of Physical Chemistry B, 103 (1999) 7743–7746.

50. W. Libbrecht, K. Vandaele, K. De Buysser, A. Verberckmoes, J.W. Thybaut, H. Poelman, J. De Clercq, P. Van Der Voort, Tuning the Pore Geometry of Ordered Mesoporous Carbons for Enhanced Adsorption of Bisphenol-A. Materials, 8 (2015) 1652-1665.

51. H. Bum An, M. Jin Yu1, J. Man Kim, M. Jin, J.K. Jeon, S. Hoon Park, S.S. Kim, Y.K. Park, Indoor formaldehyde removal over CMK-3, Nanoscale Research Letters, 7 (2012) 1-7

52. B. Glaser, J. Lehmann, W. Zech, Ameliorating physical and chemical properties of highly weathered soils in the tropics with charcoal-a review. Biology and Fertility of Soils, 35 (2002) 219–230.

53. X. Tan, S. Liu, Y. Liu, Y. Gu, G. Zeng, X. Hu, X. Wang, S. Liu, L. Jiang, Biochar as potential sustainable precursors for activated carbon production: multiple applications in environmental protection and energy storage. Bioresource Technology, 227 (2017) 359-372.

54. J.J. Manyà, Pyrolysis for biochar purposes: a review to establish current knowledge gaps and research needs. Environmental Science and Technology, 46 (2012) 7939–54.

55. J. Fanga, L. Zhana, Y. Sik Okc, B. Gao, Minireview of potential applications of hydrochar derived from hydrothermal carbonization of biomass, Journal of Industrial and Engineering Chemistry, 57 (2018) 15–21.

56. Z. Hu, M.P. Srinivasan, Mesoporous High-surface-area Activated Carbon, Microporous and Mesoporous Materials, 43 (2001) 267-275

57. D. Suhas, P. Carrott, M.M.L. Ribeiro Carrott, Lignin–From natural adsorbent to activated carbon: A review, Bioresource Technology, 98 (2007) 2301-12.

58. D. Cuhadaroglu, O. Aydemir Uygun, Production and characterization of activated carbon from a bituminous coal by chemical activation, African Journal of Biotechnology, 7 (20) (2008) 3703-3710.

59. A.S. Mestre, R.A. Pires, I. Aroso, E.M. Fernandes, M.L. Pint, R.L. Reis, M.A. Andrade, J. Pires, S.P. Silva, A.P. Carvalho, Activated carbons prepared from industrial pre-treated cork: Sustainablenadsorbents for pharmaceutical compounds removal, Chemical Engineering Journal, 253 (2014) 408–417.

60. H. Tang, Y. Duan, C. Zhu, C. Li, M. She, Q. Zhou, L. Cai, Characteristics of a biomass-based sorbent trap and its application to coal-fired flue gas mercury emission monitoring, International Journal of Coal Geology, 170 (2017) 19–27.

61. R.F.L. Ribeiro, V.C. Soares, L.M. Costa, C.C. Nascentes, Production of activated carbon from biodiesel solid residues: An alternative for hazardous metal sorption from aqueous solution, Journal of Environmental Management, 162 (2015) 123-131.

62. S. Yorgun, D. Yıldız, Preparation and characterization of activated carbons from Paulownia wood by chemical activation with H_3PO_4, Journal of the Taiwan Institute of Chemical Engineers, 53 (2015) 122–131.

63. X. Yanga, Y. Wanc, Y. Zhengb, F. Hed, Z. Yue, J. Huangf, H. Wangh, Y. Sik Okj, Y. Jianga, B. Gao, Surface functional groups of carbon-based adsorbents and their roles in the removal of heavy metals from aqueous solutions: A critical review, Chemical Engineering Journal, 366 (2019) 608–621.

64. M. Vithanage, A.U. Rajapaksha, M. Zhang, S. Thiele-Bruhn, S.S. Lee, Y.S. Ok, Acid-activated biochar increased sulfamethazine retention in soils. Environmental Science and Pollution Research, 22 (2015) 2175-2183.

65. J. Li, G. Lv, W. Bai, Q. Liu, Y. Zhang,J. Song, Modification and use of biochar from wheat straw (Triticum aestivum L.) for nitrate and phosphate removal from water, Desalination and Water Treatment, (2014) 1-13.

66. Y. Fan, B. Wang, S. Yuan, X. Wu, J. Chen, L. Wang, Adsorptive removal of chloramphenicol from wastewater by NaOH modified bamboo charcoal, Bioresource Technology, 101 (2010) 7661-7664.

67 . K. S. Ukanwa, K. Patchigolla, R. Sakrabani, E. Anthony, S. Mandavgane, A Review of Chemicals to Produce Activated Carbon from Agricultural Waste Biomass. Review, MDPI. Sustainability (2019) 1-35.

68. A. Upamali Rajapaksha, S.S. Chen, D.C.W. Tsang, M. Zhang, M. Vithanage, S. Mandal, B. Gao, N.S. Bolan, Y. Sik Ok, Engineered/designer biochar for contaminant removal/immobilization from soil and water: Potential and implication of biochar modification, Chemosphere, 148 (2016) 276-291.

69. X.R. Jing, Y.Y. Wang, W.J. Liu, Y.K. Wang, H. Jiang, Enhanced adsorption performance of tetracycline in aqueous solutions by methanol-modified biochar, Chemical Engineering Journal, 248 (2014)168-174.

70. K. O'Grady, Progress in applications of magnetic nanoparticles in biomedicine, Journal of Physics D: Applied Physics, 42 (2009) 220301

71. L. Mohammed, H.G. Gomaa, D. Ragab, J. Zhu, Magnetic nanoparticles for environmental and biomedical applications: A review, Particuology, 30 (2016) 1-14.

72. E. Aghaei, R. Diaz Alorro, A.N. Encila, K. Yoo, Magnetic Adsorbents for the Recovery of Precious Metals from Leach Solutions and Wastewater, MDPI, Metals, (2017) 1-32

73. D. Xiao, T. Lu, R. Zeng, Y. Bi, Preparation and highlighted applications of magnetic microparticles and nanoparticles: a review on recent advances. Microchimica Acta, 183 (2016) 2655–2675.

74. C.Z. Huang, B. Hu, Silica-Coated Magnetic Nano- particles Modied with Gamma-Mercaptopropyltrimethoxysilane for Fast and Selective Solid Phase Extraction of Trace Amounts of Cd, Cu, Hg, and Pb in Environmental and Biological Samples Prior to Their Determination by Inductively Coupled Plasma Mass Spectrometry, Spectrochim Acta Part B: Atomic Spectroscopy, 63 (2008) 437-444.

75. A.H. Lu, E.L. Salabas, F. Schuth, Magnetic nanoparticles: synthesis, protection, functionalization, and application, Angewandte Chemie International Edition, 46 (2007) 1222–1244.

76. S. Mangala Devi1, A. Nivetha, I. Prabha, Superparamagnetic Properties and Significant Applications of Iron Oxide Nanoparticles for Astonishing Efficacy—a Review, Journal of Superconductivity and Novel Magnetism, 32 (2019) 127–144.

77. M. Rivero-Huguet, W.D. Marshall, Reduction of hexavalent chromium mediated by micro- and nano-sized mixed metallic particles, Journal of Hazardous Materials, 169(1) (2009) 1081–1087.

78. Y. Shen, J. Tang, Z. Nie, Y.D. Wang, Y. Ren, L. Zuo, Tailoring size and structural distortion of Fe_3O_4 nanoparticles for the purification of contaminated water, Bioresource Technology, 100(18) (2009) 4139–4146.

79. K. Nee Koo, A. Fauzi Ismail, M.H. Dzarfan Othman, M.A. Rahman, T.Z. Sheng, Preparation and characterization of superparamagnetic magnetite (Fe_3O_4) nanoparticles: A short review. Malaysian Journal of Fundamental and Applied Sciences,15 (2019) 23-31.

80. W. Sumit Arora. Superparamagnetic iron oxide nanoparticles: magnetic nanoplatforms as drug carriers, International Journal of Nanomedicine, (2012) 3445-3471.

81. S. Mangala Devi1, A. Nivetha, I. Prabha, Superparamagnetic Properties and Significant Applications of Iron Oxide Nanoparticles for Astonishing Efficacy—a Review, Journal of Superconductivity and Novel Magnetism, 32 (2019) 127–144

82. H. Zhan, Y. Bian, Q. Yuan, B. Ren, A. Hursthouse, G. Zhu, Preparation and Potential Applications of Super Paramagnetic Nano-Fe3O4, Processes, 6 (2018) 1-22

83. Y.T. Lin, C.H. Weng, F.Y. Chen, Effective removal of AB24 dye by nano/micro-size zero-valent iron, Separation and Purification Technology, 64(1) (2008) 26–30.

84. P. Wang, I.M. Lo, Synthesis of mesoporous magnetic -Fe_2O_3 and its application to Cr (VI) removal from contaminated water, Water Research, 43(15) (2009) 3727–3734.

85. M.N. Alves, M. Miro, M.C. Breadmore, M. Macka, Trends in analytical separations of magnetic (nano)particles. Trends in Analytical Chemistry, 114 (2019) 89-97

86. A. Attarad, Z. Hira, M. Zia, I. ul Haq, A. Rehman Phull, J. Sarfraz Ali, A. Hussain, Synthesis, characterization, applications, and challenges of iron oxide nanoparticles, Nanotechnology, Science and Applications, 9 (2016) 49–67.

87. E.K. Athanassiou, R.N. Grass, W.J. Stark, Chemical Aerosol Engineering as a Novel Tool for Material Science: From Oxides to Salt and Metal Nanoparticles, Aerosol Science and Technology, (2010) 1521-738.

88. E. Popovicia, F. Dumitrachea, I. Morjana, R. Alexandrescua, V. Ciupinab, G. Prodanb, L. Vekasc, D. Bicac, O. Marinicad, E. Vasile, Iron/iron oxides core–shell nanoparticles by laser pyrolysis: Structural Characterization and enhanced particle dispersion, Applied Surface Science, 254 (2007) 1048–1052.

89. I. G. Gonzalez-Martinez, A. Bachmatiuk, V. Bezugly, J. Kunstmann, T. Gemming Z. Liu, G. Cuniberti M. H. Rümmeli, Electron-beam induced synthesis of nanostructures: a review, Nanoscale, 22 (2016) 11340–11362.

90. J.E. Muñoz, J. Cervantes, R. Esparza, G. Rosas, Iron nanoparticles produced by high-energy ball milling, Journal of Nanoparticle Research, 9(2007) 945–950.

91. B. Kayode Sodipo, A. Abdul Aziz, Recent advances in synthesis and surface modification of superparamagnetic iron oxide nanoparticles with silica, Journal of Magnetism and Magnetic Materials, 416 (2016) 275–291.

92. M.S. Chengyin Fu, M. Nuggehalli Ravindra, Magnetic iron oxide nanoparticles: synthesis and applications, Bioinspired, Biomimetic and Nanobiomaterials, 1 (2012) 229–244.

93. M. Faraji, Y. Yamini, M. Rezaee, Magnetic Nanoparticles: Synthesis, Stabilization, Functionalization, Characterization, and Applications, Journal of the Iranian Chemical Society, 7, (2010) 1-37.

94. A. Kumar Singh, O.N. Srivastava, K. Singh, Shape and Size-Dependent Magnetic Properties of Fe_3O_4 Nanoparticles Synthesized Using Piperidine, Nanoscale Research Letters, 12 (2017) 298.

95. M.N. Alves, M. Miro, M.C. Breadmore, M. Macka, Trends in analytical separations of magnetic (nano)particles, Trends in Analytical Chemistry, 114 (2019) 89-97

96. M. Helmi Rashid Farimani, N. Shahtahmasebi, M. Rezaee Roknabadi, N. Ghowsc, A. Kazemi, Study of structural and magnetic properties of superparamagnetic Fe3O4/SiO2 core–shell nanocomposites synthesized with hydrophilic citrate-modified Fe3O4 seeds via a sol–gel approach, PhysicaE, 53 (2013) 207–216.

97. B. Geun Cha, J. Kim, Functional mesoporous silica nanoparticles for bio-imaging applications, WIREs Nanomed Nanobiotechnol, 11(2019) 1-22.

98. O. Abu Noqta, A. Abdul Aziz, I. Adamu Usman M. Bououdina, Recent Advances in Iron Oxide Nanoparticles (IONPs): Synthesis and Surface Modification for Biomedical Applications, Journal of Superconductivity and Novel Magnetism, 32 (2019) 779–795.

99. N. Farzin Nejad, E. Shams, M.K. Amini, J.C. Bennett, Synthesis of magnetic mesoporous carbon and its application for adsorption of dibenzothiophene, Fuel Processing Technology, 106 (2013) 376–384.

100. H.S. Saroyan, D.A. Giannakoudakis, C.S. Sarafidis, N.K. Lazaridis, E.A. Deliyanni, Effective impregnation for the preparation of magnetic mesoporous carbon: application to dye adsorption, Journal of Chemical Technology and Biotechnology, 92 (2017) 1899–1911.

101. Y. Zhao, J. Feng, Q. Huo, N. Melosh, G.H. Fredrickson, B.F. Chmelka, G.D. Stucky, Triblock copolymer syntheses of mesoporous silica with periodic 50 to 300 angstrom pores, Science, 279 (1998) 548-553.

102. B.D. Cullity, S.R. Stock, Elements of X-Ray Diffraction, Prentice-Hall, 3rd Ed. (2001) 96-102.

103. S.G. Chan, P.A. Murphy, S.C. Ho, N. Kreiger, G. Darlington, E.K.F. So, P.Y.Y. Chong, Journal of Agricultural and Food Chemistry, 57 (2009) 5386–5390.

104. E.P. Barrett, L.G. Joyner, P.P. Halenda, The Determination of Pore Volume and Area Distributions in Porous Substances. I. Computations from Nitrogen Isotherms, Journal of the American Chemical Society, 73 (1951) 373 – 380.

105. S.A. Zdravkovic, Solid phase extraction in tandem with GC/MS for the determinationof semi-volatile organic substances extracted from pharmaceuticalpackaging/delivery systems via aqueous solvent systems, Journal of Pharmaceutical and Biomedical Analysis, 112 (2015) 126–138.

106. H. Kataoka, A. Ishizaki, K. Saito, Recent progress in solid-phase microextraction and its pharmaceutical and biomedical applications, Analitical Methods, 8 (2016) 5773-5788.

107. A. Rodgman, T.A. Perfetti, The chemical components of tobacco and tobacco smoke. Boca Raton, FL: CRC Press. (2009)

108. M.A. Rahman, N. Hann, A. Wilson, L. Worrall-Carter, Electronic cigarettes: patterns of use, health effects, use in smoking cessation and regulatory issues. Tobacco Induced Diseases, 12 (1) (2014) 21

109. X. Zhanga, B. Gaoc, A. Elise Creamerc, C. Caoa, Y. Li, Adsorption of VOCs onto engineered carbon materials: A review, Journal of Hazardous Materials, 338 (2017) 102–123.

110. M. Lordgooei, M.J. Rood, M. Rostam-Abadi, Modeling Effective Diffusivity of Volatile Organic Compounds in Activated Carbon Fiber, Environmental Science and Technology, 35 (2001) 613-619.

111. A. Demirbas, Potential applications of renewable energy sources, biomass combustion problems in boiler power systems and combustion related environmental issues, Progress in Energy and Combustion Science, 31 (2005) 171–92.

112. A Demirbas, Biomass resource facilities and biomass conversion processing for fuels and chemicals, Energy Conversion and Management, 42 (2001) 1357–78.

113. J. Heinimo, M. Junginger, Production and trading of biomass for energy – an overview of the global status, Biomass Bioenergy, 33 (2009) 1310–20.

114. S. Van Loo, J. Koppejan. The handbook of biomass combustion and cofiring. London (Sterling, VA): Earthscan, (2008) 442.

115. M.A. Perea-Moreno, F. Manzano-Agugliaro, A.J. Perea-Moreno, Sustainable energy based on sunflower seed husk boiler for residential buildings, Sustainability, 10 (2018) 1-20.

116. C. Xuyang, Y. Junhong, S. Xinyu, L. Wanning, H. Tao, B. Chao, Pelletization of Sunflower Seed Husks: Evaluating and Optimizing Energy Consumption and Physical Properties by Response Surface Methodology (RSM), MDPI, 2019, 1-20.

117. A.I. Casoni, M. Bidegain, M.A. Cubitto, N. Curvetto, M.A. Volpe, Pyrolysis of sunflower seed hulls for obtaining bio-oils, Bioresource Technology, 177 (2015) 406-409.

118. G. Cornelissen, N.P. Pandit, P. Taylor, B.H. Pandit, M. Sparrevik, H.P. Schmidt, Emissions and Char Quality of Flame-Curtain "Kon Tiki" Kilns for Farmer-Scale Charcoal/Biochar Production, PLOS One, 11 (2016) 0154617.

119. D. Mohan, C.U. Pittman, P.H. Steele, Pyrolysis of wood/biomass for bio-oil: a critical review, Energy Fuels, 20 (2006) 848 – 889.

120. D.J.M. Hayes, Biomass composition and its relevance to biorefining. The Role of Catalysis for the Sustainable Production of Biofuels and Bio-chemicals. Elsevier, Amsterdam, (2013) 27–65.

121. L. Singh, V.C. Kalia, Waste Biomass Management – A Holistic Approach. Springer. (2017)

122. G.M.J. Herbert, A.U. Krishnan, Quantifying environmental performance of biomass energy, Renewable and Sustainable Energy Reviews, 59 (2016) 292–308.

123. J.C. Moreno-Pirajan, L. Giraldo, Activated carbon obtained by pyrolysis of potato peel for the removal of heavy metal copper (II) from aqueous solutions. Journal of Analytical and Applied Pyrolysis, 90 (2011) 42–47.

124. M.M. Titirici, R.J. White, N. Brun, V.L. Budarin, D.S. Su, F. Monte, J.H. Clark, M.J. Mac Lachlan, Sustainable carbon materials. Chemical Society Reviews. 1 (2015) 1-41.

125. L. Zhang, C. Xu, P. Champagne. Overview of recent advances in thermochemical conversion of biomass, Energy Conversion and Management, 51 (2010) 969–82.

126. M.F. Demirbas, M. Balat, H. Balat. Potential contribution of biomass to the sustainable energy development, Energy Conversion and Management, 50 (2009) 1746–60.

127. P. Galvao, B. Henkelmann, R. Longo, J. Lailson-Brito, J.P.M. Torres, K.W. Schramm, O. Malm, Distinct bioaccumulation profile of pesticides and dioxin-like compounds by mollusk bivalves reared in polluted and unpolluted tropical bays: Consumption risk and seasonal effect. Food Chemistry, 134 (2012) 2040-2048.

128. J.L. Martínez Vidal, P. Plaza-Bolaños, R. Romero-González, A. Garrido Frenich, Determination of pesticide transformationproducts: a review of extraction and detection methods. Journal of Chromatography A, 1216 (2009) 6767 – 688.

129. S. Egodawatte, A. Datt, E.A. Burns, S.C. Larsen, Chemical Insight into the Adsorption of Chromium(III) on Iron Oxide/Mesoporous Silica Nanocomposites, Langmuir. (2015).

130. K.R. Kunduru, M. Nazarkovsky, S. Farah, R.P. Pawar, A. Basu, A.J. Domb, Nanotechnology for water purification: applications of nanotechnology methods in wastewater treatment, in: Water Purification, (2017) 33–74.

131. A. Azzouz, S.K. Kailasa, S.S. Lee, A.J. Rasco, E. Ballesteros,M. Zhang, K. Kim, Review of nanomaterials as sorbents in solid-phase extraction for environmental samples. Trends in Analytical Chemistry,108 (2018) 347 − 369.

132. M. Hua, S. Zhang, B. Pan, W. Zhang, L. Lv, Q. Zhang, Heavy metal removal from water/wastewater by nanosized metal oxides: A review, Journal of Hazardous Materials, 211–212 (2012) 317–331.

133. E. Aghaei, R. Alorro, A. Encila, K. Yoo, Magnetic Adsorbents for the Recovery of Precious Metals from Leach Solutions and Wastewater, Metals (Basel), 7 (2017) 529.

134. C. Su, Environmental implications and applications of engineered nanoscale magnetite and its hybrid nanocomposites: A review of recent literature, Journal of Hazardous Materials, 322 (2017) 48–84.

135. M. Faraji, Recent analytical applications of magnetic nanoparticles, Nanochemistry Research, 1(2) (2016) 264-290.

136. G. Giakisikli, A.N. Anthemidis, Magnetic materials as sorbents for metal/metalloid preconcentration and/or separation. A review, Analytica Chimica Acta, 789 (2013) 1–16.

137. C. Herrero-Latorre, J. Barciela-García, S. García-Martín, R.M. Peña-Crecente, J. Otárola-Jiménez, Magnetic solid-phase extraction using carbon nanotubes as sorbents: A review, Analytica Chimica Acta, 892 (2015) 10–26.

138. M. Ezoddin, B. Majidi, K. Abdi, N. Lamei, Magnetic Graphene-Dispersive Solid-Phase Extraction for Preconcentration and Determination of Lead and Cadmium in Dairy Products and Water Samples, Bulletin of Environmental Contamination and Toxicology, 95 (2015) 830–835.

139. J. Meng, J. Bu, C. Deng, X. Zhang, Preparation of polypyrrole-coated magnetic particles for micro solid-phase extraction of phthalates in water by gas chromatography-mass spectrometry analysis, Journal of Chromatography A, 1218 (2011) 1585–1591.

140. Y.W. Wu, J. Zhang, J.F. Liu, L. Chen, Z.L. Deng, M.X. Han, X.S. Wei, A.M. Yu, H.L. Zhang, Fe_3O_4@ZrO_2 nanoparticles magnetic solid phase extraction coupled with flame atomic absorption spectrometry for chromium(III) speciation in environmental and biological samples, Applied Surface Science, 258 (2012) 6772–6776.

141. L. Zhang, X. Gao, Z. Xiong, L. Zhang, B. Yu, R. Zhang, W. Zhang, Preparation of dithizone grafted poly(allyl chloride) core–shell–shell magnetic composite microspheres for solid-phase extraction of ultra-trace levels of Pb(II), Cu(II) and Cr(III) ions, Royal Society of Chemistry Advances, 5 (2015) 58873–58879.

142. F. Enache, E. Vasile, C.M. Simonescu, A. Răzvan, A. Nicolescu, A.C. Nechifor, O. Oprea, R.E. Pătescu, C. Onose, F. Dumitru, Cysteine-functionalized silica-coated magnetite nanoparticles as potential nanoadsorbents, Journal of Solid State Chemistry, 253 (2017) 318–328.

143. H. Bagheri, A. Afkhami, M. Saber-Tehrani, H. Khoshsafar, Preparation and characterization of magnetic nanocomposite of Schiff base/silica/magnetite as a preconcentration phase for the trace determination of heavy metal ions in water, food and biological samples using atomic absorption spectrometry, Talanta, 97 (2012) 87–95.

144. S. Egodawatte, A. Datt, E.A. Burns, S.C. Larsen, Chemical Insight into the Adsorption of Chromium(III) on Iron Oxide/Mesoporous Silica Nanocomposites, Langmuir, 31 (2015) 7553–7562.

145. L. Zhao, T. Szakas, M. Churley, D. Lucas, Multi-class multi-residue analysis of pesticides in edible oils by gas chromatography-tandem mass spectrometry using liquid-liquid extraction and enhanced matrix removal lipid cartridge cleanup, Journal of Chromatography A, 1584 (2019) 1−12.

146. M.L. Schmidt, N.H. Snow, Making the case for QuEChERS-gas chromatography of drugs, Trends in Analytical Chemistry, 75 (2016) 49 − 56.

147. M. Smoker, K. Tran, R.E. Smith, Determination of Polycyclic Aromatic Hydrocarbons (PAHs) in Shrimp, Journal of Agricultural and Food Chemistry, 58 (2010) 12101 − 12104.

148. T. Rejczak,T. Tuzimski, QuEChERS-based extraction with dispersive solid phase extraction clean-up using PSA and ZrO2 –based sorbents for determination of pesticides in bovine milk samples by HPLC-DAD, Food Chemistry, 217 (2017) 225 − 233

149. Y.T. Han, L. Song, N. Zou, R.H. Chen, Y.H. Qin, C.P. Pan, Multi-residue determination of 171 pesticides in cowpea using modified QuEChERS method with multi-walled carbon nanotubes as reversed-dispersive solid-phase extraction materials. Journal of Chromatography. B, Analytical Technologies in the Biomedical and Life Sciences, 1031 (2016) 99 − 108.

150. G. Ma, M. Zhang, L. Zhu, H. Chen, X. Liu, C. Lu, Facile synthesis of amine-functional reduced graphene oxides as modified quick, easy, cheap, effective, rugged and safe adsorbent for multi-pesticide residues analysis of tea, Journal of Chromatography A, 1531 (2018) 22 −31.